Analysis of glasses present in quartz and apatite phenocrysts from

Ordovician K-bentonites in the Mohawk Valley, NY

Abstract of

A thesis presented to the Faculty

of the University at Albany, State University of New York

in partial fulfillment of the requirements

for the degree of

Master of Science

College of Arts & Sciences

Department of Earth and Atmospheric Sciences

Stefanie Dannenmann

1997

ABSTRACT

More than 20 bentonites occur in the Middle Ordovician black shales of the Utica Formation that outcrop along tributaries to the Mohawk River in New York State. Pristine melt inclusions within quartz and apatite phenocrysts are commonly found in at least 40% of the bentonites. Constraints on magmatic processes can be obtained by examining the major-, minor- and trace-element variations among different melt inclusions in quartz and apatite phenocrysts from individual bentonites. The melt inclusions in apatite range in composition from rhyodacitic to rhyolitic, while those in quartz are high-silica rhyolites. Most bentonites within the Middle Ordovician sequence in New York contain melt inclusions with 5-6 wt.% K_2O (high-K). However, the bentonites within a restricted stratigraphic interval (approximately 30 m thick) that occurs in the *C. americanus* graptolite zone contain melt inclusions with 2-3 wt.% K_2O (low-K). These inclusions typically have higher MgO, CaO, MnO, TiO_2 and FeO abundances relative to the high-K glasses. Commonly in this 30 m restricted interval, bentonite layers display bimodal distributions of elemental abundances. In some cases, one of the groups of inclusions within the bimodal bentonites appears to be chemically identical to melt inclusions within other bentonites in this interval. The bimodal bentonites could be composed of the air-fall components of two different eruptions. Another possibility is that the bimodality reflects zoned magma chambers. The two different models may hold important implications for the interpretation of bentonite correlations.

Analysis of glasses present in quartz and apatite phenocrysts from Ordovician K-bentonites in the Mohawk Valley, NY

A thesis presented to the Faculty

of the University at Albany, State University of New York

in partial fulfillment of the requirements

for the degree of

Master of Science

College of Arts & Sciences

Department of Earth and Atmospheric Sciences

Stefanie Dannenmann

1997

ACKNOWLEDGMENTS

Without the support and encouragement of many people, this work would have been impossible. Thanks are due the Departments of Geological Sciences here in Albany (USA) and in Würzburg (Germany). The social and academic environment established during the development of this thesis influenced me a great deal. I appreciated the high standards that were expected by my adviser John Delano. His scientific goals were hard to follow, but allowed me to develop my own critical standards. The financial support that he generously provided is greatly acknowledged. Special thanks go to my thesis committee John Delano, Bill Kidd, Win Means and Don Rodbell for all of their thoughtful comments and constructive criticisms of the initial drafts. Of all the people in the Department, I would especially like to thank Win Means for being helpful in various situations and for his fine way in leading me to the right answers; Bill Kidd for being an expert in killing computer viruses and being available for all kinds of questions concerning computers and programs; and Greg Harper for the interesting discussions about magma chambers. Diana Paton is not only a terrific secretary, but is also a fantastic link between students, professors and advisers. Thank you so much, Diana.

There would have been no thesis if there had not been Benjamin (Ben Hanson). He was the driving power and force for my work. He provided invaluable assistance in finding my way around the wet-chemistry lab and was a patient instructor in teaching the electron microprobe during endless hours at nights and on weekends. I enjoyed a lot our, fruitful conversations, inspiring discussions and fights about our beloved melt inclusions. His rich experience of melt inclusion study has given form and substance to this work. Ben not only introduced me to the world of bentonites, but as well to the world of 'listening baseball on the radio', Howard Stern, some interesting English vocabulary, Sutters etc. . Ben, there are not enough words to express my gratitude to you.

There is no Steffi without Steff (Stefan Kosanke). Steff has been my buddy since the beginning of my university career that started ways back in Würzburg, Germany. Special thanks are accorded Steff for his patience explanations and aid in many aspects in my university career. Thanks to his wife Tobi, who took the time to read my thesis and to edit it. Life in Albany and my life at the University was

enjoyable due to my friends and fellow graduate students: Andreas, Angela, Michael, Mike, Nick, Rich and Vera. Ana, Marc & Markus thank you for the significant moral contributions and for making Morris St. the place to be.

Finally, a special word of thanks to my parents and my brother for their patience and endurance with me during my adventurous university career over the past years.

Table of Contents

LIST OF TABLES

LIST OF FIGURES

CHAPTER 1 INTRODUCTION

1.1 Terminology and Study of Paleozoic K-bentonites

Bentonites are the chemically-alterated remains of volcanic air-fall deposits. When preserved in sedimentary rocks, they are considered to be ideal time planes for correlation, because explosive eruptions distribute ash over wide geographic areas and the ash is deposited instantaneously in geologic time (Kay, 1935; Huff, 1983; Sarna-Wojcicki et al., 1987). Considerable progress has been made in correlating bentonites between different outcrops of Ordovician shales and Limestones of New York State (Delano et al., 1994; Mitchell et al., 1994).

The term bentonite is associated with a clay-rich rock containing phenocrysts of volcanic origin, such as melt inclusions, euhedral quartz and zircons, biotite and apatite phenocrysts (Fisher and Schminke, 1984). The late Ordovician bentonites of the eastern half of North America are often referred in the literature as K-bentonites (Schirnick, 1990; Delano et al., 1990, 1994). K-bentonites are rich in the clay mineral kaolinite. This study will use the term 'bentonite' to describe a clay-rich layer that can be recognized by the presence of volcanic phenocrysts, because the overall dominant clay mineral was not determined for the bentonites discussed in this study.

Volcanic ash is composed of glass and volcanic phenocrysts. Over time, the glass and chemically unstable phenocrysts become diagenetically altered to illite and smectite-rich clays. This process produces major changes in the bulk composition due to the open-system behavior of elements during diagenesis (Delano et al., 1990). Therefore, the bulk composition of the bentonite may not represent the original bulk composition of the ash. Because diagenetic processes may be very different depending on the host rock composition, the bulk composition is an unreliable "fingerprint" of the bentonite. Schirnick (1990) discovered pristine, rhyolitic glass inclusions in chemically-resistant phases (e.g., quartz, apatite and zircon) in Ordovician bentonites of New York State. These glasses have been hermetically-sealed in quartz and apatite and represent unaltered samples of the magmatic liquid from which the host mineral grew (Roedder, 1984). Delano et al. (1994) demonstrated that a host bentonite can be confidently

characterized based on the compositions of the glass inclusions. Thus, bentonites can be confidently identified at different outcrops and correlated between these outcrops.

1.2 Geological and stratigraphical background

The Upper Middle Ordovician K-bentonites of the north eastern United States are presumably the remnants of volcanic eruptions associated with the Taconic Orogenic event. During the Taconic Orogeny, an eastward dipping subduction zone developed beneath an approaching volcanic arc (Rowley & Kidd, 1981). The eastern margin of the North American continent evolved from a passive margin to a deep foreland basin into which the black graptoliferous shales of the Utica Formation were deposited. These black shales grade into the interbedded limestone and shale of the Dolgeville Formation. The Denmark, Sugar River and Rust Formation represent platform carbonates which were deposited contemporaneously with, and to the west of, the deep water foreland basin sediments (Figure 1; Mitchell et al., 1994).

Most of the bentonites in this study were collected within the Utica Formation. The Utica Formation, which consists of about 300 m of flat-lying black, often calcareous, shales, is overlain by the 5-100 meters of the Trenton Group limestones starting with the King's Falls Limestone. Additional bentonite samples were collected from the undeformed Denley member of the Denmark Formation near Carthage, New York. A trocholite bed, a stratigraphically condensed interval, marks the contact between the Sugar River Limestone and the overlying Denley member. This lithologic contact can be traced for approximately 130 km, from the Black River Valley, southeastward to the Mohwak River Valley (Lehmann et al. 1995). Mitchell et al. (1994) established a relatively precise stratigraphic framework for the Utica Formation based on the correlation of graptolite zones. Since graptolites are not found within the platform carbonates of the Denley Formation, correlations between the eastern Utica Formation and the Denly Formation have been difficult to establish. Bentonites have been used to establish a more precise correlative framework between these two formations (Mitchell et al., 1994). More detailed information about the stratigraphic units are given in Lehmann et al. (1995), Goldman et al. (1994) and Mitchell et al. (1994).

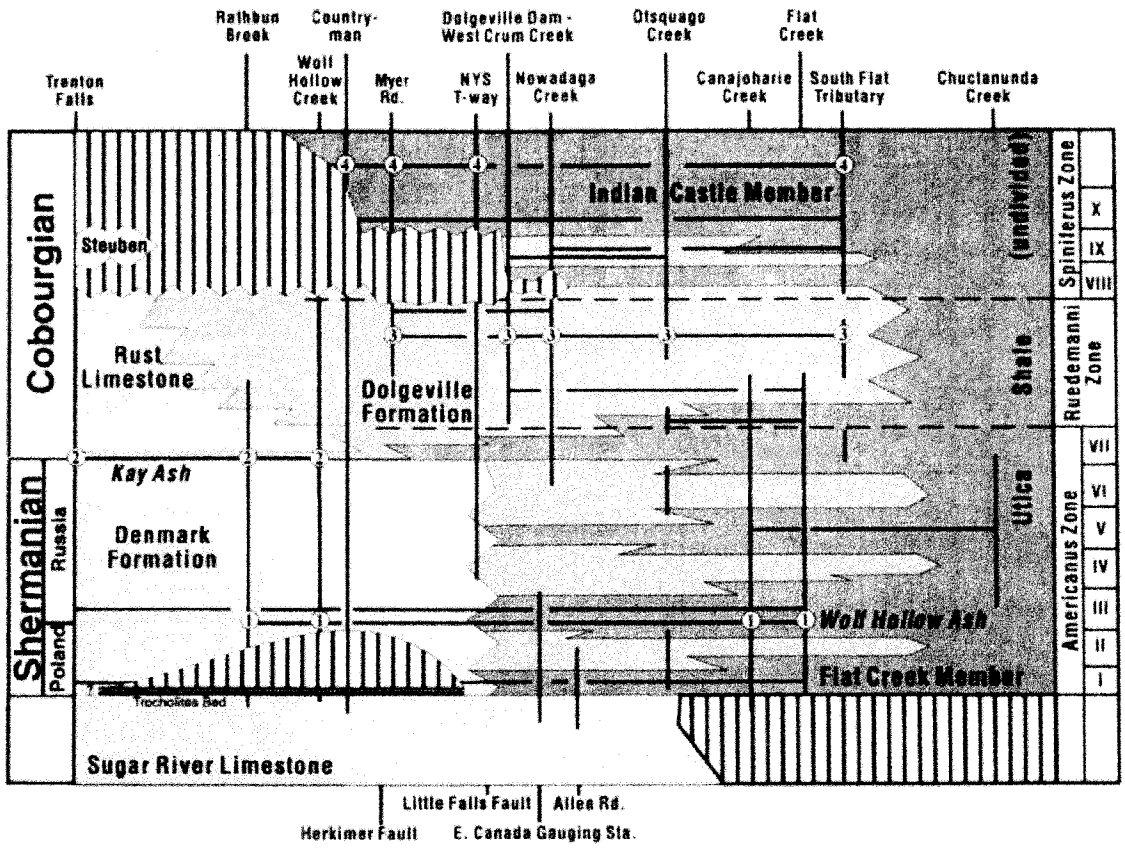

Figure 1. Chronostratigraphic cross section of late to Middle and early Upper Ordovician strata exposed along the Mohawk Valley, NY (modified from Mitchell et al., 1994), showing temporal and facies relations together with a sequence stratigraphic interpretation. Horizontal lines are the stratigraphic level of 15 correlated K-bentonites. Arabic numbers are special fingerprinted K-bentonites discussed by Mitchell et al., 1994. Areas with vertical lines represent hiatus.

1.3 Purpose of this Study

The purpose of this study was to: (a) establish detailed stratigraphic correlations among Ordovician bentonites within a complicated 30 m thick interval in the Utica Formation in order to provide much needed detail to the chronostratigraphic framework that had previously been constructed in the Mohwak Valley; (b) correlate bentonites from this interval to bentonites occurring in the western Platform carbonates of the Black River Valley; and (c) characterize the chemical diversity of melt inclusions in a unique group of bentonites which occur in a 30 m stratigraphic interval of the Utica Formation.

Bentonites have been "fingerprinted" and correlated based on the composition of glass inclusions in chemically-resistant phenocrysts. These glass inclusions are not only important for stratigraphic correlation, but also provide information about the compositions of the magma that were erupted during the Taconic Orogeny. Compositional variations among the melt inclusions within single bentonite layers may provide information pertaining to the evolution of these ancient magma chambers.

CHAPTER 2 SAMPLE LOCATION AND NOMENCLATURE

Late Ordovician bentonites are regionally distributed throughout the eastern half of North America (Huff, 1983; Cisne et al., 1982, Samson et al. 1988; Delano et al., 1990). Samples of bentonites were collected from outcrops along tributaries to the Mohawk River in Montgomery County and Herkimer County and along the Deer River Valley in Lewis County, New York (Figure 2.1).

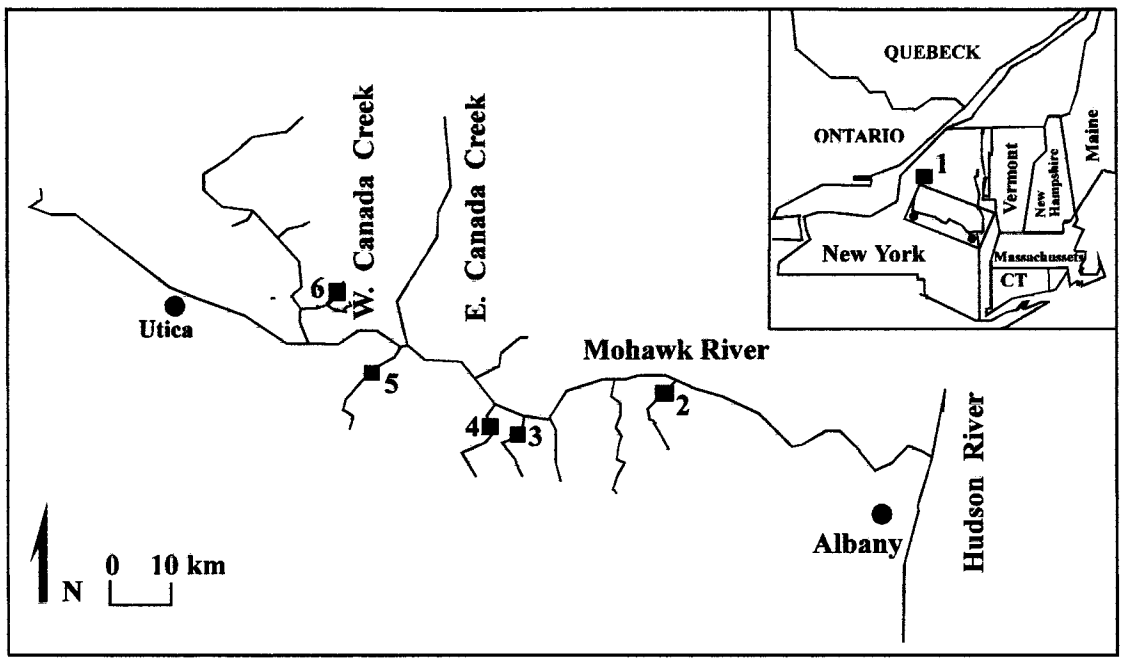

Figure 2.1 Locality map of outcrops in New York State used in this study; solid black squares represent the sampling location and the attached numbers the outcrop name: 1 = Deer River; 2 = Chuctanunda Creek; 3 = Flat Creek; 4 = Canajoharie Creek; 5 = Nowadaga Creek; 6 = North Creek tributary at Myers Road. Modified after Mitchell et al. (1994).

2.1 Canajoharie Creek, Flat Creek, Chuctanunda Creek

Bentonite samples along Canajoharie Creek, Flat Creek and Chuctanunda Creek all occur within the *upper C. americanus* and in the *O. ruedemanni* graptolite zone (Mitchell et al., 1994) of the Utica Formation.

The Canajoharie Creek locality (Figure 2.2) is located in the Wintergreen Park, 1-2 km south of the town of Canajoharie, 50 km west of Albany, and the Flat Creek section (Figure 2.3) is located 5 km to the east of Canajoharie Creek. In both sections, approximately 30 bentonites are exposed in black shales of the Utica Formation. At Canajoharie an unconformable contact exists between the Utica Shale and the King Falls Limestone at the level of the pond below the waterfall. This contact is found at Flat Creek 4 m below an interval covered by Quaternary alluvium. Bentonites in these two localities are easily accessible by walking along the creek bed. The Chuctanunda bentonites (Figure 2.4) occur in a road cut along US 5S in Montgomery County, NY, approximately 1.8 km west of Route 30, and 1.3 km southwest of the town of Amsterdam. Eleven bentonites occur in this 20 m thick outcrop. These bentonites are also easily accessible along the road cut. The geographic positions of these outcrops, marked with filled circles, are shown in Figure 2.5.1 and 2.5.2.

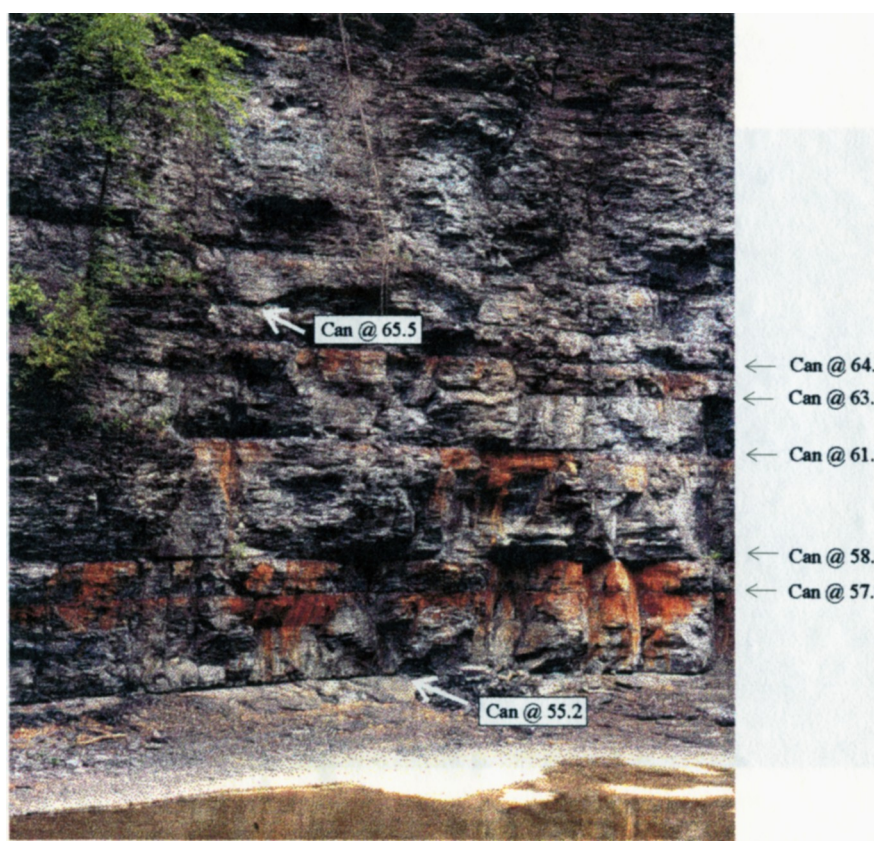

Figure 2.2 Photograph of the black shales of the Utica Formation that outcrops at Canajoharie Creek. Arrows and labels show the position of individual bentonites.

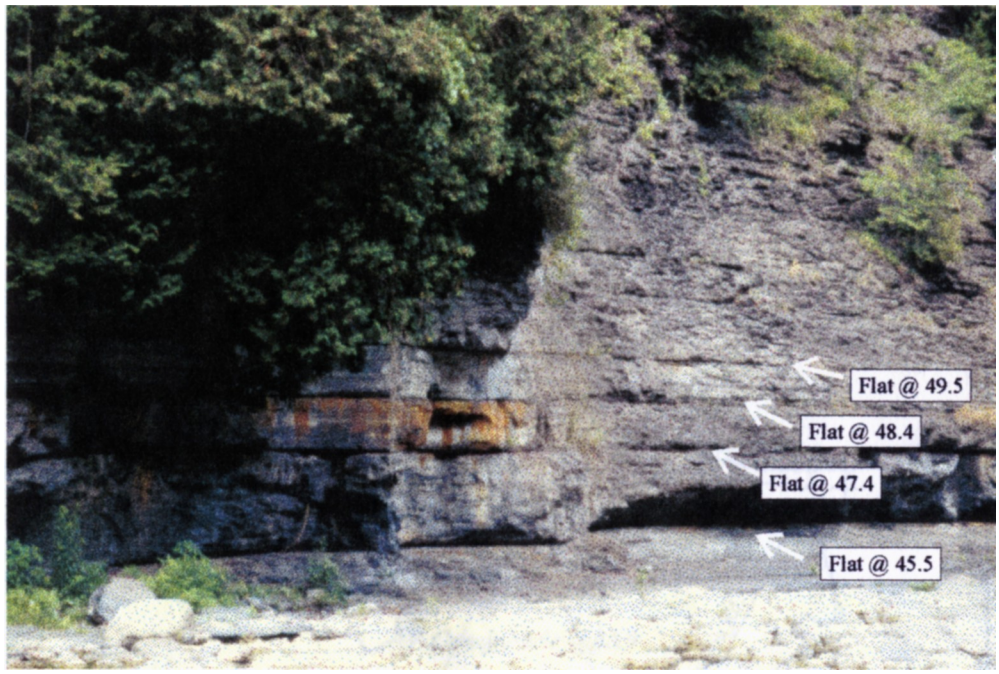

Figure 2.3 Photograph of the black shales of the Utica Shale that outcrops at Flat Creek. Arrows and labels show the position of individual bentonites.

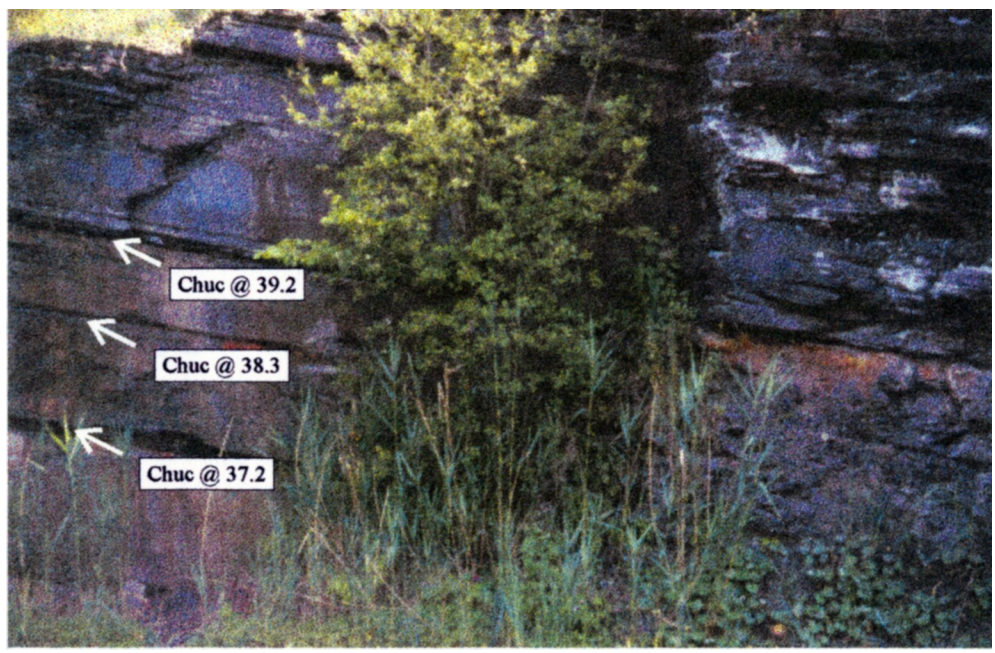

Figure 2.4 Photograph of the black shales of the Utica Formation that outcrops at Chuctanunda Creek. Arrows and labels show the position of individual bentonites.

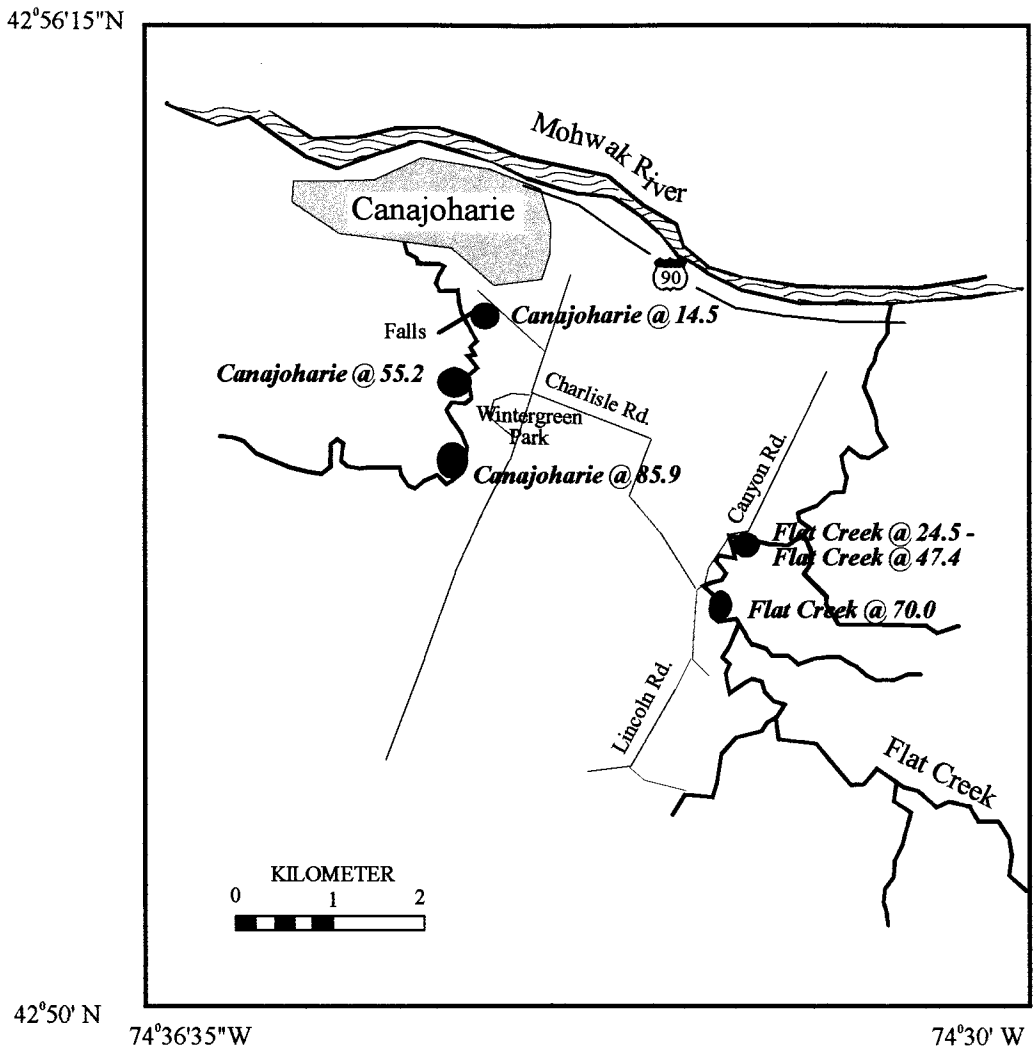

Figure 2.5.1 Map showing location of Canajoharie Creek and Flat Creek bentonites. Canajoharie @ 14.5, Canajoharie @ 55.2, and Canajoharie @ 85.9 are the locations of bentonites sampled along Canajoharie Creek at 14.5, 55.2, and 85.9 meters respectively above the King Falls Formation (Figure 2.6). Flat Creek @ 24.5, Flat Creek @ 47.4, and Flat Creek @ 70 are the locations of bentonites sampled along Flat Creek at 24.5, 47.4, and 70 meters above the Kings Falls Formation.

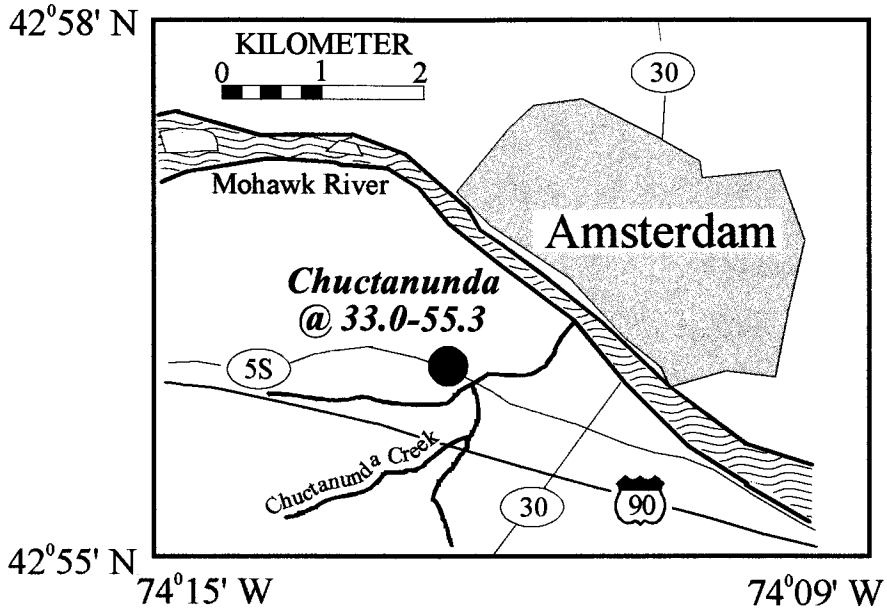

Figure 2.5.2 Map showing location of Chuctanunda Creek bentonites. All bentonites between 33.0 and 55.3 meters above the King Falls Formation were sampled at this location along the Chuctanunda Creek.

The bentonites are easily recognizable in the outcrops because they erode faster than the surrounding black shales, causing a pronounced reentrant along a stratigraphic horizon. The bentonites are also recognized by the distinct orange staining below the reentrant, which is produced during weathering of sulfides within them (see Figure 2.2). These bentonites are usually less than 15 cm thick, and are typically between two and three centimeters thick. Figure 2.6 shows the stratigraphic column of Canajoharie Creek, Flat Creek and Chuctanunda Creek sections. The horizontal lines within columns represent bentonites and the adjacent numbers represent their stratigraphic height above the contact between the Utica Formation and the Kings Falls Formation. The covered section above Flat Creek @ - 4 m is indicated by a X. In the text, bentonites are named after both their location and their position in the stratigraphic column. For example, Canajoharie @ 84.7 refers to the bentonite at Canajoharie Creek at 84.7 m above the datum. In this case, the datum is the contact between the Utica Formation and the underlying King Falls Formation.

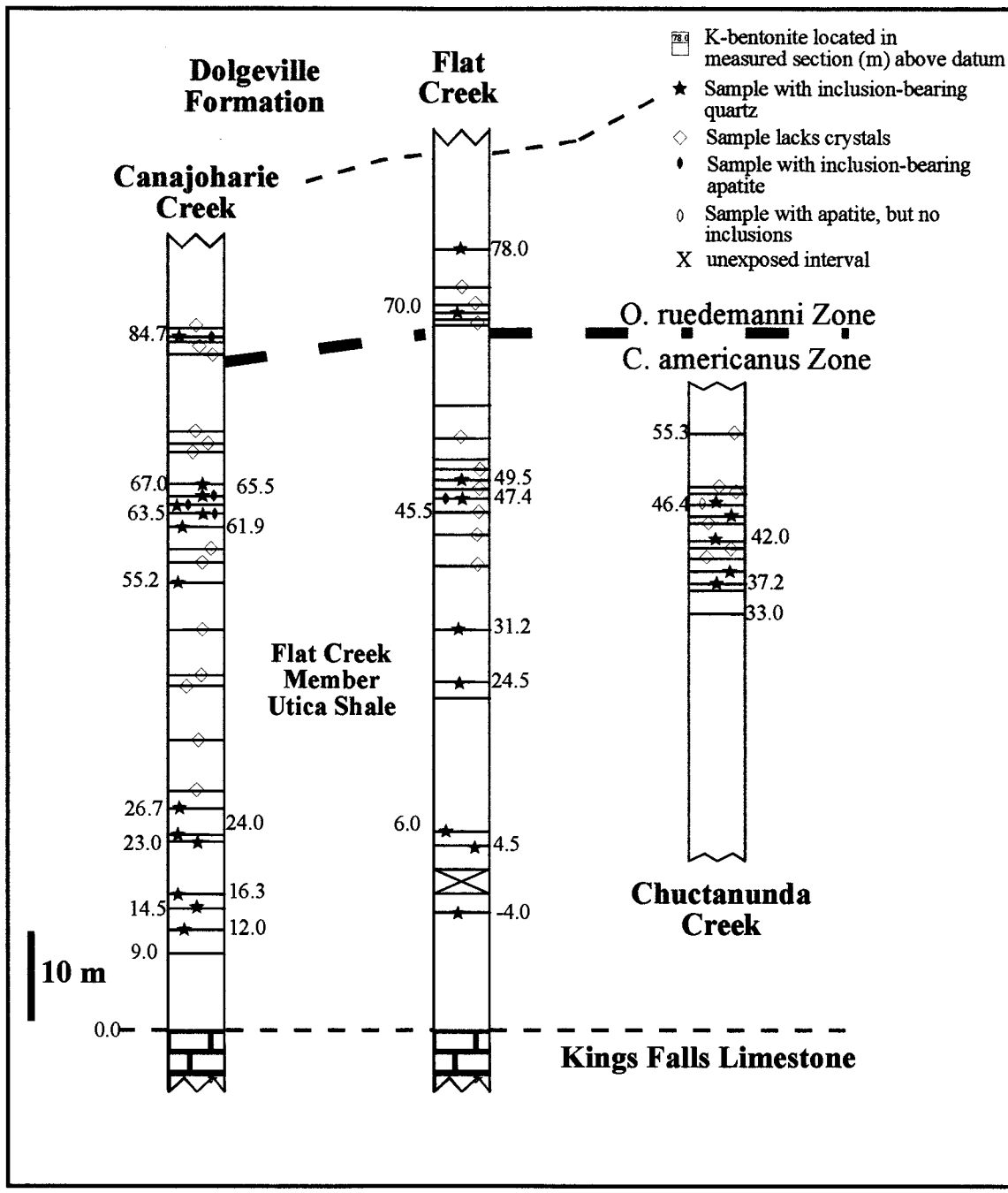

Figure 2.6. Stratigraphic columns of the Utica Formation at Canajoharie Creek, Flat Creek, and Chuctanunda Creek. Modified after Delano et al. (1994). Dashed lines connecting sections represent the boundary between the O. ruedemanni and C. americanus graptolite zones.

2.2 Deer River

The bentonites from the Deer River location were collected and provided by Dr. John W. Delano and were first described by Chenoweth (1952). They occur in the Denley limestone member of the Denmark Formation that outcrops along the Deer River in Lewis County, New York, 2 km south of the town of Carthage (Figure 2.7).

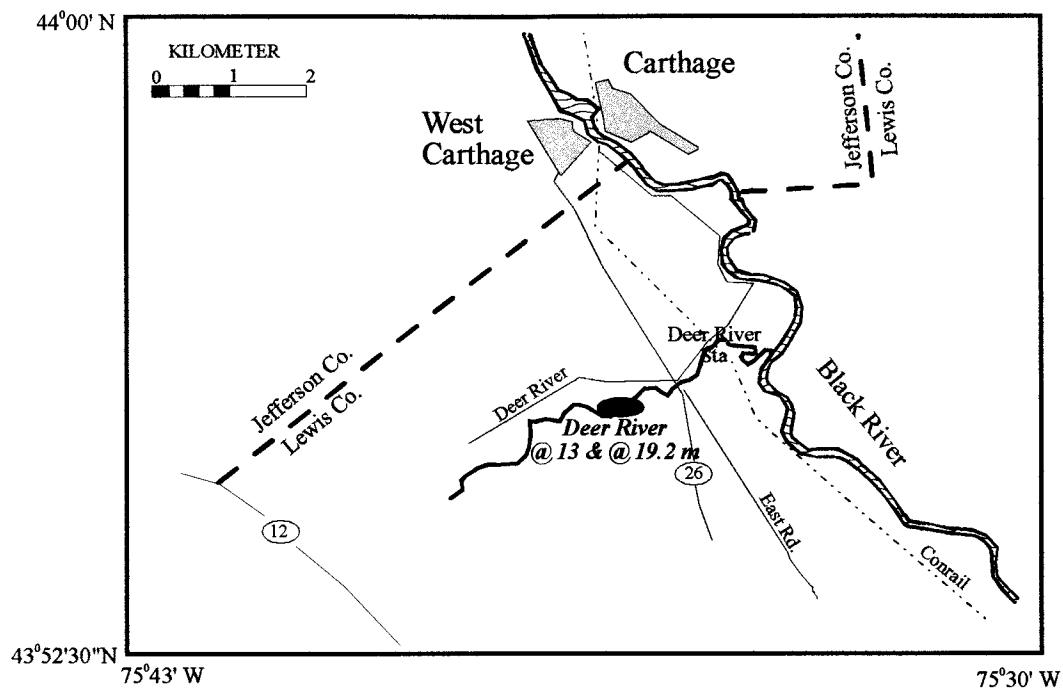

Figure 2.7. Map showing the approximate position of the bentonite sample locality at Deer River. Deer River at 13 and 19.2 m are the locations of bentonites sampled along the Deer River at 13 and 19.2 meters respectively above a Trocholite bed in the Camp Member.

Figure 2.8 shows the stratigraphic position of these bentonites. A Trocholite bed in the Camp Member of the Denley Formation is used as the datum for stratigraphic height. Deer River @ 19.2 represents a bentonite that occurs 19.2 meters above the Trocholite bed.

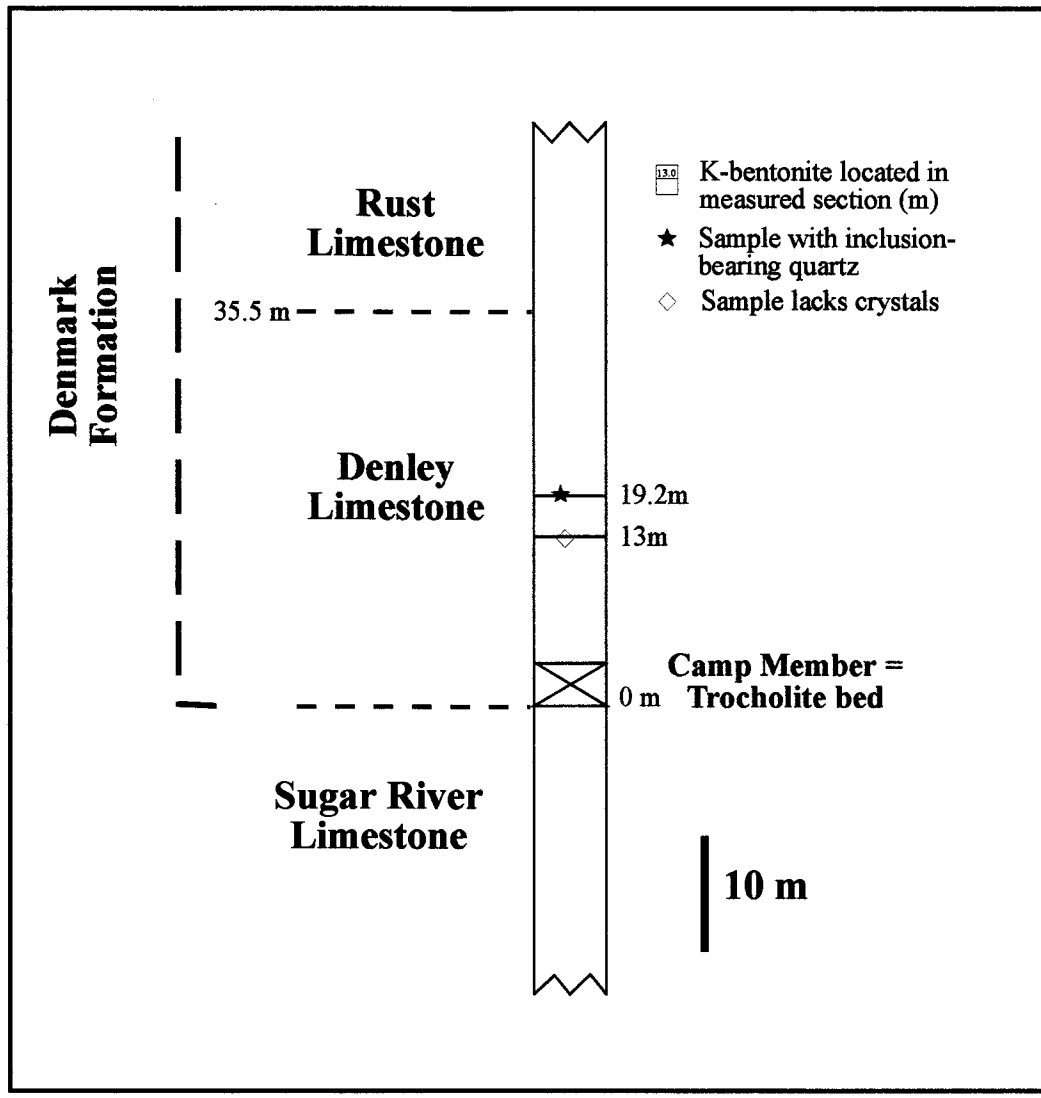

Figure 2.8. Stratigraphic column of the Denmark Formation at Deer River location. Stratigraphic data from J.W. Delano (unpublished).

2.3 Nowadaga Creek and North Creek tributary at Myers Road

Bentonites from Nowadaga Creek and North Creek tributary at Myers Road are shown in Figure 2.1. A detailed sample locality description is given in Mitchell et al. (1994). The bentonite samples were collected by J.W. Delano. Bentonites sampled for this study are Nowadaga 'B0' and Myers Road 'MC2'. Nowadaga 'B0' and Myers Road 'MC2' are also known as the "Manheim" and "Countryman" K-bentonite (Mitchell et al., 1994).

CHAPTER 3 PETROGRAPHY

Melt inclusion-bearing quartz phenocrysts (Figure 3.1.1 & 3.1.2) occur in approximately 40% of the Upper Ordovician Strata from the Mohawk valley. Apatite phenocrysts with glass inclusions (Figure 3.2.1 & 3.2.2) are rare, occurring in ~ 10 % of bentonites. The glass inclusions are of great interest because they represent pristine samples of magmatic liquid from which the host minerals grew. The unstable glass inclusions have been preserved for 450 Ma because they have been sealed within the chemically resistant phases, quartz and apatite. Quartz phenocrysts typically vary from beta-form euhedral to anhedral crystals. Shattered quartz crystals containing glass inclusions are also common. They often contain inclusions of sanidine, plagioclase, apatite, zircon, and sulfide in addition to melt inclusions. These minerals are typical of high silica rhyolites and indicate their presence in the magma at the time of quartz growth. Apatite typically occurs as stubby crystals approximately 110 μm in length, with crystal faces rarely recognizable. Apatite appears bluish in plane-polarized light. Some apatites contain inclusions of other minerals such as oxides, sulfides, quartz, monazite, or feldspar.

Glass inclusions are more abundant in quartz than in apatite phenocrysts, and range from being glassy to completely devitrified. Glass inclusions in quartz range in size from < 10 to 100 μm in diameter, whereas glass inclusions in apatite tend to be slightly smaller, ranging in diameter from 10-50 μm. Most glass inclusions are subrounded to rounded, but some display signs of faceting. Approximately 10 % of the melt inclusions in quartz phenocrysts for this study have an exsolved volatile phase (i.e., bubble), whereas no bubbles have been observed in glass inclusions in apatite phenocrysts. Vapor bubbles in glass inclusions are generally < 10 % of the inclusion volume. Although most of the inclusions in quartz are glassy, many have suffered post-entrapment crystallization (Figure 3.3). They range from being slightly crystalline, appearing speckled, to being completely crystalline, appearing opaque in transmitted light.

Hanson (1995) described the morphology of melt inclusions in quartz phenocrysts within Devonian bentonites. He classified inclusions in four different types. These same types have been

observed in the Ordovician bentonites. Most Ordovician quartz crystals contain type one (inclusions elongated parallel to the C-axis), two (oriented along one of the three crystallographic axes) and three (parallel to edges of triangular crystal faces), but rarely type four (parallel to the triangular crystal faces) has been observed. The crystal on the right in Figure 3.1.1 contains three type four inclusions. Detailed observations and chemical analyses of these types of melt inclusions found in quartz phenocrysts may provide insight into the timing of entrapment or the morphological changes experienced by the melt with time.

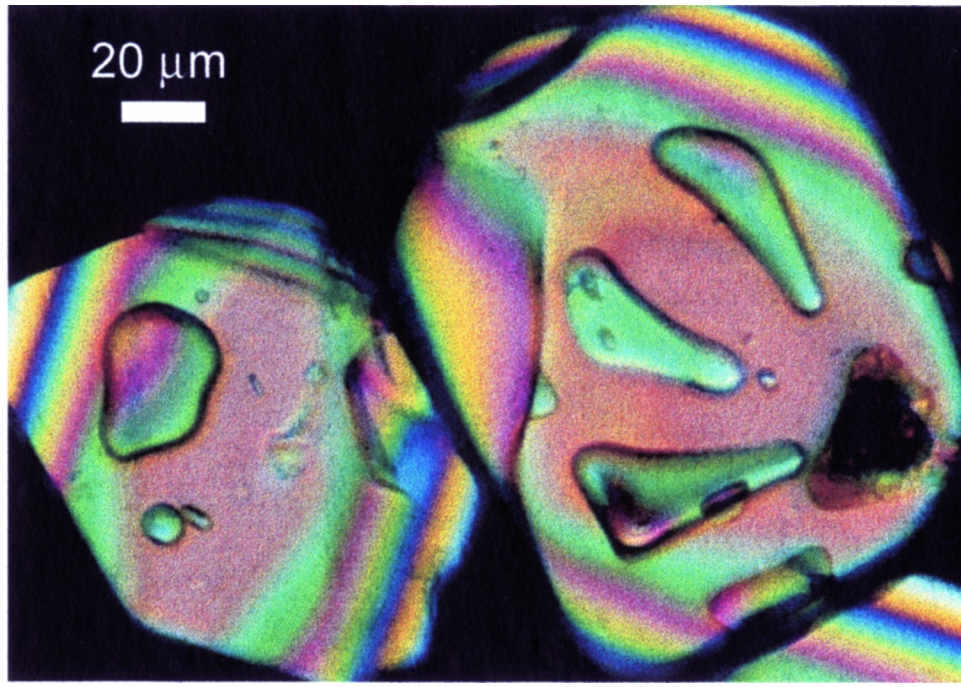

Figure 3.1.1 Photomicrograph of melt inclusions in a quartz phenocryst from Canajoharie @ 84.7.

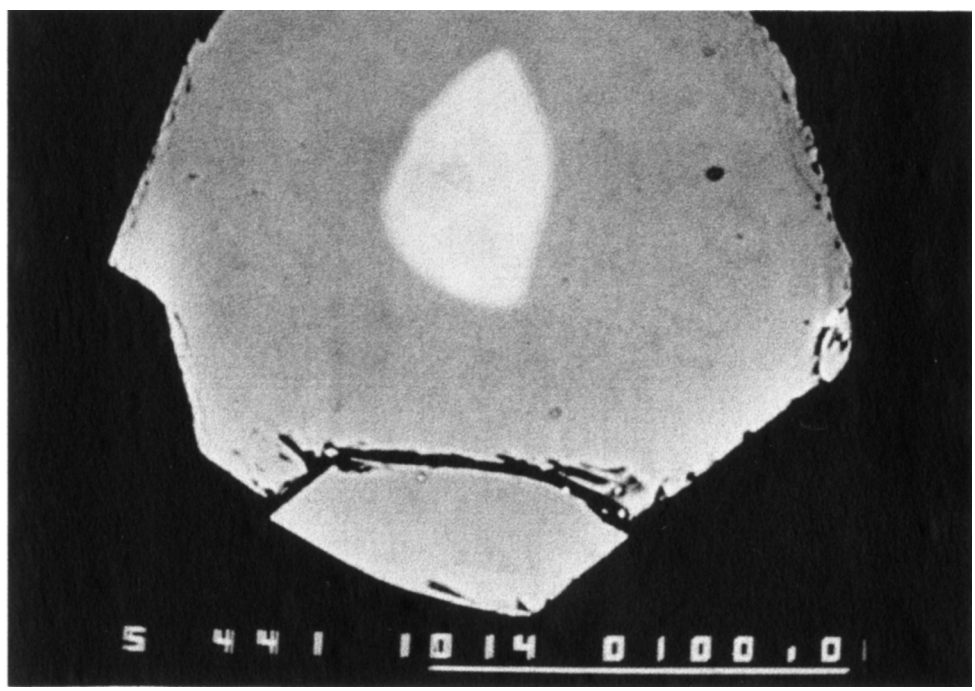

Figure 3.1.2 A backscattered electron image of a melt inclusion in a quartz phenocryst from Flat @ 78.0. The black is epoxy, the gray is quartz and the light gray is the glass inclusion. Note the scale bar in the bottom right is 100 µm.

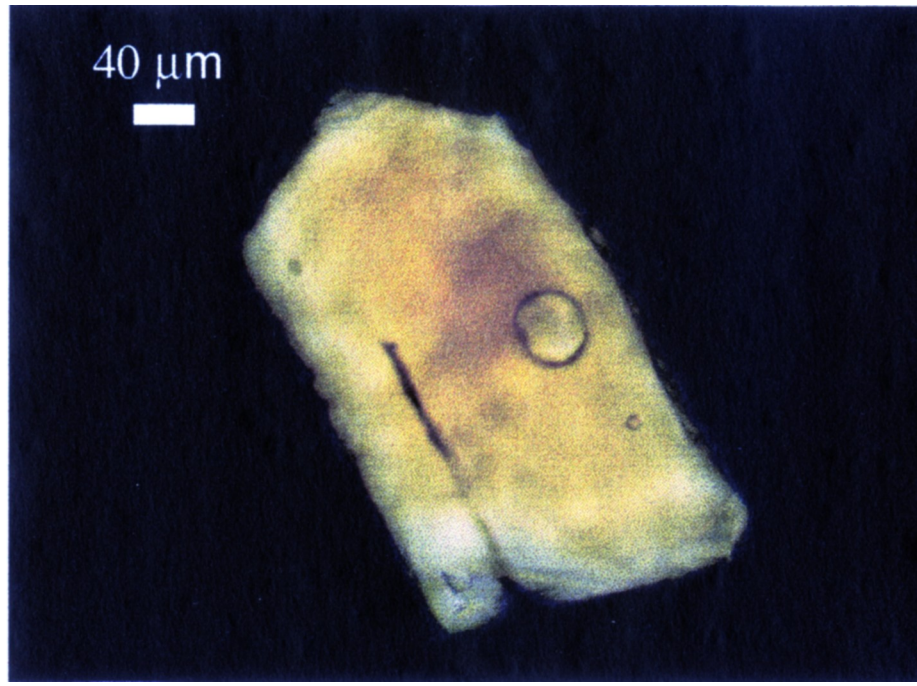

Figure 3.2.1 Photomicrograph of a melt inclusion in an apatite phenocryst from Canajoharie @ 84.7.

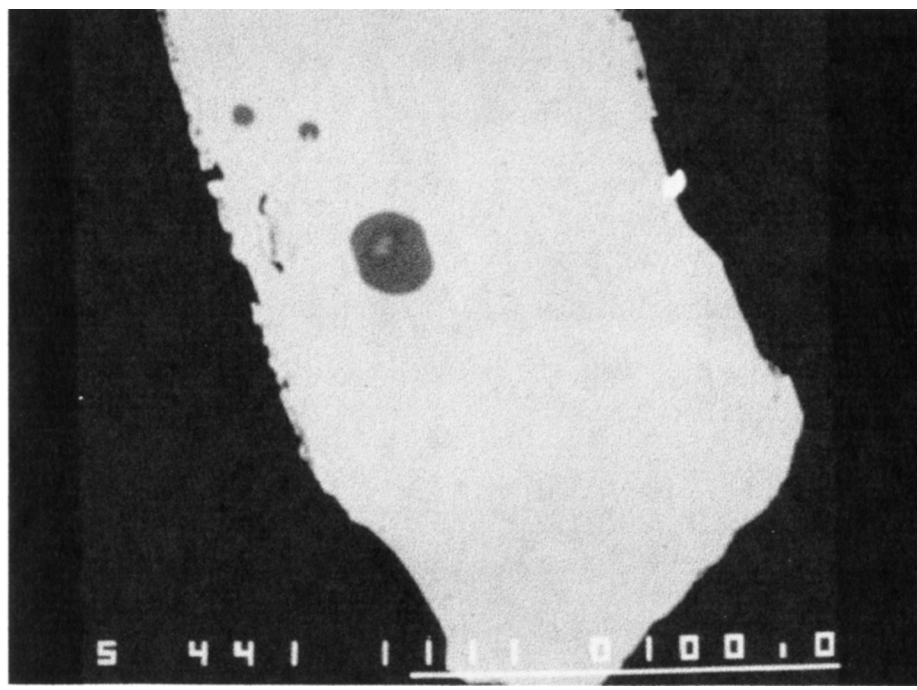

Figure 3.2.2 A backscattered electron image of a melt inclusion in an apatite phenocryst from Canajoharie @ 84.7. The black is epoxy, the gray is apatite and the dark gray is the glass inclusion. Note the scale bar in the bottom right is 100 µm.

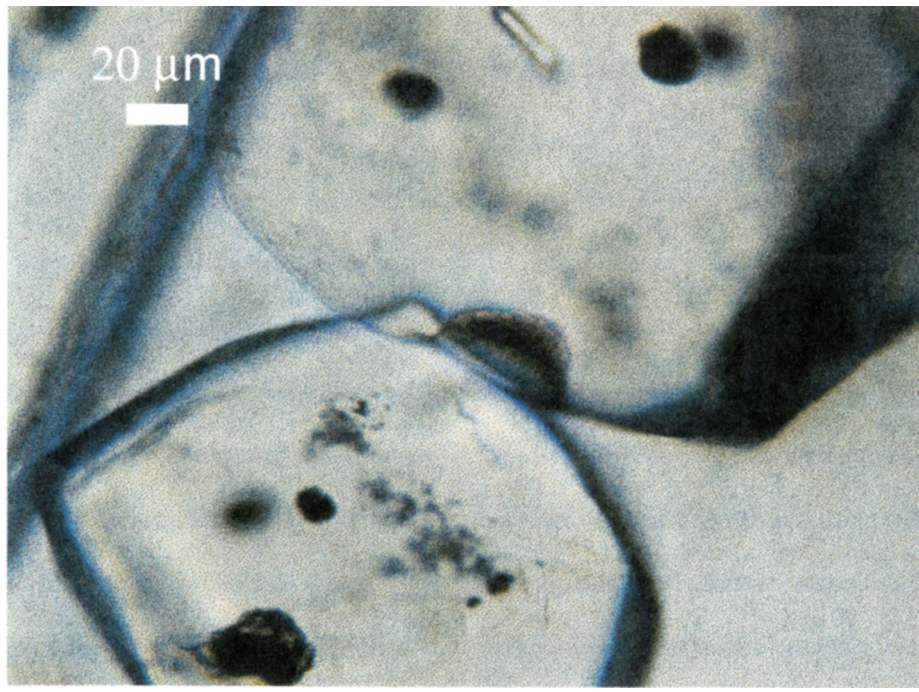

Figure 3.3 Photograph of crystallized melt inclusions in quartz phenocrysts from Canajoharie @ 87.4.

CHAPTER 4 SAMPLE PREPARATION AND ANALYSIS

4.1 Sample Preparation

1-2 kg of bentonite sample was wet sieved, and the size fraction greater than 105 μm was retained. After drying, this fraction was passed through a Frantz Isodynamic magnetic separator to concentrate quartz and apatite crystals. Apatite was separated using bromoform. The light fraction was then treated with concentrated HCl and HNO_3 to remove carbonates, sulfides and clays adhering to the crystals, then resieved. Samples were placed in immersion oil, and hand-picked using tweezers under a binocular microscope. Crystals containing melt inclusions were further inspected at 400x in a petrographic scope. Only melt inclusions with no crystals were individually mounted in epoxy and then ground and polished for electron microprobe analysis. Crystallized inclusions were treated separately as described below.

4.2 Experimental melting of crystallized inclusions

Crystallized melt inclusions were prepared for analysis using the techniques described by Hanson (1995). Quartz crystals containing devitrified inclusions were cleaned in trichloroethylene to remove oil and placed in platinum foil pouches. The pouches were gently closed and then held in an one-atmosphere furnace for 14 days at a temperature of 1075 °C. The experiments were quenched in air by rapid removal from the furnace. The melted inclusions were again immersed in oil and examined under high magnification. Only inclusions containing no visible crystals were prepared for electron microprobe analysis.

4.3 Electron Microprobe Analysis

Electron microprobe analyses were performed at the Rensselaer Polytechnic Institute using a JEOL 733 superprobe. The high-precision electron microprobe technique described by Hanson et al. (1996) was used to analyze major (Al_2O_3, SiO_2, FeO, CaO, Na_2O, K_2O), minor (Cl, TiO_2), and trace-

elements (MgO, MnO). If possible one melt inclusions of at least 12 crystals per bentonite at one site were analyzed. During an analytical session, three groups of five elements were analyzed in separate steps. The first package of elements included Na, K, Al, Si and Fe. At a beam current of 5 - 20 nA, five 20 second analyses were performed on each inclusion to monitor the Na-loss. Na-loss during exposure to the electron beam was corrected for using a technique modified from Nielson and Sigurdsson (1981), which is described in detail in Hanson et al. (1996). After this set of analyzes, the second package of elements (Mg, Ti, Al, Cl, Fe) was analyzed for 180 seconds at a beam current of 45 nA. Under the same analytical conditions the third and final package of elements (Mg, Ca, Al, Mn, Fe) were analyzed. The Al abundances determined from the first set of analyses is used as a normalizing element.

During the experimental heating, the crystallized glass inclusions are diluted by SiO_2 due to melting of the host phenocryst. This results in a proportional decrease in all of the other elemental abundances. This dilution can be corrected for by normalizing all of the data to the Al_2O_3 abundance of the originally entrapped melt. We have no way, however, of determining independently the original Al-content. Hanson et al. (1995 and 1997 in prep.) determined an average of 11.8 wt. % Al_2O_3 in 102 non-crystalline glass inclusions in quartz phenocrysts from 23 different Ordovician and Devonian bentonites. In order to correct for Si-addition all experimental data have been normalized to 11.8 wt.% Al_2O_3. Because all inclusions do not actually contain 11.8 wt. % Al_2O_3, the normalized data is an estimate of the actual abundances and hence the accuracy is not perfect. The total range in Al_2O_3 observed so far is 11.0 to 12.3 wt.% within the average being around 11.8. Inclusions normalized to 11.8 wt.% Al_2O_3 are referred in the text with an asterix (e.g., FeO*).

A set of three working standards was analyzed before every session to monitor the precision and reproducibility of analyses from one analytical session to another. The working standards were hydrous, rhyolitic melt inclusions from separate, unrelated, compositional distinct eruptive events (Hanson et al., 1996). The result of 24 analyses on each of the three working standards (Figure 4.1) not only demonstrates the analytical precision and reproducibility of data, but also the ability to unambiguously distinguish different rhyolitic glass compositions.

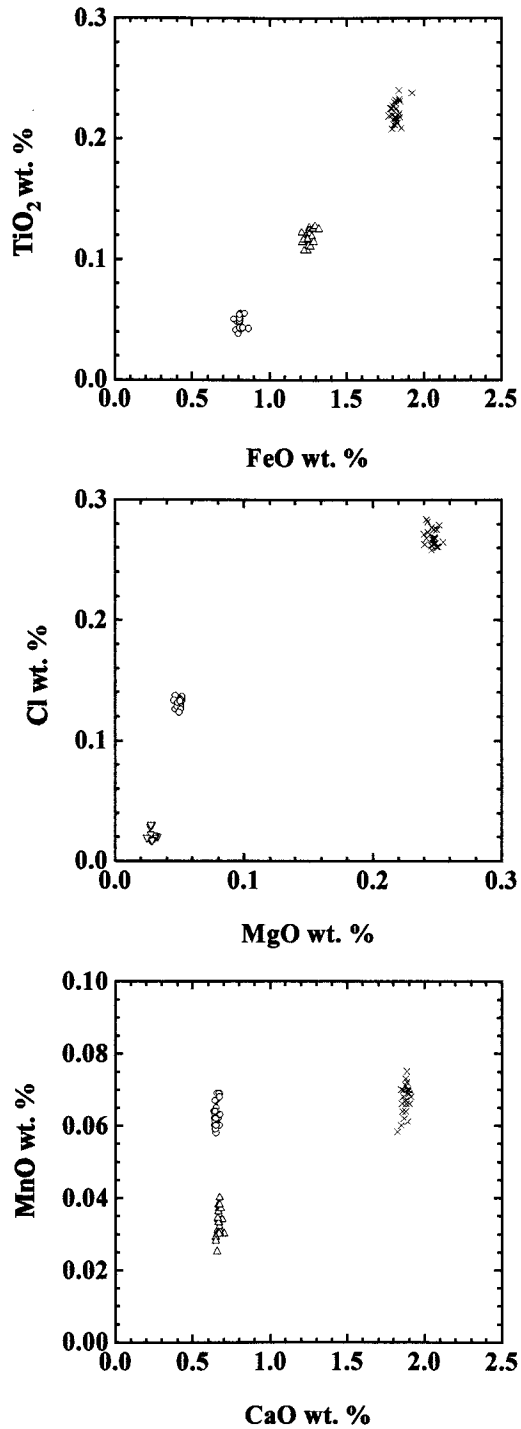

Figure 4.1. Results of 24 replicate analyses of rhyolitic glass inclusions in quartz that were used as working standards during this study. These data were acquired during the collection of element packages #2 and #3 (Hanson et al., 1996) and analyzed once before each analytical session.

CHAPTER 5 STRATIGRAPHIC CORRELATION OF BENTONITES BASED ON MELT INCLUSION COMPOSITION

The bentonites examined in this study were collected from the broad basin sequence of the Trenton Group, exposed in the Mohwak and Black River Valleys of central and north-western New York State. Many long and continuous sections of the Trenton Group are very well exposed between Canajoharie, New York, and Lake Ontario. There are thought to be no unconformities or significant diastems in the Trenton Group, which represents a period of perhaps 8 my of continuous carbonate deposition (Titus, 1989).

Chronostratigraphic horizons in sedimentary sequences can be produced by geological instantaneous events such as explosive volcanic eruptions (Kay, 1935; Huff, 1983; Sarna-Wojcicki et al., 1987). Individual bentonite layers can be confidently identified and distinguished based on the compositions of glass inclusions within their phenocrysts. Although a number of geochemical correlations have already been established in the Mohwak river sections by Delano and coworkers (1994), the stratigraphic goal of this study was to provide very detailed correlations in a smaller, more complicated interval. This particular 30 m interval (Figure 5.1) is of interest because it contains bentonites with melt inclusions of a curious, never-before seen composition. This is described in detail in chapter 6. A further goal of this study was to attempt to correlate this 30 m interval to the bentonites that occur in the platform carbonate sequence that outcrops along the Deer River to the northwest. A correlation between the Mohawk and Black River Valleys is important because there are few biostratigraphic features common to both the black shales of the Utica Formation and the platform carbonates of the Denmark Formation.

5.1 Canajoharie @ 65.5 m - Flat Creek @ 49.5 m

The composition of pristine melt inclusions in quartz phenocrysts from Canajoharie @ 65.5 m (Appendix A.4.1) and Flat Creek @ 49.5 m (Appendix B.3.1) are shown in Figure 5.2 a, b, c, and d. The compositions of these melt inclusions suggest that these two bentonites are equivalent. There appears to

be two, chemically-different groups of inclusions in quartz from this bentonite (Figure 5.4), and they can be best recognized in their TiO_2 and Cl content. Group I is distinguished from group II by a higher concentration in TiO_2, and Cl. The TiO_2 -concentration in Group I is > 0.16 wt. % and Cl-concentration is > 0.12, whereas in Group II, TiO_2 -concentration is < 0.12 wt. % and Cl-concentration is < 0.11. These two groups can be recognized at both Canajoharie @ 65.5 and Flat Creek @ 49.5. Both bentonites are identical in containing these two groups.

Experimentally-melted crystallized inclusions have also been analyzed from both bentonites. These data are shown in Figure 5.3 and in Appendices A.4.2 and B.3.2. Here again the melt compositions are indistinguishable. The composition of both the pristine and experimentally melted inclusions support the chemical equivalencies of these bentonites. The two groups observed among the pristine inclusions are also observed among the crystallized inclusions (Figure 5.4 b). Group I has a higher concentration in Cl and TiO_2 than Group II. Although the majority of pristine melt inclusions belong to group I and the majority of the remelted inclusions to group II, both groups are represented. The chemical signatures of both the crystalline and non-crystalline inclusions strongly suggest that these bentonites represent the same eruption. This correlation is parallel to a correlation previously established between Canajoharie @ 84.7 and Flat Creek @ 70 (see Figure 5.1) by Delano et al. (1994) and therefore this correlation is reasonable.

All bentonites were included in the calculation of a melt inclusion chemistry-based correlation matrix, for which similarity coefficients (= $d_{(A, B)}$) (Borchardt et al., 1972) were calculated for all combination of bentonites. The similarity coefficient is an average of the relative abundances of melt inclusions in two different bentonites. The equation used in this study are based on the equations used by Borchardt et al. (1972). The equation #1 in Borchardt et al. (1972) is a strict comparison of mean abundances for all elements, and therefore blind to any real compositional ranges that are characteristic for the bentonite. Keeping this in mind it is useful under special circumstances (e.g., Canajoharie @65.5 and Deer River @ 19.2) to compare the two groups in Canajoharie @ 65.5 separately (i.e., identify each group separately in the matrix).

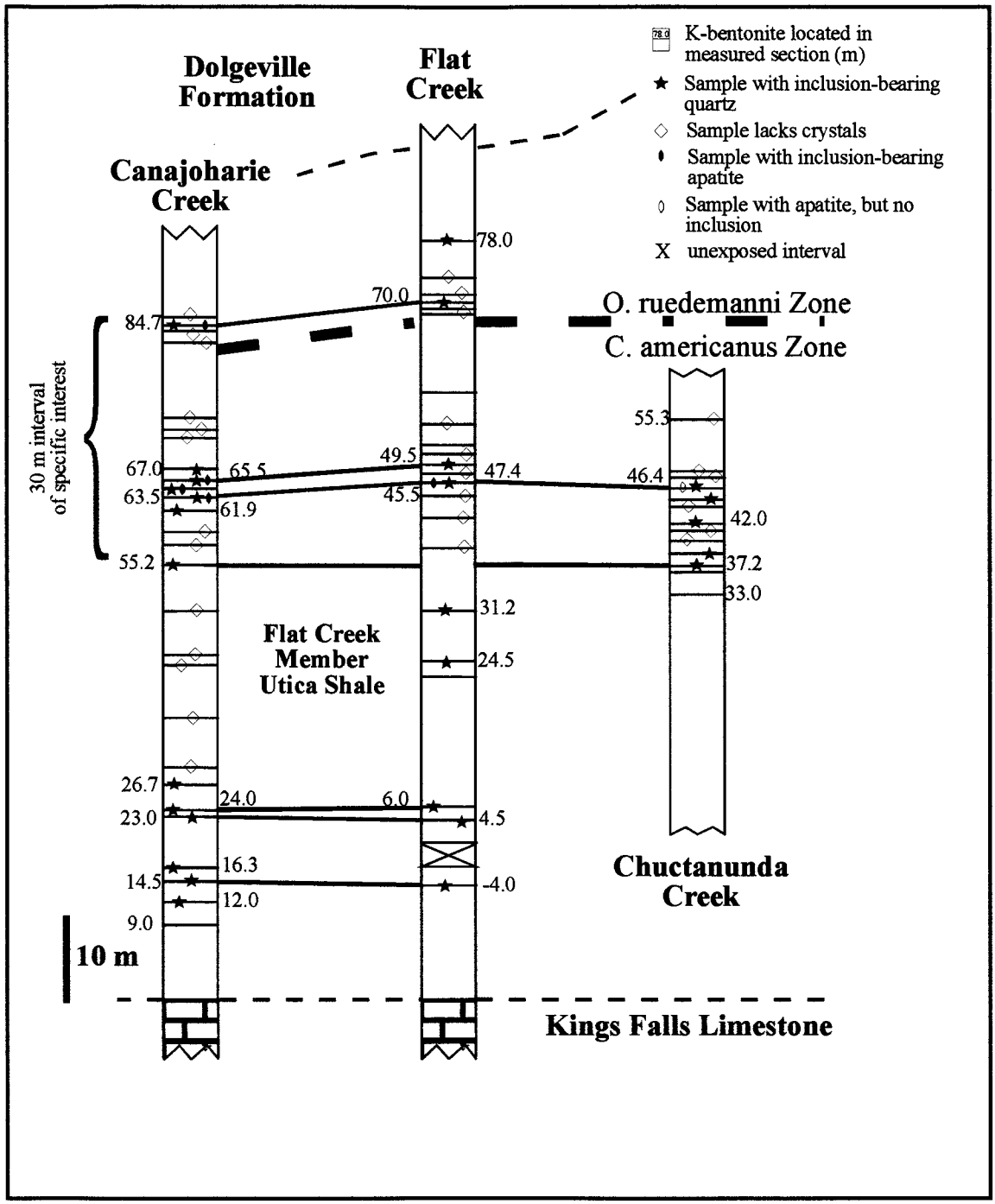

Figure 5.1. Stratigraphic column of the Utica Formation at Canajoharie Creek, Flat Creek, and Chuctanunda Creek. Continuos lines between two sections indicate correlation based on the geochemistry of the melt inclusions. See also Delano et al. (1994) for the first bentonite correlations in this area.

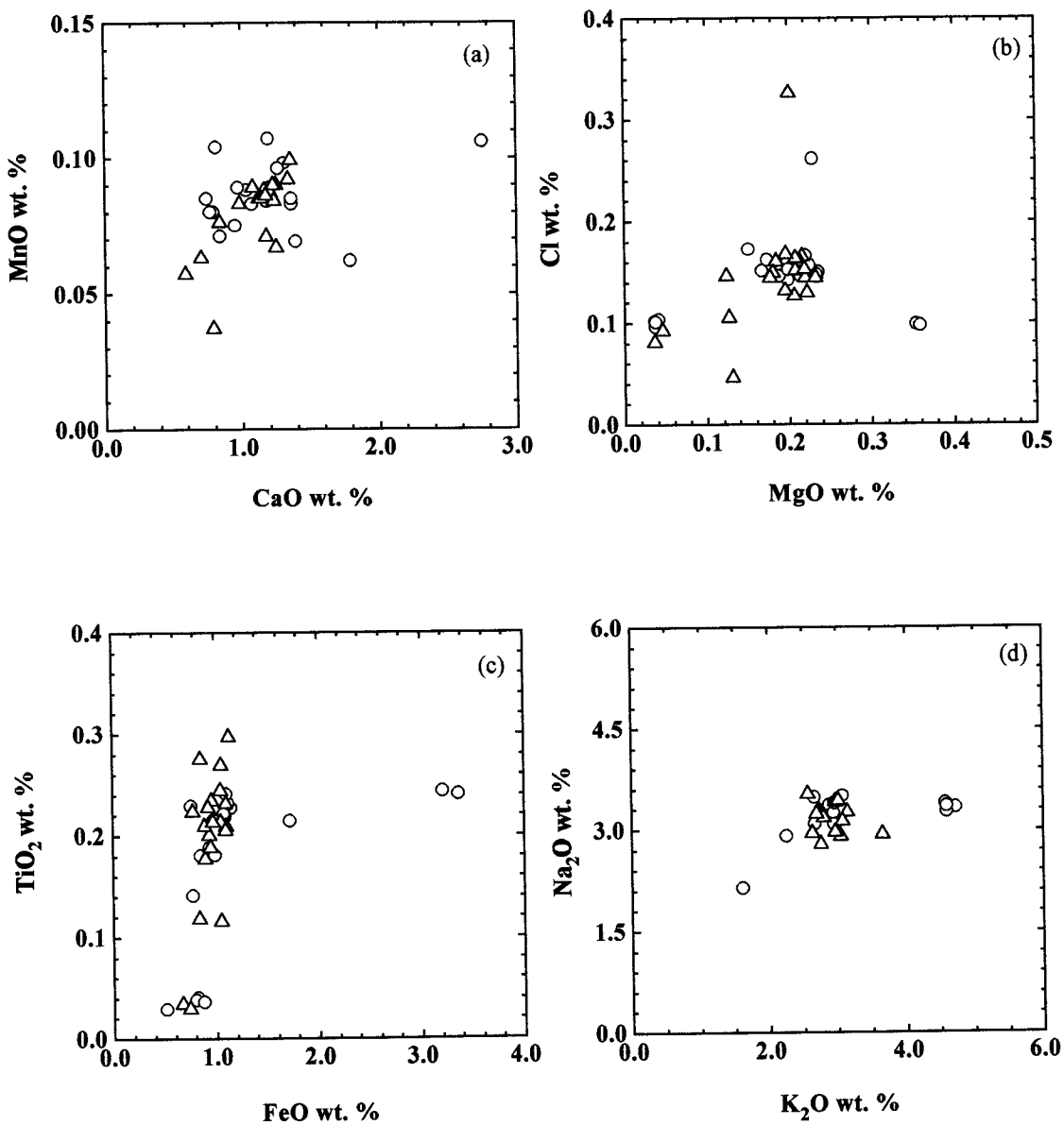

Figure 5.2. Plot of (a) MnO vs. CaO, (b) Cl vs. MgO, (c) TiO_2 vs. FeO, and (d) Na_2O vs. K_2O in glassy melt inclusions in quartz phenocrysts from a bentonite correlated from Canajoharie @ 65.5 m (open circles) to Flat Creek @ 49.5 m (open triangles). Analytical precision as in Figure 4.1.

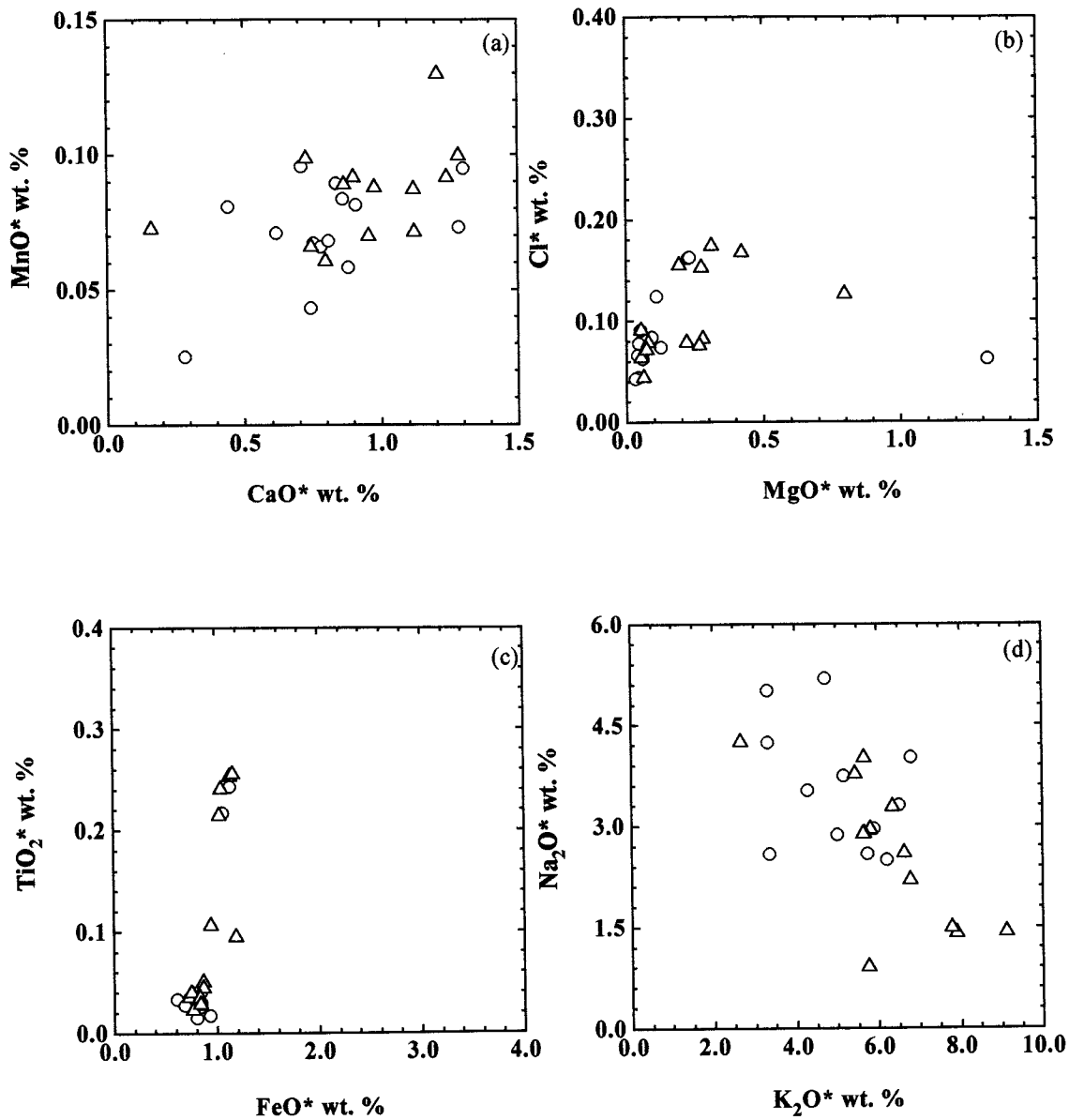

Figure 5.3. Plot of (a) MnO* vs. CaO*, (b) Cl* vs. MgO*, (c) TiO_2* vs. FeO*, and (d) Na_2O* vs. K_2O* in glassy melt inclusions in quartz phenocrysts from a bentonite correlated from Canajoharie @ 65.5 m (open circles) to Flat Creek @ 49.5 m (open triangles). All of these melt inclusions were crystallized and were experimentally melted in a one-atmosphere furnace. Analytical precision as in Figure 4.1.

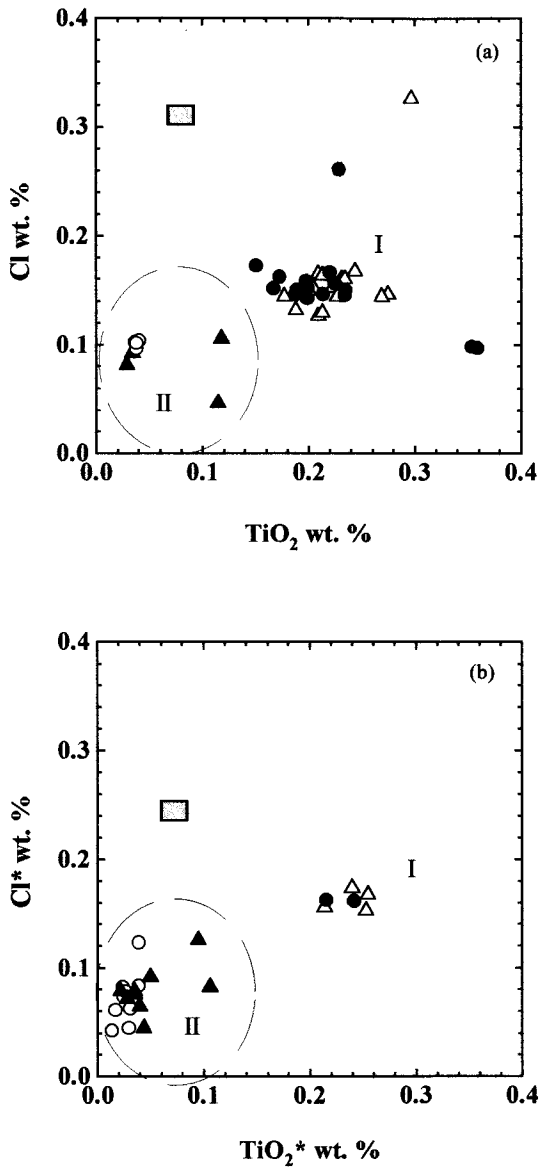

Figure 5.4. Plot of (a) TiO_2 vs. Cl in glassy melt inclusions in quartz phenocrysts from Canajoharie @ 65.5 m (circles) to Flat Creek @ 49.5 m (upwards triangles). Plot of (b) TiO_2* vs. Cl* from experimentally melted bentonite from Canajoharie @ 65.5 m (circles) to Flat Creek @ 49.5 m (upwards triangles). The shaded box shows the analytical precision.

For those bentonites that show a continuos range (trend rather then individual groups), one needs to use the standard deviation for comparing the "similarity of trends" among different bentonites. Borchardt et al. (1972) used typically one bulk analysis for each bentonite to establish their comparison, whereas this study has a much richer data-set. The parameter "gi" of Borchardt et al. (1972) is not of any help in this study either for several reasons (e.g., analytical uncertainty is the least of the problems in this study, but was the greatest concern to Borchardt et al. (1972)). As well the coefficient of '0.33' in the denominator is irrelevant, since it was merely defined by Borchardt et al. (1972) as being the maximum analytical error (i.e., 33 %) that would be permitted into the elements used for their similarity coefficient. Therefore, a small variation on Equation #1 of Borchardt et al. (1972) is suggested in order use a similarity coefficient in this study. The following equation gives equal weighting to (a) comparison of means and to (b) comparison of standard deviations (Delano, 1997 pers. communication).

$$d_{(A,B)} = \frac{\sum_{i=1}^{n} (M_i + D_i)}{2n} \quad \text{, for 'n' elements}$$

$$\text{where } M_i = \frac{X_{iA}}{X_{iB}} \quad \text{, where } X_{iB} > X_{iA} \text{ (i.e., } M_i < 1) \text{ for '} X_i \text{' = mean abundances of i}$$

$$\text{or} \quad \frac{X_{iB}}{X_{iA}} \quad \text{, where } X_{iA} > X_{iB} \text{ (i.e., } M_i < 1)$$

$$\text{where } D_i = \frac{\sigma_{iA}}{\sigma_{iB}} \quad \text{, where } \sigma_{iB} > \sigma_{iA} \text{ (i.e., } D_i < 1) \text{ for '} \sigma_i \text{' = standard deviation of element i}$$

$$\text{or} \quad \frac{\sigma_{iB}}{\sigma_{iA}} \quad \text{, where } \sigma_{iA} > \sigma_{iB} \text{ (i.e., } D_i < 1)$$

Since each element 'i' has two parameters being used in which a perfect correlation will have ($M_i + D_i$) for each element equaling 2, the dominator becomes '2n'.

The first criterion is given by the standard deviation of the working standards (see chapter 4) in this study: $TiO_2 = 0.01$, $FeO = 0.035$, $MnO = 0.007$, $MgO = 0.006$, $CaO = 0.03$, $K_2O = 0.04$, $Na_2O = 0.2$ and $Cl = 0.008$. If standard deviation of one bentonite is greater than the given criterion then the above equation has been used for determine the similarity coefficient. If the standard deviation is less than the given criterion then

$d_{(A, B)} = \Sigma Mi/n$ (= Equation #1 of Borchardt et al. (1972)) has been used.

Finally, Table 1 - 3 are the results of this data compilation for analyses from pristine melt inclusions in quartz and apatite phenocrysts and from experimentally remelted inclusions in quartz phenocrysts. Bentonites believed to be correlated yield similarity coefficients greater than 0.750. Therefore, the $d_{(A, B)}$ criterion suggesting correlation is ≥ 0.750. Hence, Canajoharie Creek @ 65.5 (I), Flat Creek @ 49.5 (I) are not only correlated visually by comparing the chemistry in diagrams (Figure 5.2), but as well by their similarity coefficient (= 0.845 in Table 1). The same is applied to Canajoharie Creek @ 61.9, Flat Creek @ 47.4 and Chuctanunda Creek @ 46.4.

Difficulties for defining $d_{(A, B)}$ appear with the similarity coefficient of experimentally remelted inclusions (Table 2). Correlations defined by the similarity coefficient in pristine melt inclusions (indicated with '*' in Table 2) cannot be positively identified with the similarity coefficient of experimentally remelted inclusions. At this stage of the study no explanation is available for this occurrence and therefore the similarity coefficient for experimentally remelted inclusions in quartz phenocrysts is not a criterion to determine a stratigraphic correlation.

Table I **Similarity coefficients ($d_{(A,B)}$) for pristine melt inclusions in quartz phenocrysts (see text for detailed explanation)**

Bentonite Sample	Can@61.9	Can@63.5	Can@65.5 (I)	Can@65.5 (II)	Can@67.0 (I)	Can@67.0 (II)	Can@84.7
Can@61.9	1						
Can@63.5	0.604	1					
Can@65.5 (I)	0.656	0.628	1				
Can@65.5 (II)	0.453	0.711	0.548	1			
Can@67.0 (I)	0.625	0.476	0.645	0.495	1		
Can@67.0 (II)	0.550	0.683	0.551	0.678	0.508	1	
Can@84.7	0.509	0.470	0.641	0.500	0.791	0.500	1
Flat@31.2	0.635	0.590	0.576	0.402	0.599	0.533	0.450
Flat@47.4	0.595	0.791$	0.620	0.667	0.497	0.621	0.425
Flat@49.5 (I)	0.627	0.695	0.845	0.565	0.647	0.499	0.642
Chuc@42.0	0.697	0.567	0.679	0.426	0.730	0.494	0.606
Chuc@46.4	0.660	0.764	0.566	0.649	0.456	0.664	0.411
Deer River @19.2	0.512	0.693	0.583	0.842	0.477	0.722	0.443

Can = Canajoharie Creek
Flat = Flat Creek
Chuc = Chuctanunda Creek
(I) = group I and (II) = group II

$ $d_{(A,B)}$ criterion suggesting correlation > 0.75

Table I **Similarity coefficients ($d_{(A,B)}$) for pristine melt inclusions in quartz phenocrysts (continued)**

	Flat@31.2	Flat@47.4	Flat@49.5 (I)	Chuc@42.0	Chuc@46.4	Deer River @19.2
Flat@31.2	1					
Flat@47.4	0.569	1				
Flat@49.5 (I)	0.522	0.645	1			
Chuc@42.0	0.622	0.557	0.626	1		
Chuc@46.4	0.612	0.810	0.578	0.571	1	
Deer River @19.2	0.397	0.640	0.551	0.488	0.577	1

Table II **Similarity coefficients ($d_{(A,B)}$) for experimentally remelted inclusions in quartz phenocrysts**

Bentonite Sample	Can@63.5	Can@65.5 (I)	Can@65.5 (II)	Flat@47.4	Flat@49.5 (I)	Flat@49.5 (II)	Chuc@46.4	Deer River @19.2
Can@63.5	1							
Can@65.5 (I)	0.563	1						
Can@65.5 (II)	0.686	0.541	1					
Flat@47.4	0.710*	0.582	0.755	1				
Flat@49.5 (I)	0.635	0.794*	0.601	0.573	1			
Flat@49.5 (II)	0.686	0.621	0.706	0.718	0.632	1		
Chuc@46.4	0.657*	0.644	0.779	0.739*	0.548	0.603	1	
Deer River @19.2	0.717	0.609	0.701*	0.707	0.635	0.779	0.658	1

Can = Canajoharie Creek
Flat = Flat Creek
Chuc = Chuctanunda Creek
(I) = group I and (II) = group II

* correlation established in Table 1

Table III **Similarity coefficients ($d_{(A,B)}$) for melt inclusions in apatite phenocrysts**

Bentonite Sample	MC2	B0
MC2	1	
B0	0.723	1

MC2 = Myers Road 'MC 2'
B0 = Nowadaga 'B0'

5.2 Canajoharie @ 63.5 m, Flat Creek @ 47.4 m and Chuctanunda @ 46.4 m

The composition of pristine and experimentally melted inclusions in quartz phenocrysts from Canajoharie @ 63.5 (Appendix A.3.1), Flat Creek @ 47.4 (Appendix B.2.1) and Chuctanunda @ 46.4 (Appendix C.1.1) are shown in Figure 5.5 and Figure 5.6 a, b, c, and d.

Although the inclusions from these three bentonites are generally very similar in their chemical composition, there are subtle chemical differences. Chuctanunda @ 46.4 can be distinguished from Canajoharie @ 63.5 and Flat Creek @ 47.4 by the TiO_2 and FeO abundances among the melt inclusions (Figure 5.5. c). Chuctanunda has a low and a high TiO_2 group (~ 0.8 wt.% and ~ 1.5 wt.%) and FeO group (up to 0.8 wt.% and ~ 1.4 wt.%), whereas the data from Canajoharie and Flat Creek lie between these two groups. The similarity coefficient (Table 1) for these bentonites on the other hand suggests that these layers are correlation. Here, the strongest correlation is indicated between Flat Creek @ 47.4 and Chuctanunda @ 46.4 with a similarity coefficient of 0.810.

Although the pristine inclusions from Canajoharie and Flat Creek appear similar, the crystallized inclusions are chemically-different. The melted inclusions from the Canajoharie bentonite display a wider range in MgO* than the bentonite in Flat Creek or at Chuctanunda. The difference among all three bentonites is best identified in their Na_2O* and K_2O* compositions (Figure 5.6. d). The Alkalis clearly demonstrate the difference between these three bentonites.

Schirnick (1990) correlated Canajoharie @ 63.5 with Flat Creek @ 47.4 bentonite based on melt inclusion composition and zircon morphology. Because Canajoharie @ 63.5 and Flat Creek @ 47.4 are both two meters below the correlated bentonite described in chapter 5.1, it might be expected that these bentonites are equivalent, but the compositions of the melt inclusions of these two layers in this study contradict this conclusion. This contradiction highlights the need for extreme caution in assuming bentonite correlations using relative stratigraphic positions.

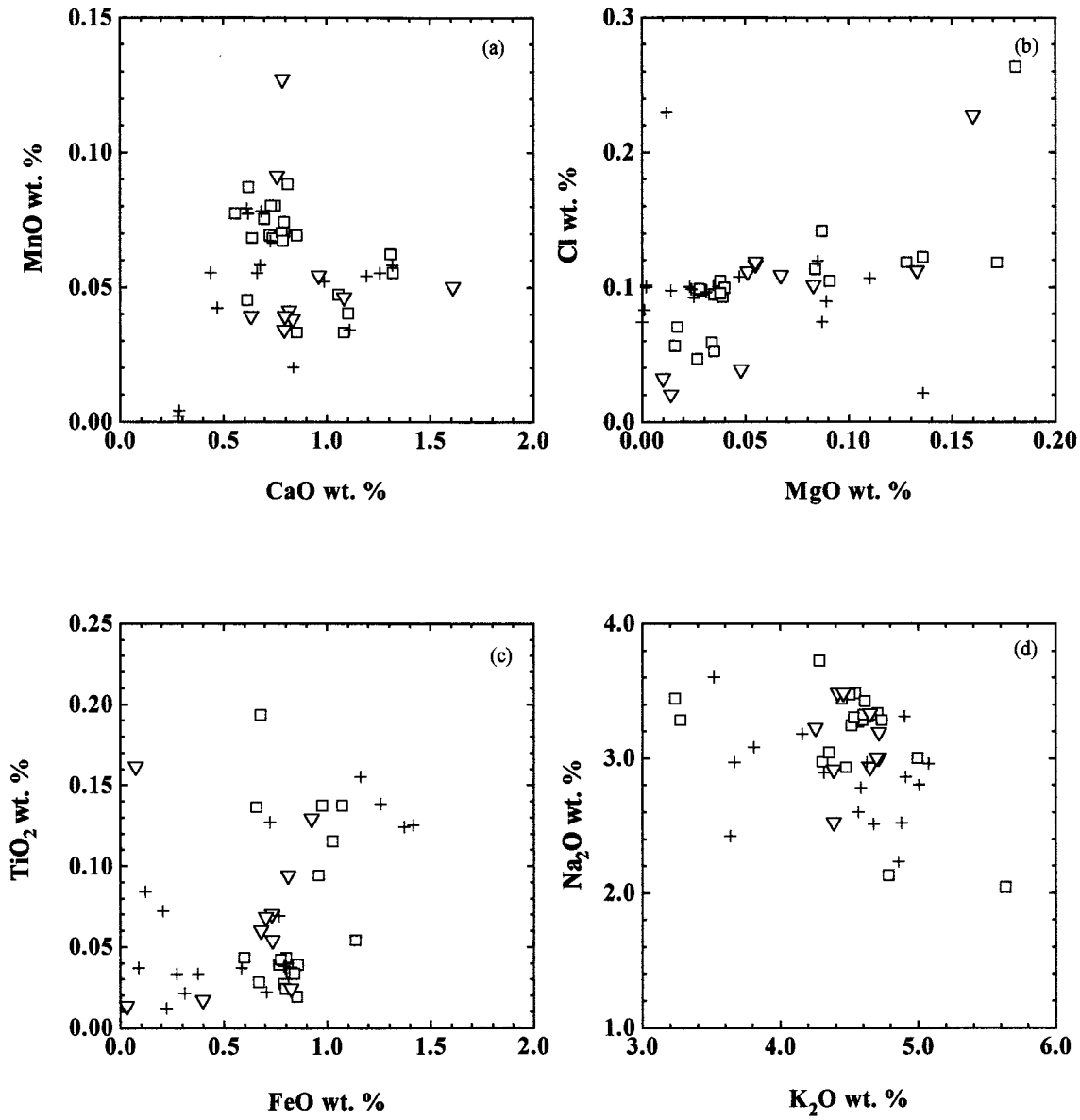

Figure 5.5. Plot of (a) MnO vs. CaO, (b) Cl vs. MgO, (c) TiO_2 vs. FeO, and (d) Na_2O vs. K_2O in melt inclusions in quartz phenocrysts from bentonites at Canajoharie @ 63.5 m (open squares) to Flat Creek @ 47.4 m (open down triangles) and Chuctanunda @ 46.4 m (crosses). Analytical precision as in Figure 4.1.

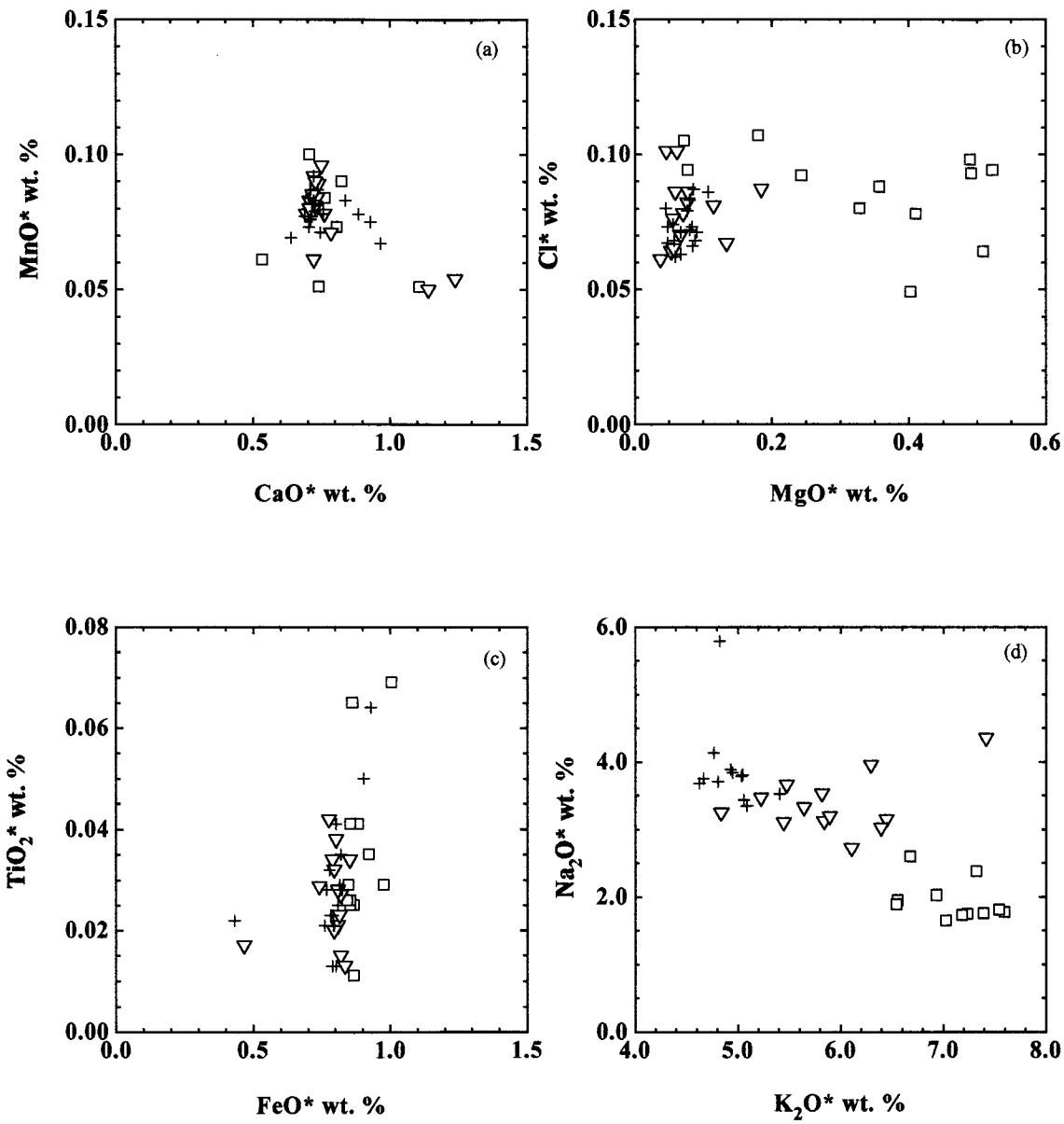

Figure 5.6. Plot of (a) MnO* vs. CaO*, (b) Cl* vs. MgO*, (c) TiO_2* vs. FeO*, and (d) Na_2O* vs. K_2O* in melt inclusions in quartz phenocrysts from bentonites at Canajoharie @ 63.5 m (open squares) to Flat Creek @ 47.4 m (open down triangles) and Chuctanunda @ 46.4 m (crosses). All of these melt inclusions were crystallized and were remelted in a one-atmosphere furnace. Analytical precision as in Figure 4.1.

5.3 "Test for chemical variability within Flat Creek @ 47.4"

Flat Creek @ 47.4 m was sampled at various locations along a 45 meter transect of the outcrop (Figure 5.7) to search for petrographic differences or differences in the composition of inclusions in the same layer. Melt inclusions in quartz from two of the five samples have been analyzed (Appendices B.2.2 and B.2.3) and compared to previous data. These two were chosen because they appeared to be petrographically different from the other samples and from the previously-collected samples of this bentonite. These samples contained smaller phenocrysts (200 μm vs. 500 μm), are richer in quartz phenocrysts, and had generally more inclusions (both pristine and crystallized) than the other three samples. The compositions of these inclusions, however, showed no obvious differences (Figure 5.8). Data points lying outside the group contained bubbles and are therefore chemically different from the ones with no bubbles (bubbled inclusions will be discussed in chapter 6.3). It seems, that the bentonites are "well mixed" at the km-scale and the cm-scale.

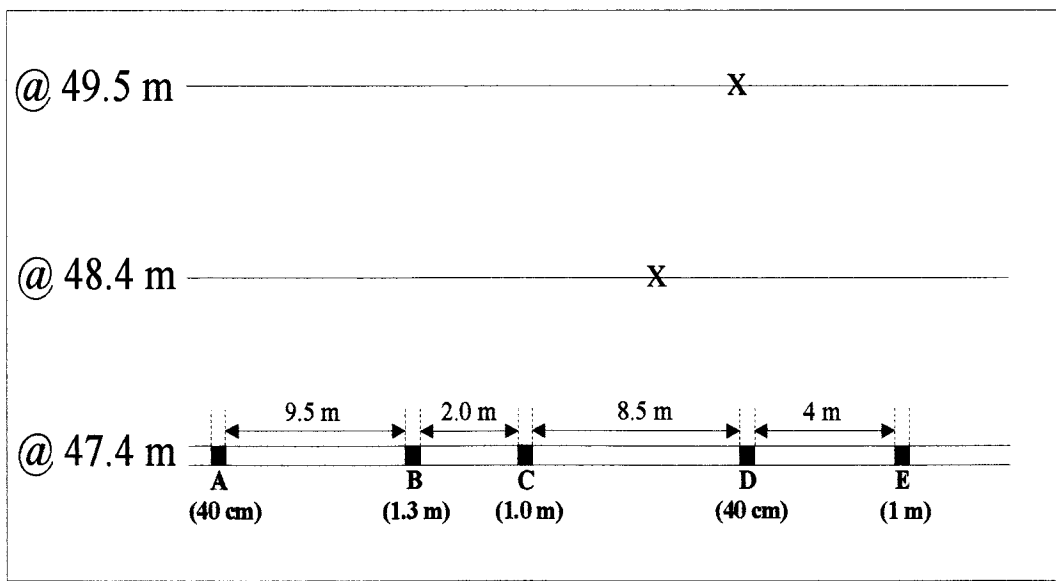

Figure 5.7. Locations (letters) and widths (number in parenthesis) of Flat Creek @ 47.4 m along the outcrop (see Figure 2.5.1). Sample side "A" was 40 cm wide and was located 9.5 meters to the west of sample "B". X's represent locations of samples from the bentonites above Flat Creek @ 47.4.

5.4 Canajoharie @ 61.9 m and Chuctanunda @ 42.0 m

The composition of pristine melted inclusions in quartz phenocrysts from Canajoharie @ 61.9 (Appendix A.2) and Chuctanunda @ 46.4 (Appendix C.2) are shown in Figure 5.9 a, b, c, and d. The chemical composition of the inclusions from these two bentonites is very similar. It is most likely that these melt inclusions compositions are the same, but more data from Chuctanunda @ 42.0 are needed in order to make a firm conclusion.

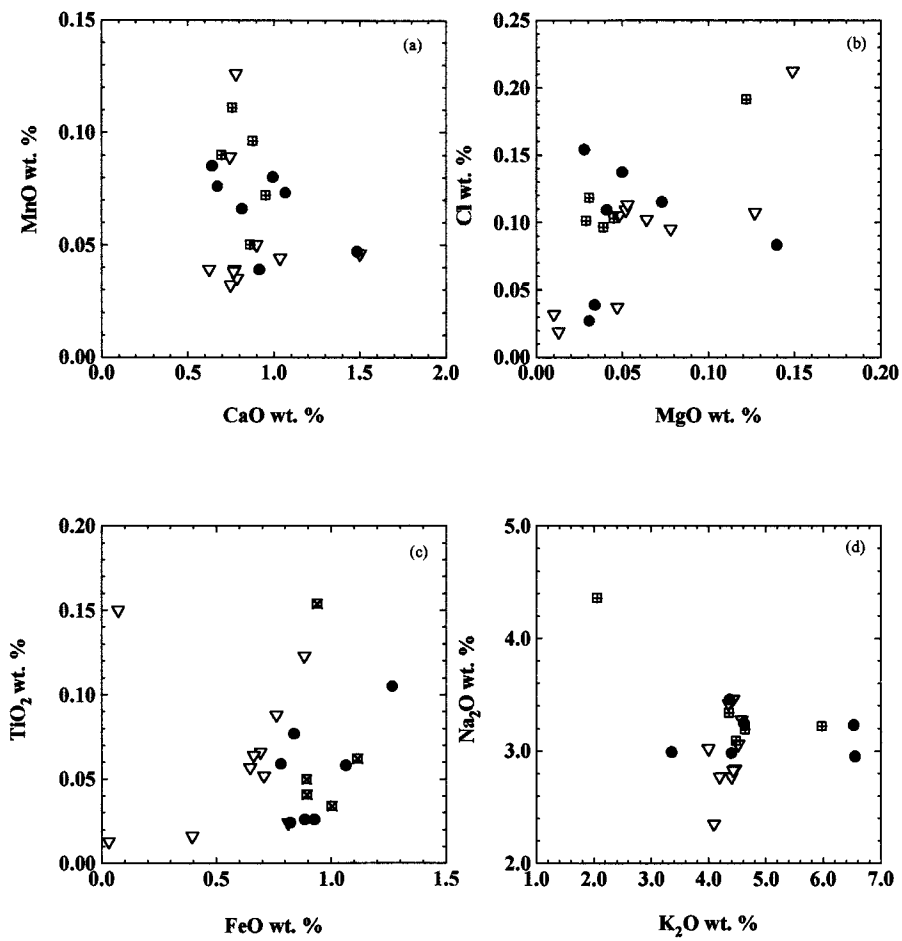

Figure 5.8. Plot of (a) MnO vs. CaO, (b) Cl vs. MgO, (c) TiO_2 vs. FeO, and (d) Na_2O vs. K_2O in glassy melt inclusions in quartz phenocrysts from bentonites at Flat Creek @ 47.4 m (open down triangles), Flat Creek @ 47.4 m 'C' (squares with a cross in the center) and Flat Creek @ 47.4 m 'E' (filled circles). Analytical precision as in Figure 4.1.

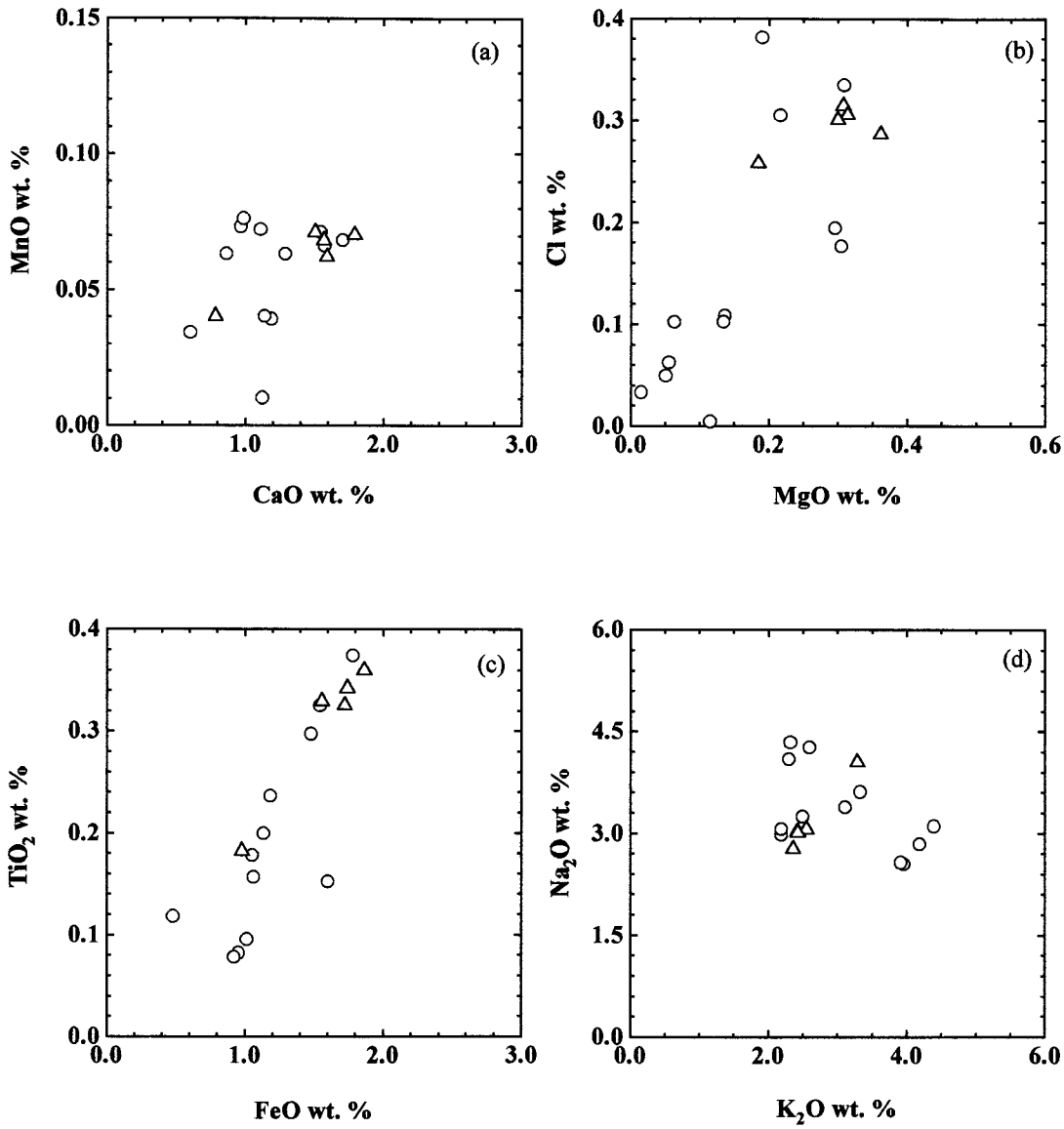

Figure 5.9. Plot of (a) MnO vs. CaO, (b) Cl vs. MgO, (c) TiO_2 vs. FeO, and (d) Na_2O vs. K_2O in glassy melt inclusions in quartz phenocrysts from bentonites at Canajoharie @ 61.9 m (open circles) and Chuctanunda @ 42.0 m (open triangles). Analytical precision as in Figure 4.1.

5.5 Deer River @ 19.2 and Canajoharie @ 65. 5 m

The Trentonian paleontology and stratigraphy have been the subject of detailed studies by Titus (1989, 1992). Titus studied variations in the trimeric columnals (one of the plates that form the stems of crinoids) of the crinoid genus *Ectenocrinus* through a sequence of nearly 100 m of the lower, middle, and upper Trenton Limestone. These columnals display both temporal and spatial patterns of variation. Titus (1989) pointed out that, the biostratigraphy is only of value if the outcrops have been correctly correlated. One of the first investigators who attempted to correlate between outcrops in this region was Kay (1937), who used biostratigraphic constraints and bentonite patterns to argue that the Denley Limestone is a time-stratigraphic unit (Kay, 1953). Chenoweth (1952) extended these correlations from the Black River Valley into the Mohawk River Valley on the basis of faunal assemblages and bentonite patterns. Later Delano et al. (1994) and Mitchell et al. (1994) established a stratigraphic framework for the Taconic foredeep based on the compositions of glasses preserved in quartz phenocrysts within bentonites and on graptolite biostratigraphic units. Outcrops in the Utica Shale in the Mohwak Valley have become the standard graptolite biostratigraphy for the upper Middle Ordovician of Eastern and midcontinental North America (Goldman et al., 1994). Graptolites are rare or absent in the Trenton Group, but bentonites are relatively numerous. Stratigraphically separate bentonite beds can be readily distinguished and correlated between geographically separate localities. By precise correlation of bentonites using glass composition, Delano et al. (1994) and Mitchell et al. (1994) have been able to compare these two correlation techniques. Additional bentonites have been sampled between the Mohawk River Valley and the Deer River Valley in order to add detail to this stratigraphic framework.

Only two bentonites have been found at the Deer River locality and only one of these contains quartz phenocrysts with melt inclusions. The compositions of melt inclusions from this bentonite (Deer River @ 19.2) are displayed in Appendix D.1.1 and D.1.2. The compositions of these inclusions are most similar to those from Canajoharie @ 65.5 (Figure 5.10 a, b, c, d and Figure 5.11 a, b, c, d). As previously mentioned (see 5.1) two chemical groups can be discerned within the pristine melt inclusions at Canajoharie @ 65.5. The Deer River inclusions appear to be chemically identical to the group II

inclusions from Canajoharie @ 65.5. This is as well confirmed by the similarity coefficient in Table 1 (0.842). No inclusions from Deer River @ 19.2, however, belong to group I from Canajoharie @ 65.5. The compositions of remelted inclusions from those two bentonites are also quite similar. The only element within the remelted inclusions that distinguishes the two bentonites is MgO. The Deer River bentonite shows a greater variation in MgO* (~ 0.08 - 1.4 wt. %) than the Canajoharie bentonite (mostly ~ 0.03 - 0.2 wt. %; see also Figure 5.11. b). On the basis of these data, no definite correlation can be made, even though the compositions are strikingly similar.

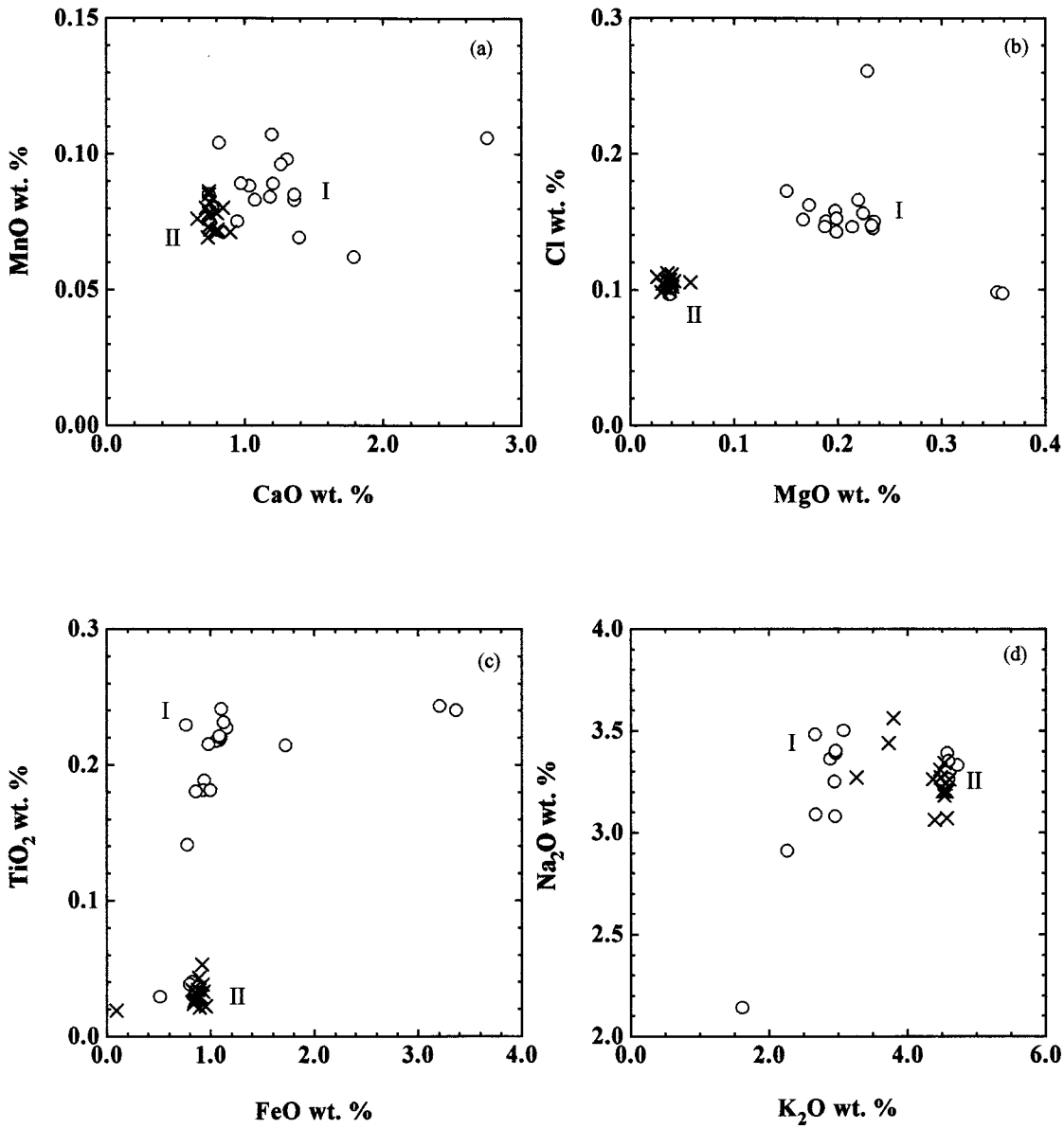

Figure 5.10. Plot of (a) MnO vs. CaO, (b) Cl vs. MgO, (c) TiO_2 vs. FeO, and (d) Na_2O vs. K_2O in glassy melt inclusions in quartz phenocrysts from the bentonites at Canajoharie @ 65.5 m (open circles) and Deer River @ 19.2 m (crosses). Analytical precision as in Figure 4.1.

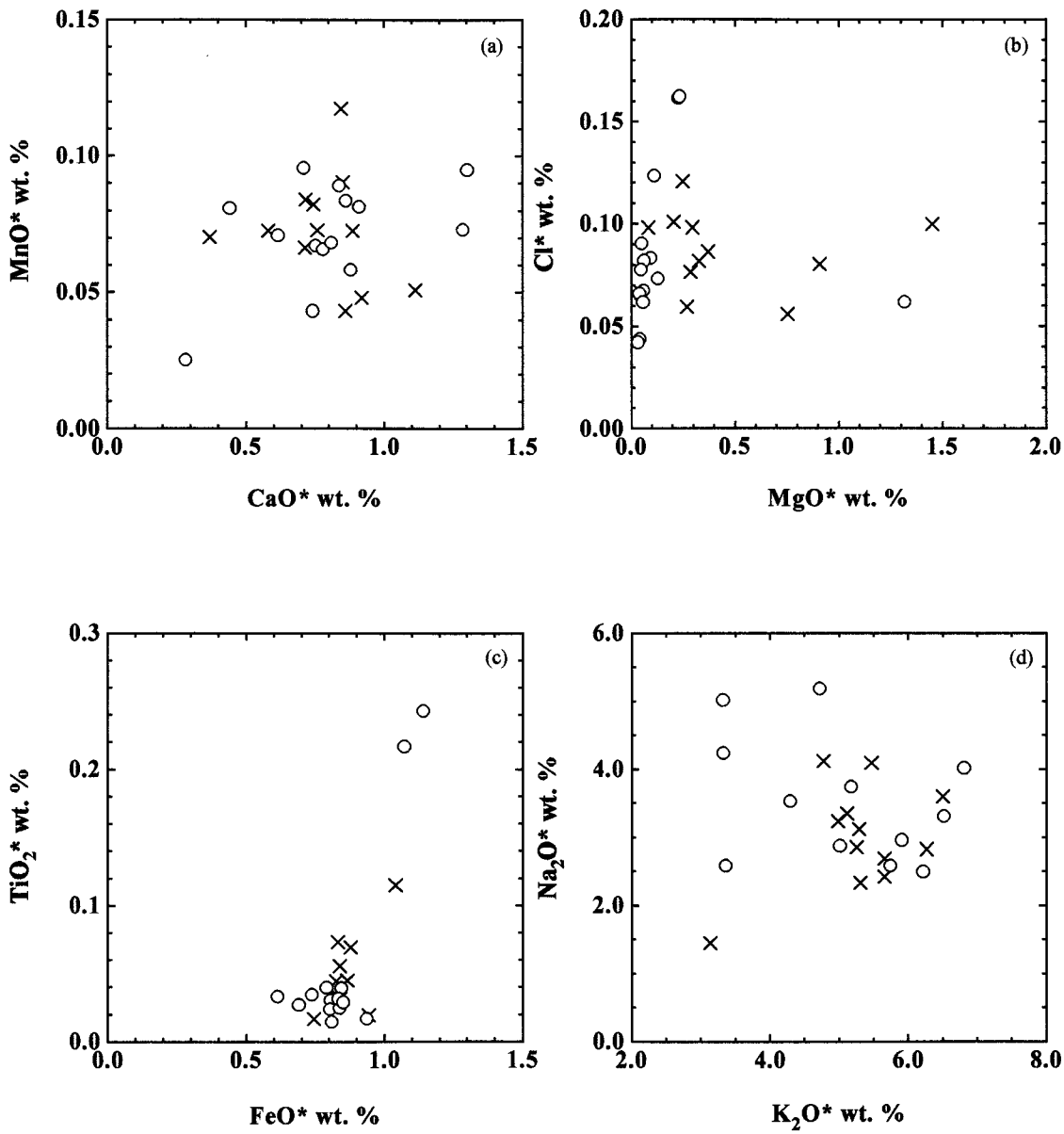

Figure 5.11. Plot of (a) MnO* vs. CaO*, (b) Cl* vs. MgO*, (c) TiO_2* vs. FeO*, and (d) Na_2O* vs. K_2O* in melt inclusions in quartz phenocrysts from the bentonites at Canajoharie @ 65.5 m (open circles) and Deer River @ 19.2 m (crosses). All of these melt inclusions were crystallized and were experimentally melted in a one-atmosphere furnace. Analytical precision as in Figure 4.1.

5.6 Nowadaga 'B0' (Manheim) and Myers Road 'MC2' (Countryman)

The chemical compositions of melt inclusions in apatite phenocrysts, as well those in quartz can be used for correlating K-bentonites. In Figure 5.12 a, b, c, d (Appendix E.1 and E.2) data of melt inclusions in apatite phenocrysts from Nowadaga 'B0' and Myers Road 'MC2' are shown. Previous work (analysis on pristine melt inclusion in quartz phenocrysts - Mitchell et al., 1994; apatite analysis - Samson et al., 1995) has shown that Myers Road 'MC2' is similar to, but distinct from, Nowadaga 'B0'. Figure 5.12 a, b and c show their similarity, but in Figure 5.12 d the difference is clearly resolved by the high K_2O values (9-11 wt. %) for the Myers Road 'MC2' (open diamonds) compared to the 4-6 wt. % K_2O of the Nowadaga 'B0' bentonite.

5.7 Conclusions

1. The bentonites of the Utica Formation at Canajoharie @ 65.5 m and Flat Creek @ 49.5 m have been correlated by the chemical composition of both pristine and experimentally melted inclusions in quartz phenocrysts.
2. Two chemically separate groups have been identified within the chemical composition of Canajoharie @ 65.5 m and Flat Creek @ 49.5 m bentonites. These groups are represented in both the pristine and the experimentally melted inclusions. Only one of these two groups has been identified at the Deer River @ 19.2 m melt inclusions. Therefore, no definite correlation can be made from the Deer River bentonite to the Canajoharie and Flat Creek bentonite.
3. Melt inclusions from Canajoharie @ 63.5 m, Flat Creek @ 47.4 m and Chuctanunda @ 46.4 m are very similar in their chemical composition, but there are subtle chemical differences.
4. The chemical compositions from Canajoharie @ 61.9 m and Chuctanunda @ 42.0 m seem to be equivalent. More data are needed to confirm this correlation.
5. Melt inclusion composition in apatite phenocrysts from the Nowadaga 'B0' and Myers Road 'MC2' bentonite confirms that these two bentonites are chemically distinct from each other.

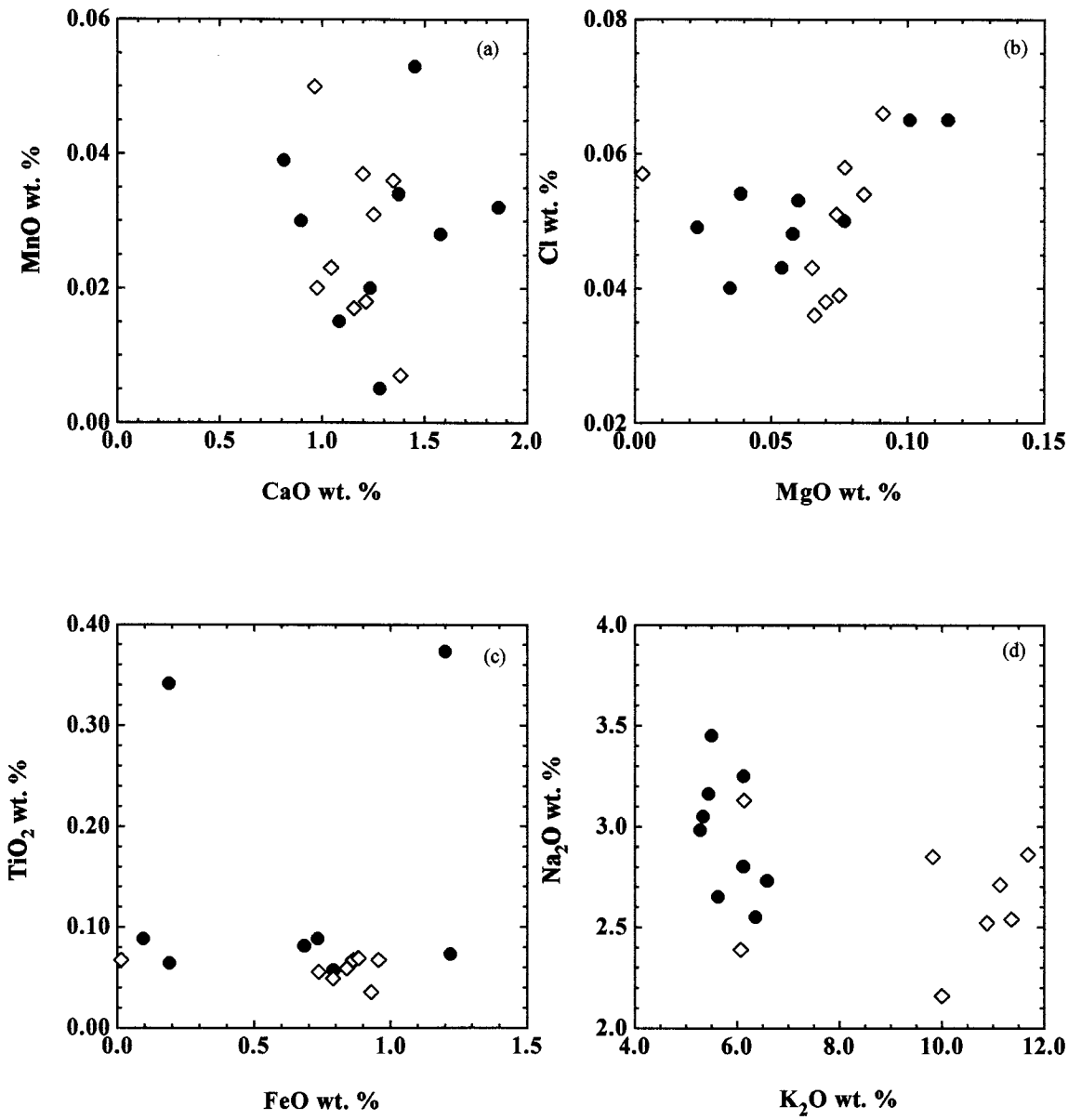

Figure 5.12. Plot of (a) MnO vs. CaO, (b) Cl vs. MgO, (c) TiO_2 vs. FeO, and (d) Na_2O vs. K_2O in melt inclusions in apatite phenocrysts from the bentonites at Myers Road 'MC2' (open diamonds) and Nowadaga 'B0' (solid circles). Analytical precision as in Figure 4.1.

CHAPTER 6 GEOCHEMISTRY

6.1 Melt inclusion composition

The glass inclusions within apatite phenocrysts from the Ordovician bentonites range in composition from rhyodacites to high silica rhyolites. Most glasses in quartz phenocrysts have 5-6 wt.% K_2O (referred to as 'high-K' in the text) and 2-3 wt.% Na_2O. These high-K inclusions typically contain $\leq$ 0.2 wt.% MgO. The melt inclusions from the stratigraphic sequence at Canajoharie Creek within the specific studied 30 m interval are chemically distinct from glasses in the other bentonites within the Ordovician strata of New York (Figure 6.1 a). Specifically, these inclusions have distinctive abundances of K_2O. Several bentonites contain melt inclusions with distinctly lower K_2O abundances (2-3 wt.%, referred as 'low-K') (e.g., Canajoharie @ 84.7 m, @ 61.9 m, @ 63.5 m). In addition, these inclusions typically contain higher abundances, of MgO, CaO, MnO, TiO_2 and FeO relative to the high-K inclusions, suggesting that these melts are less evolved in nature. Some of the low-K bentonites display a wide range in composition (Canajoharie @ 63.5 m and Canajoharie @ 61.9 m) and some display bimodal distributions as of minor and trace elements, as for example at Canajoharie 67.0 m and Canajoharie 65.5 m (Figure 6.1 a). These distinctive bentonites occur in a restricted stratigraphic interval (approximately 30 m thick) in the upper *C. americanus* graptolite zone of the Utica Formation (Mitchell et al., 1994), and have not been observed in any other part of the Ordovician strata. The glass inclusions in apatite phenocrysts from the 30 m interval at Canajoharie, like the melt inclusions in quartz, range from low-K rhyolite to high-K rhyolites (Figure 6.1 b). However, these inclusions in apatite display a much wider range in SiO_2. This is discussed below. In the Myer's Road 'MC2' bentonites, which is not a member of the 30 m section, glass inclusions in apatites are ultrapotassic with K_2O contents varying from 6 to 11 wt.% and ranging from 67 to 73 wt. % in SiO_2 (Appendix E.1). This is discussed in section 6.4.

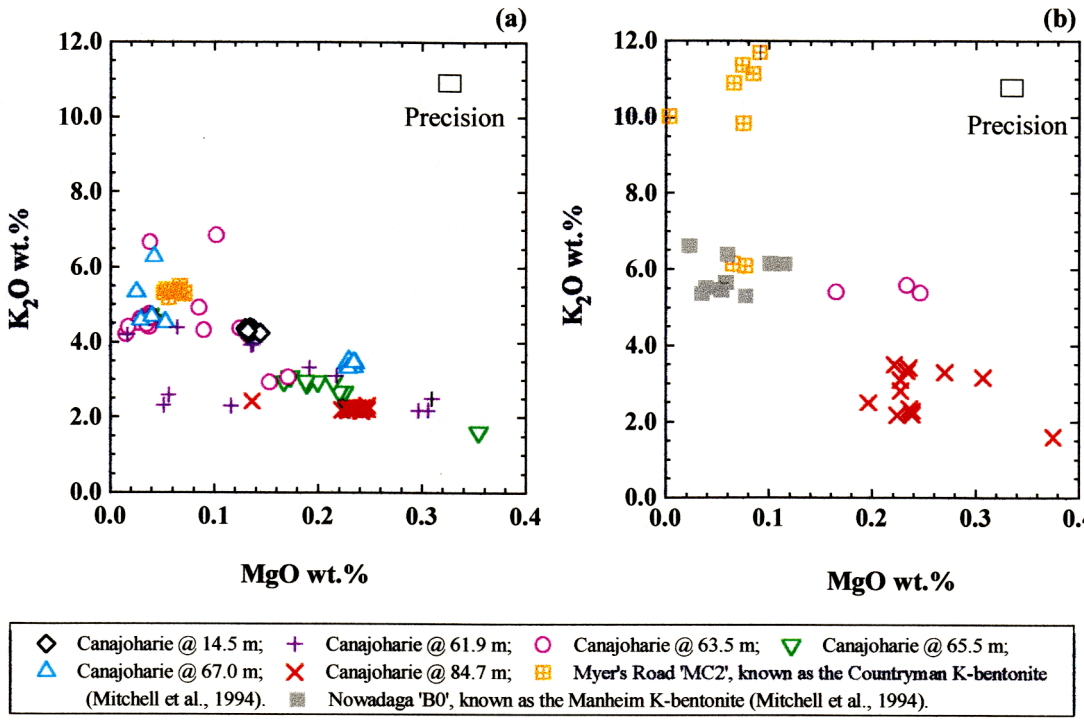

Figure 6.1 a, b Plots of electron microprobe results from melt inclusions in quartz phenocrysts (a) and apatite phenocrysts (b) from Bentonites of the Mohawk Valley. The box in all diagrams represents the analytical precision and reproducibility of the analyses. Each symbol represents an analysis of a single inclusion and each group of symbols represents a bentonite layer.

6.2 Comparison of melt inclusions in quartz and apatite phenocrysts

Figure 6.2 a, b represents the results of analyses of 23 different inclusions in quartz and 15 inclusions in apatite phenocrysts from the Canajoharie Creek @ 84.7 m (Appendices A.6.1 and A.6.2). The glass inclusions in quartz phenocrysts from Canajoharie Creek @ 87.4 m display little chemical variation and are identical within analytical precision, whereas the melt inclusions in apatite phenocrysts from this particular bentonite vary by a factor of approximately 2 in MgO, MnO, FeO, and TiO_2. Melt inclusions in apatites compositionally overlap, within analytical uncertainty, those in quartz phenocrysts, but often define a larger compositional range (Dannenmann et al., 1996).

It seems that the quartz phenocrysts in these bentonites entrapped melt of more constant composition. A similar relationship between melt inclusions in quartz and apatite phenocrysts has been observed by Hanson (1995) in Devonian bentonites from New York State. Since the compositions of melt inclusions in quartz and apatite phenocrysts are so similar, it seems unlikely that they represent different eruptive events (Hanson, 1995). It is more likely that melt inclusions are samples of (a) compositionally-zoned magma chamber or (b) were entrapped at different times during the evolution of a magma chamber as suggested by Hanson (1995). In these scenarios, the quartz would have (a) crystallized within a restricted region of a zoned chamber, or (b) crystallized during an abrupt event during evolution of the magma chamber.

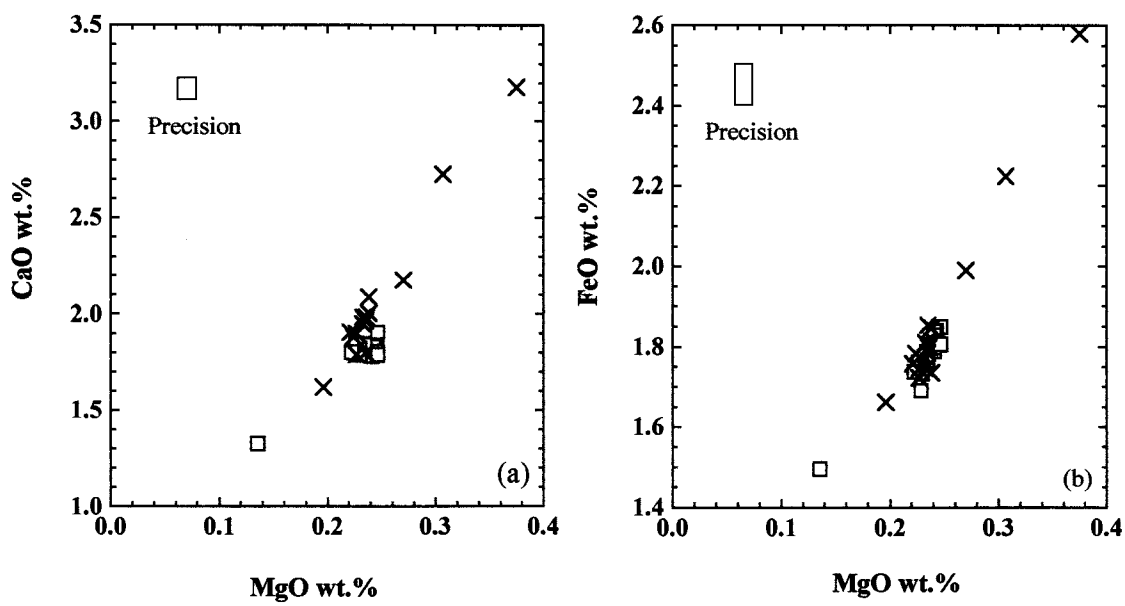

Figure 6.2 a, b Comparison of 23 melt inclusions in quartz phenocrysts (open squares) to 15 melt inclusions in apatite phenocrysts (crosses) from the bentonite layer at Canajoharie @ 84.7 m.

Apatite phenocrysts entrap a wider range in melt composition, and hence contain valuable information regarding the magma evolution or zoning (Figure 6.3). Spulber and Rutherford (1983) conducted hydrothermal experiments on Kilauea oceanic tholeites at P_{fluid}= 1 kb and at different temperatures. As the temperature decreased, the SiO_2 content in these melts increases, as expected. P_2O_5 content also increases until the melt becomes saturated with apatite (Green and Watson, 1982). With decreasing temperature apatite progressively crystallizes removing P_2O_5 from the melt. Apatite crystallizes following the saturation surface. Since apatite starts to crystallize around 63 wt.% and quartz is not seen until 67 wt.%, apatite crystallizes long before quartz and, correspondingly, melt inclusions in apatite provide a wider range (rhyodacite to high-silica rhyolite) in melt composition. It is not implied here that the bentonite inclusions represent highly fractionated basalts, only that apatite phenocrysts exist over a wider range in SiO_2-content than quartz phenocrysts.

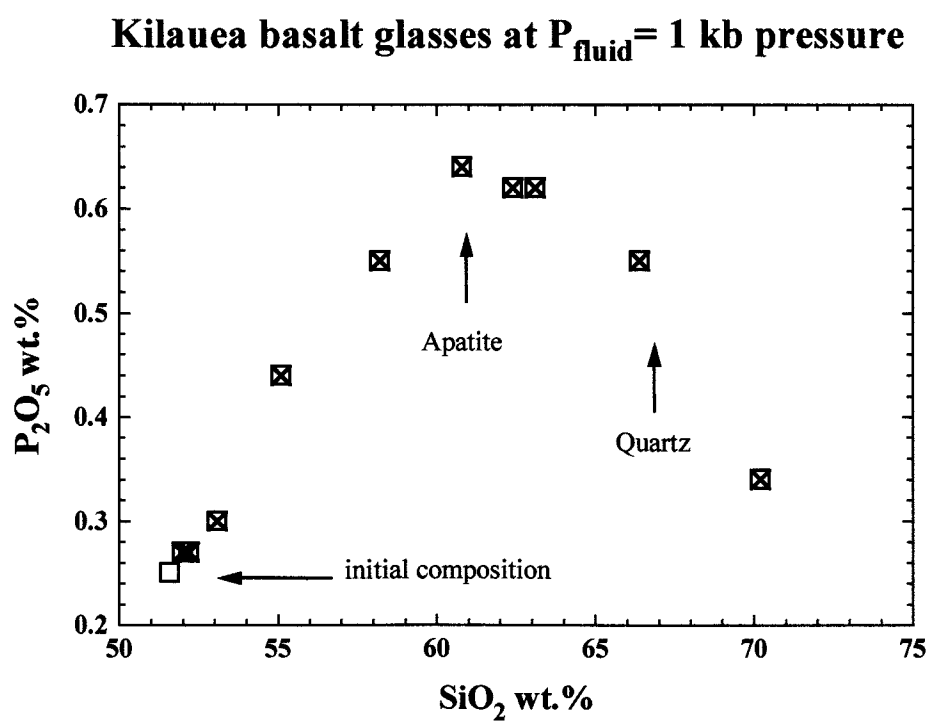

Figure 6.3 Residual melt chemistry for experiments on Kilauea basalts at P_{fluid} = 1 kb pressure. Data from Spulber and Rutherford (1983).

6.3. Vapor bubbles

Non-crystallized glass inclusions in quartz phenocrysts may contain bubbles; these vapor bubbles are generally < 10 % of the inclusion volume. As mentioned in chapter 5.3, data points lying outside normal compositional groups of melt inclusions from a single bentonite are often inclusions that contain bubbles. In this study, bubbles are observed in inclusions from Canajoharie @ 67.0, Canajoharie @ 63.5, Flat Creek @ 31.2, Flat Creek @ 47.4 'C' & 'E' and Chuctanunda @ 46.4. The bubble-bearing inclusions of these bentonites all show the same characteristics (Figure 6.4). It is assumed that the deviation in the sum of the major oxides from 100 % is an approximate measure of volatile content in the glass inclusions (Anderson, 1973; Beddoe-Stephens et al., 1983; Rutherford et al., 1985; Devine et al. 1995; Hanson et al., 1996). Typical oxide totals of the bubble bearing inclusions are near to 100 %, suggesting that the glasses have lost their volatiles. Less than 2 years are required for H_2O in a 50 μm diameter inclusion of rhyolitic melt at the center of a 2 mm diameter quartz crystal to reach 95% reequilibration with external melt at 800 ° C (Qin et al., 1992). Thus, melt inclusions have enough time to vesiculate in the magma chamber.

Figure 6.4 and Figure 6.5 are a comparison of melt inclusions with bubbles (solid circles) and without bubbles (open diamonds) from the bentonite layer at Chuctanunda @ 46.4. The bubble bearing inclusions generally contain more Al_2O_3, MnO, K_2O and Na_2O and less TiO_2, FeO, MgO and SiO_2 than the melt inclusions without bubbles. Bubbles may contain the vapor lost from the melt. If H_2O is lost, then SiO_2 will precipitate on the inclusion wall of the host quartz crystals (Webster, 1991) and produces a relative increase in Al_2O_3 and everything else in the glass. The SiO_2 content increases with the increasing volatile content from increased dilution of melt with SiO_2. The reason for this is that the liquidus is suppressed in the melt-quartz system by dissolved volatiles. Due to H_2O loss, inclusions could reach the liquidus and crystallize quartz and possibly other phases. In order to determine the original elemental abundance the bubble bearing melt inclusion data has to be normalized to 11.8 wt. % Al_2O_3. This normalization will lower the data to an estimation of the actual abundances (see Figure 6.4 open red circles).

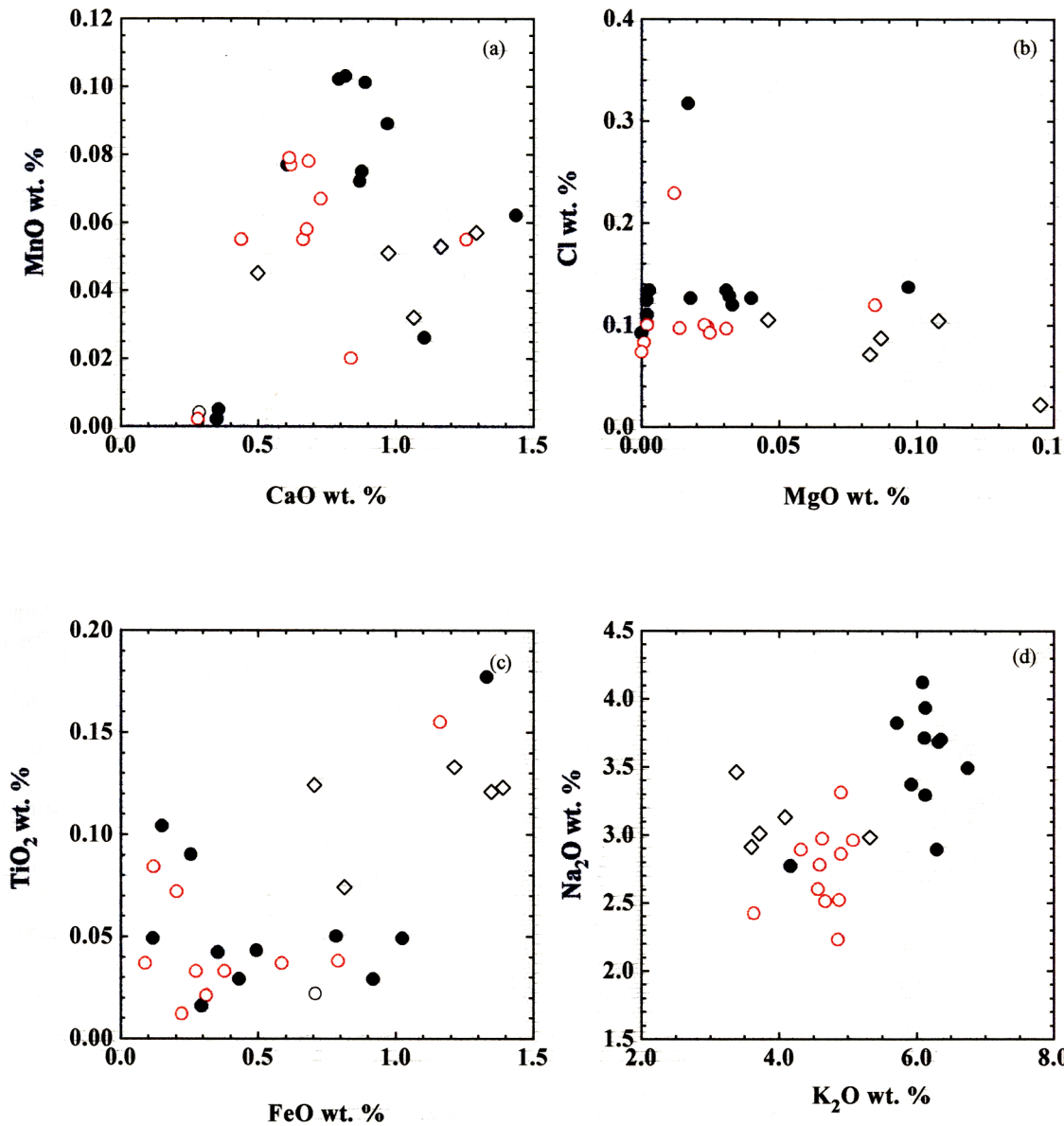

Figure 6.4 Plot of (a) MnO vs. CaO, (b) Cl vs. MgO, (c) TiO_2 vs. FeO, and (d) Na_2O vs. K_2O in melt inclusions in quartz phenocrysts from the bentonite at Chuctanunda @ 46.4 m. Melt inclusions with bubbles are presented by solid circles and without by open diamonds. Red open circles are melt inclusions with bubble data normalized to 11.8 wt. % Al_2O_3. See text for explanation.

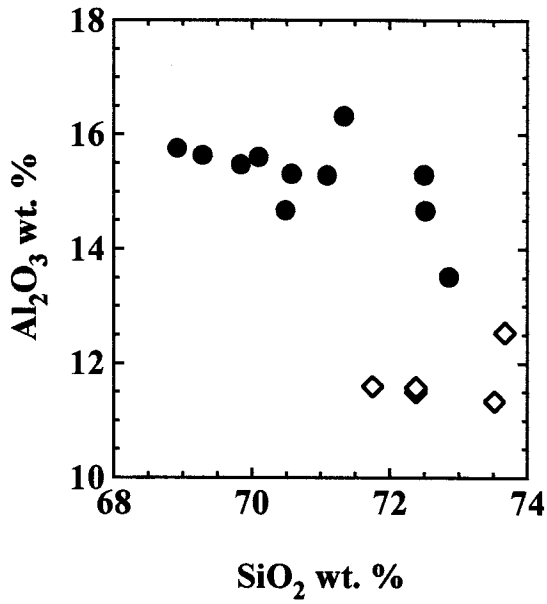

Figure 6.5 Plot of Al_2O_3 vs. SiO_2 in melt inclusions in quartz phenocrysts from the bentonite at Chuctanunda @ 46.4 m. Melt inclusions with bubbles are presented by solid circles and without by open diamonds.

6.4 Ultrapotassic Inclusions

Melt inclusions in the apatites from Myer's Road 'MC2' show a range from 6 wt.% to around 11 wt.% in their K_2O content. This is the reason why it is possible to distinguish it from the otherwise chemically similar Nowadaga 'B0' bentonite (see Figure 5.11). Except for the K_2O content, all other elements in these two bentonites seem to be comparable.

Schirnick (1990) observed heterogeneous inclusions of ultrapotassic content in quartz phenocrysts. The heterogeneity in these inclusions is not necessarily visible in transmitted light microscopy: Only under backscattered electron image have chemically different domains been observed. The chemistry of these inclusions not only differs in the K_2O composition, but in other elements as well (e.g., poor in Na_2O and CaO). Phenomena like the above have not been observed in the Myer's Road 'MC2' bentonite. If the ultrapotassic content reflects the true composition of these melts and they are not heterogeneous, than a possible explanation might be found in their relationship to the Tectonic setting.

Ninkovich and Hays (1972) observed that potash versus silica increases with increasing depth of underlying earthquakes. They studied the relationship between the chemical composition of volcanic rocks and the depth of intermediate and deep focus earthquakes in the Benioff zone (where melts are generated) and they concluded that the contents of volcanic rocks from Batu Tara (north of the island Flores, Indonesia) and Muriah (northern coast of Java) are about 10.5 wt.% in K_2O and 69 wt.% in SiO_2. These rocks are from volcanoes whose underlying earthquakes reach depths between 200 and 300 km

(Hamilton, 1979). Volcanoes with similar distances to the Benioff Zone (100-150 km) have an increase in potassium and other incompatible elements in a direction towards the collision near Timor, and, furthermore, show an increase of potassium with increasing distance from the Benioff Zone (Van Bergen et al., 1989, 1993). Van Bergen et al. (1992) observed at Batu Tara a progressive increase in potassium and incompatible trace element concentrations away from the trench. Since a broadly similar scenario to the tectonic setting during the Taconic Orogeny is present in the Banda Sea region and the ultrapotassic magmas of the Eastern Sunda Arc lie between the 200 and 300 km -depth Benioff zone, the magma containing ultrapotassic melt inclusions in apatite crystals from Myer's Road 'MC2' possibly came from around the same depth as the magma from Batu Tara or Muriah. But it has to be considered that previous work in relating the chemical variations of potassium to the Benioff Zone has been based on bulk-rock geochemistry. No detailed study exists so far for ultrapotassic content within the glass composition.

CHAPTER 7 DISCUSSION

Many melt inclusions in different bentonite layers at the outcrop at Canajoharie show a wide and bimodal distribution of elemental abundances. There are several possible explanations for this observation, for example: These bentonite layers may be composed of two or more distinct eruptions, erupted through multiple previous deposited ash layers; they are composed of a single eruption from a large heterogeneous (i.e., zoned) magma chamber, influenced by partial melting or wall rock assimilation etc.. In this study the case of muliple eruptive events and the case of a heterogeneous magma chamber are closer examined.

7.1 Multiple eruptive events

It is easy to imagine that two or more eruptive events might occur within a small enough time period that their air fall components would be preserved in the same layer, especially if, during this time, the sedimentation rate is low (Hanson 1997, in preparation). Hanson et al. (1997, in preparation) suggested that a Devonian bentonite within the Central Appalachian Basin is a composite of two air-fall components from different eruptive events. One component was preserved at all six localities, while the other was found at only three of these six localities, suggesting that one of these eruptions was distributed over a wide area whereas the other eruption was only more locally preserved.

In chapter 5.1 Canajoharie @ 65.5 is correlated with Flat Creek @ 49.5, which occurs 3 km to the west. Figure 5.4 indicates that two different groups of inclusions occurs in this layer, which could be interpreted as two eruptive events preserved in the same layer. The melt inclusions from the Deer River bentonite, 140 km north of the Canajoharie Creek locality (see Figure 5.9), contain inclusions that are chemically identical to one of the groups at Canajoharie @ 65.5 and Flat Creek @ 49.5. If two eruptive events are indicated by these groups, then the Deer River bentonite only contains evidence for one of these eruptive events.

7.2 Heterogeneous magma chamber

The processes that give rise to compositional variations in silicic magma chambers have been a prominent topic in igneous petrology and the subject of considerable debate (Smith, 1979, Hildreth, 1979). It is generally accepted that crystal fractionation is the dominant mechanism generating zonation in closed-system magma chambers. Open-system processes, such as assimilation of wall rock and recharge, also contribute to the development of zoning. Trends produced by crystal fractionation can also be produced by partial melting, but the processes are difficult to distinguish. Partial melting is controlled by the chemistry of solid phases being added to the melt and is considered to occur at significant depths in the mantle whereas fractional crystallization is a crustal phenomenon.

Island arc volcanics are very often related to fractional crystallization. On the basis of major- and trace-element chemistry and isotopic analyses it has been concluded that most of the andesites cannot be primary mantle melts but are derived from fractional crystallization (Ewart, 1982). After Ewart (1982), a typical Harker variation diagram for a rhyolite-andesite-basalt suite shows the smooth patterns of increasing Al_2O_3, MgO, FeO, CaO, and TiO_2 content or decreasing Na_2O and K_2O content relative to the SiO_2 content. These patterns indicate a relatively orderly fractionation relationship among all members of the suite. Normally a Harker diagram is based on a function of SiO_2 because there is considerably more variation in SiO_2 content than in MgO content. Since in the earlier melt inclusion analyses SiO_2 has not been analyzed, the Harker diagram is based on a function of MgO content for the Mohawk valley section. Figure 7.1 shows the oxides content (measured in weight percent) of melt inclusions in quartz phenocrysts from the Mohawk valley bentonite at Canajoharie Creek and the result of the experimental glass data from Kilauea Tholeiites (Spulber and Rutherford, 1983). Na_2O and K_2O content decreases and CaO, FeO, TiO_2 increases relative to MgO, which is typical for island arc magmas.

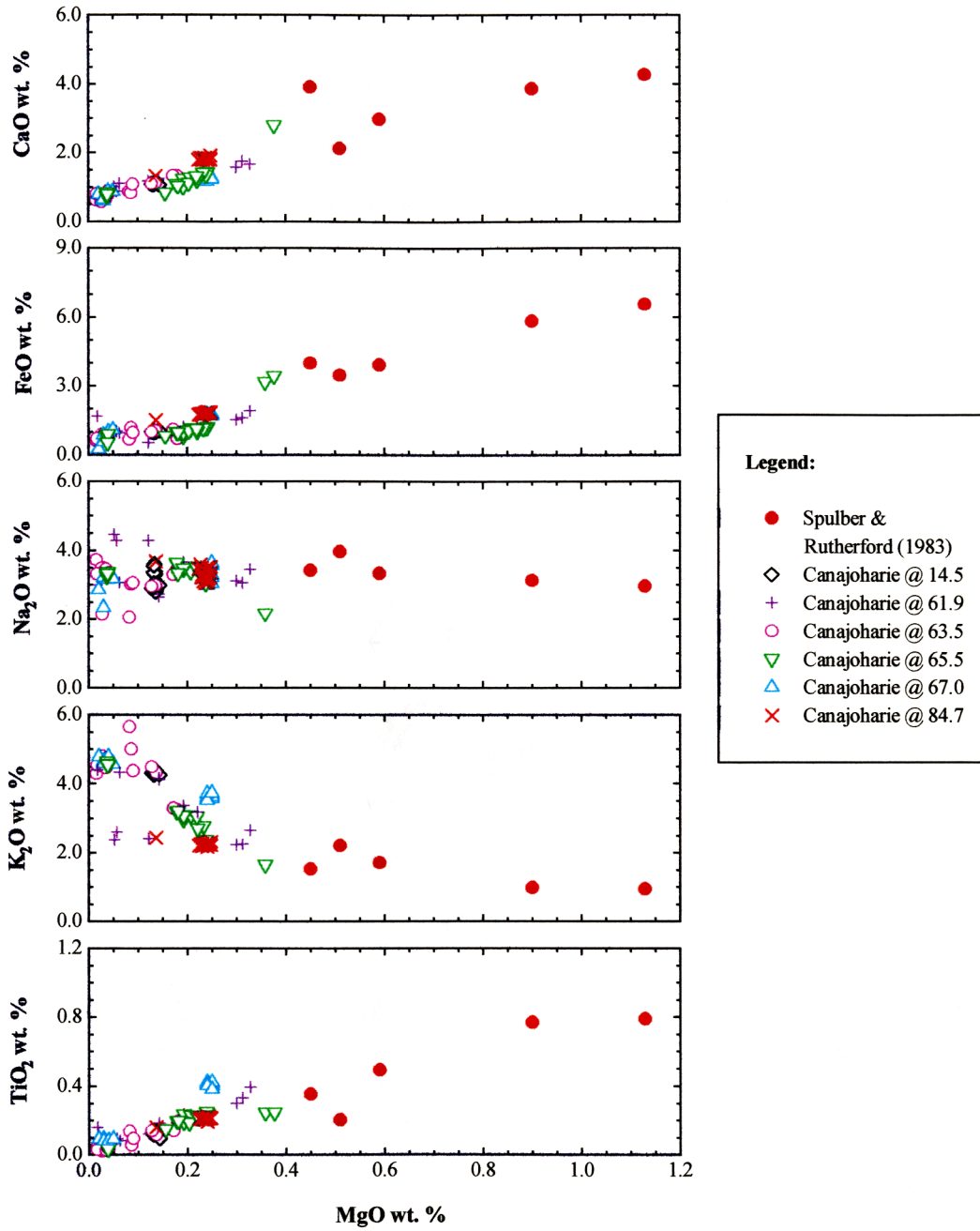

Figure 7.1. Harker MgO content variation diagram for glass data from Canajoharie Creek Bentonites and experimental glass data of Kilauea basalts at different temperatures from Spulber & Rutherford (1983).

Another common chemical technique for distinguishing rock suites that involve fractionation is the AFM diagram, a ternary plot of total content of alkalis ($Na_2O + K_2O$) versus total FeO and MgO contents. Within a rock suite the trend of rock compositions on this diagram will depend on one or more mineral phases being removed from initial parent by liquid fractionation. Figure 7.2 is such a AFM-diagram on which Canajoharie Creek melt inclusion data and the data from Spulber & Rutherford (1983) is plotted.

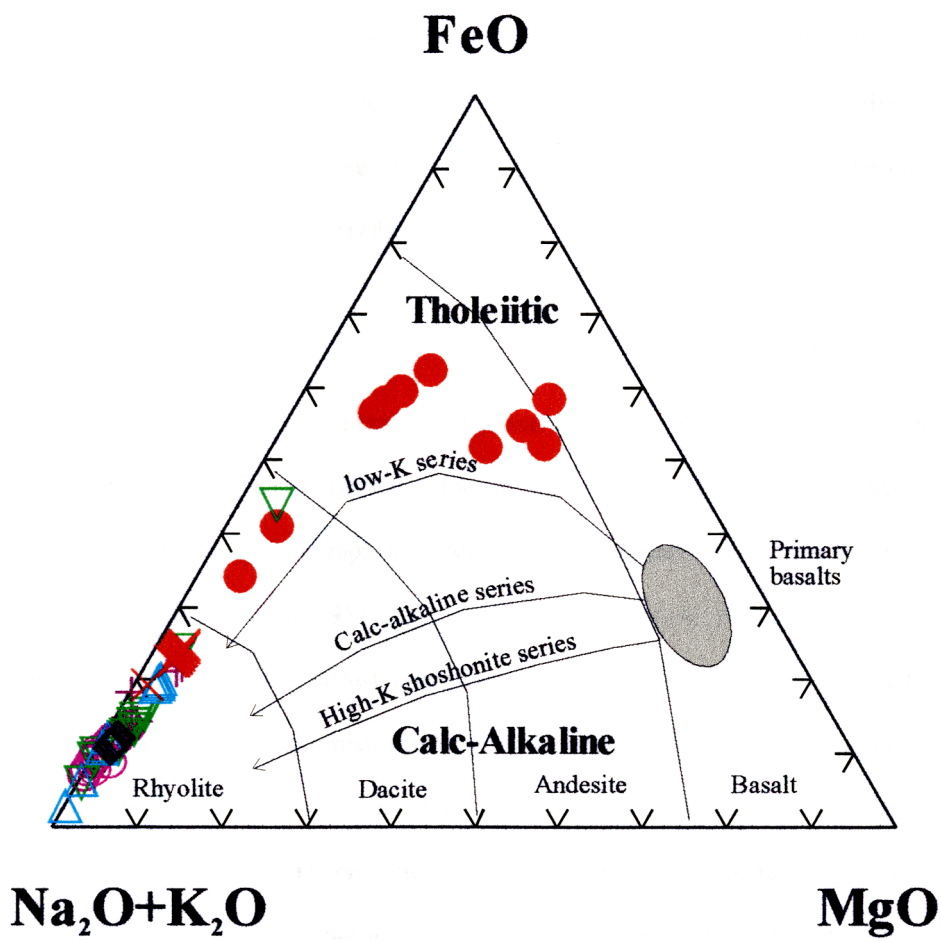

Figure 7.2. AFM diagram showing the calc-alkalic trends, including the low-K series, the calc-alkaline series, and the high-K shoshonite series. Approximate compositional ranges for basalt, andesite, dacite, and rhyolite are shown, as is the field of compositions for primary, mantle derived basalts. The colored symbols are as in Figure 7.1, melt inclusion data from bentonites at Canajoharie Creek and the experimental of Spulber & Rutherford (1983). This graph is modified after Blatt & Tracy, 1995.

The glass data from Canajoharie Creek is trending towards the low-K series. After Blatt & Tracy (1995) the low-K series are dominated by basalts and basaltic andesites. They represent initial stages of mantle melting beneath an island arc with subsequent fractionation of these initial melts. Even though the AFM diagram divisions are determined for whole rock analyses, it can be inferred that these bentonites evolve from a low-K series.

Most likely the case of fractionation cannot be applied for this study, because one would expect a systematic increase in the elemental abundances. Figure 5.2 c is an example showing only an increase in the TiO_2 abundances, but no increase in FeO. In the case of crystal fractionation there would be an enrichement in FeO. Another argument against liquid fractionation is that the proportion of crystals (phenocrysts) to glass in some rhyolites is so small that the compositional variations in the liquid cannot have resulted from fractionation of crystals (Hildreth, 1981).

7.3 Zoning and Mixing

Chemical variations in ash flows represent chemical variations within individual magma bodies. Zoned eruptive sequences is a possible explanation for the different compositions seen in the Canajoharie Creek glass data. The following paragraph is a brief summary about typical features of zonation as observed by Smith (1979) and Hildreth (1981).

Zonation may be the result of diffusion-convection-controlled differentiation mechanisms which develop along the temperature gradient which results from the establishment of volatile gradients. These further lead to gradients in melt structure, which, together with the other factors (stress & thermal region, crustal composition, crystallization history, magma chamber geometry, parental magma composition, eruptive drawdown, and organization), appear to control the relative enrichment or depletion of elements in the non-convecting, highly differentiated roof portion of the magma chamber. All pyroclastic eruptions exceeding 1 km^3 are compositionally zoned and many much smaller ones show pronounced zonations as well. Erupted parts of magma chambers range from nearly uniform rhyolitic composition to strongly contrasting basalt-rhyolite compositions. Many large ash-flow sheets exhibit either a small compositional

gap (1% to 4% SiO_2) or a transition from rhyolite to rhyodacite. With depth, magma columns become hotter, more mafic and more phenocryst-rich. There are pre-eruptive gradients in T, F_{O2}, major and trace element and isotopic composition, volatiles (H_2O, Cl, F) and in types, abundance and composition of phenocrysts. A zoned magma column may be vertically layered with abrupt transitions between zoned subunits. Wide compositional gaps are common at all levels of SiO_2 - concentration and must have developed within a magmatic system (sometimes reflecting simultaneous tapping of two chambers or arrival of new basic magma triggering eruption. Small-volume systems tend to show stronger compositional contrasts than large-volume systems.

As mentioned above, small compositional gaps (1% to 4% SiO_2) or a rapid transition from rhyolite to rhyodacite can be observed for zoned magma chambers. Compositional gaps are observed in glasses of the Canajoharie Creek bentonites at 65.5 m and 67.0 m. At Canajoharie at 61.9 m and 63.5 m a transition from rhyolitic to rhyodacitic melt inclusion compositions have been observed. Figure 7.3 is a comparison of melt inclusions in quartz phenocrysts from Canajoharie Creek bentonites to melt inclusions from three well-studied, chemically zoned ash flow sheets from the southwest Nevada Volcanic field (Vogel & Aines, 1996). Vogel & Aines (1996) demonstrated that analyses of melt inclusions in feldspar and quartz phenocrysts, glass matrix and pumice fragments from the same ash flow are mostly of the same chemical composition. The pumice fragments in these ash flow sheets have been previously interpreted to represent eruptions from chemically zoned magma bodies (Hildreth, 1981). Glass data from the Canajoharie bentonites follow the compositional trend of the three ash flow sheets from the southwest Nevada volcanic field (represented by the solid black symbols). This observation, along with the occurrence of small compositional gaps and a rapid transition from rhyolitic to rhyodacitic composition, suggests that the melt inclusions from these bentonites come from a chemically zoned magma chamber.

Figure 7.4 is a enlargement from Figure 7.3. Two trends can be observed. Trend #1 is represented by the high-K group (see chapter 6), and trend #2, represented by the low-K group and mostly by melt inclusions from Canajoharie @ 65.5 and Canajoharie @ 84.7. This low-K trend can be seen in Figure 6.1 a. Mixing with more mafic magma would serve as an explanation of the origin of the

observed trend #2. Small amounts of mixing within an inhomogenous magma chamber could provide enough changes in the chemical environment of a magma chamber, so that large-scale mixing of two discreet magma types is not required to produce these differences.

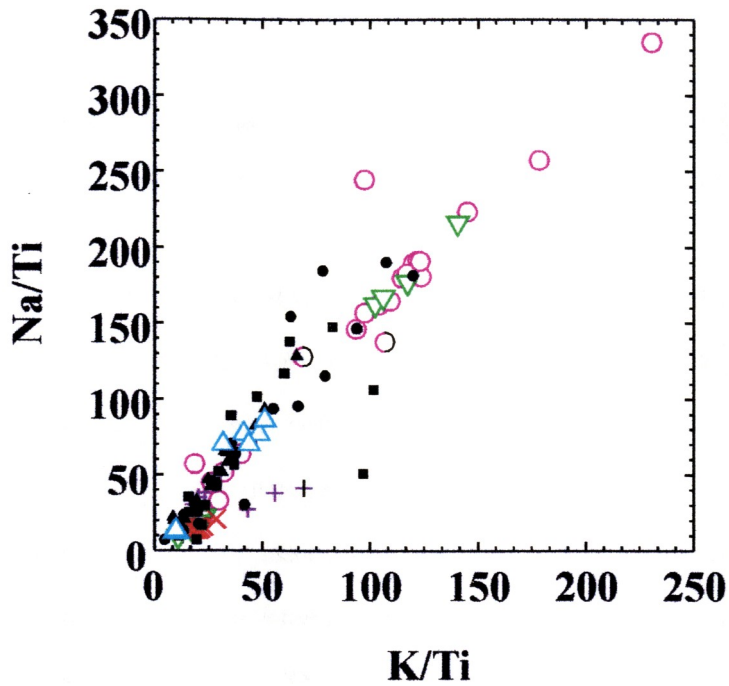

Figure 7.3 Bivariate plot of the molecular proportion of Na/Ti vs. K/Ti for the melt inclusions in quartz phenocrysts data of Canajoharie Creek (symbols as in Figure 7.1) and melt inclusions from chemically zoned ash flow sheets from the southwest Nevada Volcanic Field (Topopah Spring Tuff (solid black triangles), Rainer Mesa Tuff (solid black circles) and Ammonia Tanks Tuff (solid black squares)) (Vogel and Aines, 1996).

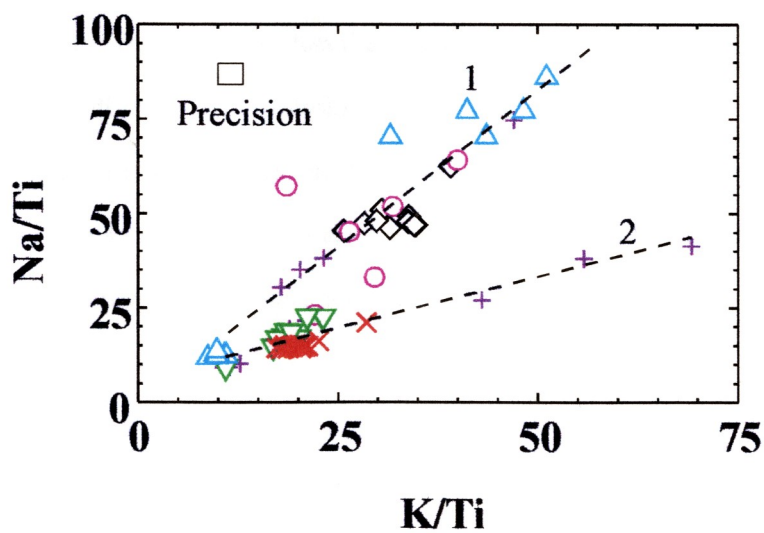

Figure 7.4 Enlargement of lower part of Figure 7.3. Data of the melt inclusions from the Southwest Nevada Volcanic Field are not included. Numbers represent different trends observed in these data.

CHAPTER 8 CONCLUSIONS

The main conclusions reached as a result of this analytical study of melt inclusions in quartz and apatite phenocrysts of Ordovician bentonites from the Utica and Denmark Formations are the following:

1. Of the approximately 26 layers sampled and examined within the 30 m interval in the black shales of the Utica Formation, 11 of these were bentonites that contained melt inclusion-bearing quartz phenocrysts. Of the 2 layers collected in the carbonates of the Denmark Formation, only one layer contained melt inclusion-bearing quartz phenocrysts.
2. Pristine glassy inclusions have been identified in quartz and apatite phenocrysts within Ordovician bentonites. Devitrified inclusions have been identified in quartz phenocrysts and were experimentally melted in a one-atmosphere furnace. These types of inclusions have been used for fingerprinting different ash layers.
3. Within the 30 m interval only one additional correlation can been added between the outcrops at Canajoharie Creek and Flat Creek. A correlation between bentonites within this interval to bentonites occurring in the western Platform carbonates of the Black River Valley has not been estabished.
4. Major-, minor-, and trace elements from the analyzed melt inclusions within the 30 m interval show generally bimodal distribution or a transition from rhyolite to rhyodacite.
5. Difficulties in correlating bentonites in this particular studied area are possible due to individual bentonite layers being composed of the products of two or more distinct eruptions or being composed of eruptions from heterogenous (zoned) magma chamber.

Bibliography

Anderson, A.T., **1973**, The before-eruption water contents of some high-alumina magmas. *Bulletin Volcanologique*, v. 37, p. 530-552.

Beddoe-Stephens, B., Aspden, J.A., and Shepherd, T.J., **1983**, Glass inclusions and melt compositions of the Toba Tuffs, Northern Sumatra. *Contributions to Mineralogy and Petrology*, v. 83, p. 278-287.

Blatt, H., and Tracy, R., **1995**, Evolution of magmas: Fractional crystallization and contamination. *In:* Petrology: Igneous, Sedimentary, & Metamorphic. W.H. Freemann, 2nd edition, p. 119-189.

Borchardt, G.A., Aruscavage, P.J., and Millard, H.T., Jr., **1972**, Correlation of the Bishop Ash, a Pleistocene marker bed, using instrumental neutron activation analysis. *Journal of Sedimentary Petrology*, v. 42, p. 301-306.

Chenoweth, P.A., **1952**, Statistical Methods applied to Trentonian Stratigraphy in New York. *Bulletin of the Geological Society of America*, v. 63, p. 521-560.

Cisne, J.L., Karig, D.E., Rabe, B.D., and Hay, B.J., **1982**, Topography and Tectonics of the Taconic outer trench slope as revealed through gradient analyses of fossil assemblages. *Lethaia*, p. 229-246.

Dannenmann, S., Hanson, B., and Delano, J.W., **1996**, Composition of magmas erupted explosively during the Taconic Orogeny: Analysis of glasses preserved in quartz and apatite phenocrysts from bentonites. *Geological Society of America Abstracts With Programs*, vol. 28, no. 3, p. 47.

Delano, J.W., Schirnick, C., Bock, B., Kidd, W.S.F., Heizler, M.T., Putnam, G.W., DeLong, S.E., and Ohr, M., **1990**, Petrology and Geochemistry of Ordovician K-bentonites in New York State: Constrains on the Nature of a Volcanic Arc. *Journal of Geology*, v. 98, p. 157-170.

Delano, J.W., Tice, S.J., Mitchell, C.E, and Goldman, D., **1994**, Rhyolitic glass in Ordovician K-Bentonites: A new stratigraphic tool. *Geology*, v. 22, p. 115-118.

Devine, J.D., Gardner, J.E., Brack, H.P., Layne, G.D., and Rutherford, M.G., **1995**, Comparison of microanalytical methods for estimating H_2O contents of silicic volcanic glasses. *American Mineralogist*, v. 80, p. 319-328.

Dunbar, N.W., Hervig, R.L., and Kyle, P.R., **1989**, Determination of pre-eruptive H_2O, F, and Cl contents of silicic magmas using melt inclusions: examples from the Taupo Volcanic Center. *Bulletin of Volcanology*, v. 51, p.177-184.

Ewart, A., **1982**, The mineralogy and petrology of Tertiary-Recent orogenic volcanic rocks with special reference to the andesitic-basaltic composition range. *In*, Thorpe R.S. (ed.), Andesites. Wiley, Chichester, p. 25-87.

Fisher, R.V., and Schminke, H.-U., **1984**, Pyroclastic Rocks. *Springer-Verlag Berlin Heidelberg*, 472 pp.

Goldmann, D., Mitchell, C.E., Bergström, S.M., Delano, J.W., and Tice, S., **1994**, K-bentonites and graptolite biostratigraphy in the Middle Ordovician of New York State and Quebec: A new chronostratigraphic model. *Palaios*, v. 9, p. 124-143.

Green, T.H., and Watson, E.B., **1982**, Crystallization of Apatite in Natural Magmas Under High Pressure, Hydrous Conditions, with Particular Reference to 'Orogenic' Rock Series. *Contributions to Mineralogy and Petrology*, v. 79, p. 96-105.

Hamilton, W., **1979**, Tectonics of the Indonesian region. *U.S. Geol. Surv., Prof. Pap. 1078*, 345 pp.

Hanson, B., **1995**, A Geochemical Study of ryholitic melt inclusions in igneous phenocrysts from lower Devonian bentonites. *Unpublished Doctoral Dissertation*, The State University of New York at Albany, Albany, 481 pp.

Hanson, B., Delano, J.W., and Lindstrom, D.J., **1996**, High-precision analysis of rhyolitic melt inclusions in quartz phenocrysts using the electron microprobe and INAA. *American Mineralogist*, v. 81, p. 1249-1262.

Hanson, B., Kiparski, W. von, and Delano, J.W., **1997**, A chemical study of rhyolitic glass inclusions in quartz phenocrysts in bentonites from the Lower Devonian Helderberg Group and Esopus Formation, northeastern United States. *in preparation*

Hildreth, W., **1981**, Gradients in silicic magma chambers: Implications for lithospheric magmatism. *Journal of Geophysical Research*, v. 86, p. 10153-10192.

Hildreth, W., **1979**, The Bishop Tuff: Evidence for the origin of compositional zonation in silicic magma chambers. *Geological Society of America, Special Paper 180*, p 43-75.

Huff, W.D., **1983**, Correlation of Middle Ordovician K-bentonites based on chemical fingerprinting. *Journal of Geology*, v. 91. p. 113-123.

Kay, G.M., **1935**, Distribution of Ordovician altered volcanic materials and related clays. *Geol. Soc. American Bulletin*, v. 6, p. 225-244.

Kay, G.M., **1937**, Stratigraphy of the Trenton Group. *Geol. Soc. American Bulletin*, v. 48, p. 233-302.

Kay, M., **1953**, Geology of the Utica quadrangle, New York. *New York State Museum Bulletin*, v. 347, pp. 126.

Lehmann, D., Brett, C. E., Cole, R., and Baird, G., **1995**, Distal sedimentation in a peripheral foreland basin: Ordovician black shales and associated flysch of the western Taconic foreland, New York State and Ontario. *Geological Society of America Bulletin*, v. 107, p. 708-724.

Mitchell, C.E., Goldman, D., Delano, J.W., Samson, S.D., and Bergstrom, S.M., **1994**, Temporal and spatial distribution of biozones and facies relative to geochemically correlated K-bentonites in the Middle Ordovician Taconic foredeep. *Geology*, v. 22, p. 715-718.

Nielsen, C.H., and Sigurdsson, H., **1981**, Quantitative methods for electron microprobe analysis of sodium in natural and synthetic glasses. *American Mineralogist*, v.66, p. 547-552.

Ninkovich, D., and Hays, J.D., **1972**, Mediterranean island arcs and origin of high potash volcanoes. *Earth and Planetary Science Letters*, v. 16, p. 331-345.

Qin, Z., Lu, F., and Anderson, A.T., Jr., **1992**, Diffusive reequilibration of melt and fluid inclusions. *American Mineralogist*, v. 77, p. 565-576.

Rutherford, M.J, Sigurdsson, H., Carey, S., and Davis, A., **1985**, The May 18, 1980, Eruption of Mount St. Helens 1. Melt composition and Experimental Phase Equilibria. *Journal of Geophysical Research*, v. 90, No. B4, p. 2929-2947.

Roedder, E., **1984**, Fluid inclusions. *Mineralogical Society of America, Review in Mineralogy*, v. 12, 644 pp.

Rowley, D.B., and Kidd, W.S.F., **1981**, Stratigraphic relationships and detrital composition of the medial Ordovician flysch of western New England: Implications for the tectonic evolution of the Taconic Orogen. *Journal of Geology*, v. 89, p. 200-218.

Samson, S.D., Kyle, P.R., and Alexander, E.C., Jr., **1988**, Correlation of North American Ordovician bentonites by using apatite chemistry. *Geology*, v. 6, p.444-447.

Samson, S.D., Matthews, S., Mitchell, C.E., and Goldman, D., **1995**, Tephrochronology of highly altered ash beds: The use of trace element and strontium isotope geochemistry of apatite phenocrysts to correlate K-bentonites. *Geochimica et Cosmochimica Acta*, v. 59, No. 12, p. 252, p. 2527-2536.

Sarna-Wojcicki, A.M., Morrison, S.D., Meyer, C.E., and Hillhouse, J.W., **1987**, Correlation of upper Cenozoic tephra layers between sediments of the western United States and eastern Pacific Ocean and comparison with biostratigraphic and magnetostratigraphic age data. *Geological Society of America Bulletin*, v. 98, p. 207-223.

Schirnick, C., **1990**, Origin, sedimentary geochemistry, and correlation of Middle and Late Ordovician K-bentonites: Constrains from melt inclusions and zircon morphology. *Unpublished M.S. Thesis*, The State University of New York at Albany, Albany, 209 pp.

Smith, R.L., **1979**, Ash-flow magmatism. *Geological Society of American Bulletin Special Paper*, v. 180, p. 5-27.

Spulber, D.S., and Rutherford, M.J., **1983**, The Origin of Rhyolite and Plagiogranite in Oceanic Crust: An Experimental Study. *Journal of Petrology*, v. 24, p. 1-25.

Titus, R., **1989**, Clinal Variation in the Evolution of Ectenocrinus Simplex. *Journal of Paleontology*, v. 63, No. 1, p. 81-91.

Titus, R., **1992**, Clinal Variation, Heterochrony, and Facies in the Trentonian Sowerbyella Lineage (Ordovician, New York State). *Journal of Paleontology*, v. 66, No. 5, p. 758-771.

Van Bergen, M.J., Erfan, R.D., Sriwana, T., Suharyono, K., Poorter, R.P.E., Varekamp, J.C.,Vroon, P.Z., and Wirakusumah, A.D., **1989**, Spatial Geochemical Variations of Arc Volcanism around the Banda Sea. *Netherlands Journal of Sea Research*, v. 24 (2/3), p. 313-322.

Van Bergen, M.J., Vroon, P..Z., Varekamp, J.C., and Poorter, R.P.E., **1992**, The Origin of the Potassic rock suite from Batu Tara volcano (East Sunda Arc, Indonesia). *Lithos*, v. 24, p. 261-282.

Van Bergen, M.J., Vroon, P.Z., and Hoogewerff, J.A., **1993**, Geochemical and tectonic relationships in the east Indonesian arc-continent collision region: implications for the subduction of the Australian passive margin. *Tectonophysics*, v. 223, p. 97-116.

Vogel, T.A., and Aines, R., **1996**, Melt inclusions from chemically zoned ash flow sheets from the Southwest Nevada Volcanic Field. *Journal of Geophysical Research*, v. 101, No. B3, p. 5591-5610.

Webster, J.D., and Duffield, W.A., **1991**, Volatiles and lithophile elements in Taylor Creek Rhyolites: Constrains from glass inclusion analysis. *American Mineralogist*, v. 76. p. 1628-1645.

Appendix A

Canajoharie Creek

Appendix A.1 Results of electron microprobe analyses of rhyolitic melt inclusions in quartz phenocrysts from Canjoharie @ 14.5 m.
All data are in weight percent.

	SiO_2	TiO_2	Al_2O_3	FeO*	MnO	MgO	CaO	K_2O	Na_2O	Cl	Total‡
1	72.74	0.128	11.81	0.986	0.044	0.134	1.121	4.34	3.60	0.118	95.02
2	72.89	0.123	11.85	0.991	0.041	0.136	1.108	4.38	3.37	0.117	95.01
3	73.20	0.133	11.77	0.993	0.040	0.136	1.102	4.37	2.77	0.122	94.64
4	72.40	0.131	11.96	1.001	0.035	0.137	1.115	4.37	3.34	0.116	94.61
5	72.18	0.124	11.93	0.959	0.049	0.134	1.106	4.30	3.39	0.114	94.29
6	73.29	0.126	11.69	0.965	0.040	0.132	1.100	4.27	3.52	0.113	95.25
7	72.82	0.131	11.82	0.997	0.037	0.136	1.112	4.34	n.a.	0.115	-
8	72.47	0.124	11.86	1.014	0.036	0.134	1.100	4.40	n.a.	0.114	-
9	72.31	0.128	11.98	1.003	0.045	0.130	1.100	4.38	2.93	0.117	94.12
10	72.77	0.118	11.81	0.978	0.041	0.131	1.070	4.34	2.91	0.111	94.28
11	70.86	0.094	11.76	1.033	0.047	0.144	1.066	4.25	2.97	0.116	92.34
12	72.87	0.124	11.67	0.950	0.048	0.132	1.072	4.31	2.99	0.112	94.28

* total iron as FeO

‡ Difference of totals from 100 % is due to the presence of volatiles

Analyst: Delano, J.W.

Appendix A.2 Results of electron microprobe analyses of rhyolitic melt inclusions in quartz phenocrysts from Canajoharie @ 61.9 m.
All data are in weight percent.

	SiO_2	TiO_2	Al_2O_3	FeO*	MnO	MgO	CaO	K_2O	Na_2O	Cl
1	n.a.	0.374	11.15	1.784	0.066	0.309	1.576	2.50	3.25	0.334
2	n.a.	0.082	11.99	0.958	0.072	0.064	1.112	4.40	3.10	0.102
3	n.a.	0.152	11.25	1.602	0.034	0.016	0.605	4.19	2.84	0.033
4	n.a.	0.325	11.54	1.547	0.068	0.305	1.707	2.19	2.98	0.176
5	n.a.	0.236	11.67	1.187	0.073	0.191	0.971	3.33	3.61	0.381
6	n.a.	0.297	11.64	1.481	0.071	0.296	1.550	2.19	3.06	0.194
7	n.a.	0.095	11.80	1.018	0.063	0.056	0.864	2.60	4.27	0.062
8	n.a.	0.156	11.38	1.067	0.039	0.137	1.192	3.96	2.55	0.108
9	n.a.	0.178	11.18	1.057	0.040	0.135	1.142	3.92	2.57	0.102
10	n.a.	0.118	11.30	0.482	0.010	0.116	1.124	2.30	4.09	0.004
11	n.a.	0.199	11.59	1.137	0.063	0.217	1.288	3.11	3.38	0.304
12	n.a.	0.078	11.54	0.925	0.076	0.051	0.990	2.32	4.34	0.049

* total iron as FeO
Analyst: Delano, J.W.

Appendix A.3.1 Results of electron microprobe analyses of rhyolitic melt inclusions in quartz phenocrysts from Canajoharie @ 63.5 m.
All data are in weight percent.

	SiO_2	TiO_2	Al_2O_3	FeO*	MnO	MgO	CaO	K_2O	Na_2O	Cl	Total[‡]
1	n.a.	0.035	12.00	0.851	0.088	0.029	0.634	4.63	3.54	0.099	-
2	n.a.	0.035	11.90	0.835	0.075	0.037	0.803	4.75	3.36	0.098	-
3	n.a.	0.042	11.62	0.592	0.044	0.015	0.607	4.22	3.66	0.055	-
4	n.a.	0.034	11.89	0.838	0.081	0.037	0.755	4.68	3.34	0.098	-
5	n.a.	0.036	11.77	0.823	0.069	0.035	0.724	4.65	3.31	0.094	-
6	n.a.	0.039	11.80	0.768	0.075	0.034	0.697	4.57	3.27	0.058	-
7 (ves)[§]	n.a.	0.165	14.34	0.801	0.040	0.102	1.039	6.86	2.48	0.137	-
8	n.a.	0.053	11.61	1.122	0.087	0.085	0.801	4.92	2.95	0.138	-
9	n.a.	0.112	11.50	1.002	0.039	0.133	1.078	4.20	2.89	0.118	-
10	n.a.	0.019	11.78	0.854	0.077	0.027	0.558	4.50	3.46	0.046	-
11	n.a.	0.043	11.57	0.787	0.067	0.038	0.725	4.51	3.22	0.090	-
12	71.62	0.039	11.84	0.865	0.080	0.037	0.732	4.64	3.43	0.101	93.38
13	72.73	0.033	11.48	0.809	0.067	0.037	0.834	4.40	3.15	0.101	93.64
15	72.01	0.093	11.70	0.952	0.047	0.090	1.050	4.32	3.01	0.103	93.38
16	72.46	0.027	11.45	0.654	0.068	0.017	0.770	4.41	3.20	0.068	93.12
17	70.29	0.024	11.86	0.805	0.069	0.035	0.644	4.47	3.46	0.052	91.71
18	73.62	0.183	11.19	0.644	0.059	0.171	1.242	3.07	3.26	0.249	93.69
19	75.30	0.123	10.55	0.961	0.049	0.153	1.181	2.93	2.93	0.106	94.28
20	71.54	0.033	11.82	0.846	0.070	0.040	0.784	4.62	3.33	0.099	93.18
21	73.09	0.134	11.51	0.957	0.033	0.125	1.060	4.37	2.86	0.115	94.25
22	71.56	0.041	11.57	0.761	0.066	0.038	0.774	4.65	3.22	0.094	92.77

* total iron as FeO

[§] (ves) inclusion contains a bubble

n.a. = not analyzed

[‡] Difference of totals from 100 % is due to the presence of volatiles

Analyst: Delano, J.W.

Appendix A.3.2 Results of electron microprobe analyses of experimentally remelted rhyolitic melt inclusions in quartz phenocrysts from Canajoharie @ 63.5 m
All data are in weight percent and normalized to 11.8 wt.% Al_2O_3.

	SiO_2	TiO_2	Al_2O_3	FeO*	MnO	MgO	CaO	K_2O	Na_2O	Cl
1	81.45	0.041	11.80	0.884	0.089	0.078	0.731	6.68	2.59	0.094
2	81.58	0.069	11.80	1.007	0.051	0.329	1.109	6.94	2.02	0.080
3	n.a.	0.029	11.80	0.851	0.081	0.181	0.740	n.a.	n.a.	0.107
4	81.68	0.035	11.80	0.924	0.073	0.510	0.807	7.24	1.74	0.064
5	81.73	0.011	11.80	0.869	0.083	0.358	0.713	7.60	1.77	0.088
6	81.45	0.025	11.80	0.868	0.090	0.244	0.825	6.56	1.94	0.092
7	80.79	0.025	11.80	0.855	0.091	0.490	0.731	7.40	1.75	0.098
8	80.99	0.065	11.80	0.863	0.051	0.411	0.742	7.19	1.73	0.078
9	83.17	0.029	11.80	0.979	0.061	0.403	0.537	6.55	1.88	0.049
10	82.53	0.041	11.80	0.855	0.100	0.073	0.707	7.33	2.37	0.105
11	81.09	0.026	11.80	0.856	0.084	0.492	0.765	7.55	1.80	0.093
12	80.66	0.026	11.80	0.845	0.082	0.523	0.717	7.03	1.64	0.094

* total iron as FeO
Analyst: Dannenmann, S., Hanson, B.

Appendix A.3.3 Results of electron microprobe analyses of rhyolitic melt inclusions in apatite phenocrysts from Canajoharie @ 63.5 m.
All data are in weight percent.

	SiO_2	TiO_2	Al_2O_3	FeO*	MnO	MgO	CaO	K_2O	Na_2O	Cl	Total‡
1	73.19	0.162	12.70	1.492	0.029	0.233	0.775	5.59	2.56	0.030	96.76
2	73.86	0.143	12.79	1.299	0.050	0.165	0.743	5.41	2.84	0.033	97.34
3	72.64	0.173	12.90	1.625	0.066	0.246	1.085	5.40	2.65	0.016	96.80

* total iron as FeO

‡ Difference of totals from 100 % is due to the presence of volatiles

Analyst: Dannenmann, S., Hanson, B.

Appendix A.4.1 Results of electron microprobe analyses of rhyolitic melt inclusions in quartz phenocrysts from Canajoharie @ 65.5 m.
All data are in weight percent.

	SiO_2	TiO_2	Al_2O_3	FeO*	MnO	MgO	CaO	K_2O	Na_2O	Cl	Total‡
1	72.05	0.040	12.06	0.823	0.085	0.038	0.743	4.73	3.33	0.096	94.00
2	74.20	0.229	11.54	0.768	0.107	0.189	1.197	2.89	3.36	0.150	94.63
3	73.00	0.214	11.37	1.728	0.062	0.229	1.791	2.26	2.91	0.261	93.83
4a†	72.62	0.218	11.33	1.090	0.089	0.199	1.207	2.95	3.25	0.142	93.10
4b	n.a.	0.217	n.a.	1.056	n.a.	0.198	n.a.	n.a.	n.a.	0.158	-
5	71.47	0.038	11.91	0.803	0.071	0.037	0.843	4.60	3.26	0.102	93.14
6	73.48	0.188	11.43	0.941	0.088	0.173	1.035	3.08	3.50	0.162	94.08
7a	n.a.	0.227	n.a.	1.160	0.069	0.235	1.395	n.a.	n.a.	0.150	-
7b	n.a.	0.231	n.a.	1.132	0.083	0.234	1.362	n.a.	n.a.	0.145	-
8a	73.45	0.181	11.52	0.934	0.089	0.188	0.975	2.97	3.39	0.146	93.84
8b	n.a.	0.181	n.a.	0.999	0.083	0.199	1.075	n.a.	n.a.	0.152	-
9a	73.09	0.243	11.68	3.214	n.a.	0.354	n.a.	1.62	2.14	0.098	92.45
9b	n.a.	0.240	n.a.	3.371	0.106	0.359	2.757	n.a.	n.a.	0.097	-
11	75.18	0.180	10.92	0.861	0.075	0.167	0.952	2.96	3.08	0.151	94.52
12	n.a.	0.141	n.a.	0.779	0.104	0.151	0.815	n.a.	n.a.	0.172	-
13	73.96	0.220	11.44	1.099	0.085	0.225	1.361	2.68	3.09	0.156	94.32
14	71.19	0.036	11.94	0.883	0.080	0.041	0.793	4.58	3.39	0.103	93.03
15	71.25	0.029	11.93	0.516	0.080	0.038	0.771	4.60	3.35	0.101	92.66
16	73.31	0.215	11.70	0.988	0.084	0.220	1.183	2.67	3.48	0.166	94.01
17	73.54	0.221	11.54	1.087	0.096	0.214	1.265	2.97	3.40	0.146	94.48

* total iron as FeO

† Sample numbers with letters represent analyses of different inclusions in the same phenocryst

n.a. = not analyzed

‡ Difference of totals from 100 % is due to the presence of volatiles

Analyst: 1-12 Dannenmann, S., Hanson, B.
13-17 Delano, J.W.

Appendix A.4.2 Results of electron microprobe analyses of experimentally remelted rhyolitic melt inclusions in quartz phenocrysts from Canajoharie @ 65.5 m. All data are in weight percent and normalized to 11.8 wt.% Al_2O_3.

	SiO_2	TiO_2	Al_2O_3	FeO*	MnO	MgO	CaO	K_2O	Na_2O	Cl
1	79.20	0.030	11.80	0.755	0.067	0.045	0.806	3.34	4.23	0.044
2	79.67	0.033	11.80	0.744	0.043	0.061	0.614	5.91	2.96	0.067
3	79.94	0.039	11.80	0.882	0.058	0.096	0.845	6.22	2.49	0.083
4	81.23	0.014	11.80	0.711	0.095	0.035	0.811	6.52	3.30	0.042
5	80.50	0.242	11.80	1.303	0.095	0.229	1.143	4.73	5.18	0.161
6	80.08	0.216	11.80	1.287	0.073	0.234	1.074	5.19	3.73	0.162
7a†	75.99	0.034	11.80	0.864	0.084	0.042	0.739	4.31	3.52	0.066
7b	78.27	0.024	11.80	0.912	0.081	0.063	0.805	5.02	2.86	0.082
8	80.70	0.025	11.80	0.782	0.066	0.129	0.839	7.30	n.a.	0.073
9a	76.88	0.027	11.80	0.839	0.089	0.048	0.692	5.75	2.58	0.078
9b	79.96	0.017	11.80	0.285	0.025	0.132	0.938	3.33	5.01	0.061
10	77.56	0.039	11.80	0.444	0.081	0.113	0.793	6.82	4.01	0.123
11	80.85	0.031	11.80	0.618	0.071	0.059	0.835	3.37	2.58	0.062

* total iron as FeO

† Sample numbers with letters represent analyses of different inclusions in the same phenocryst

n.a. = not analyzed

Analyst: Hanson, B.

Appendix A.5 Results of electron microprobe analyses of rhyolitic melt inclusions in quartz phenocrysts from Canajoharie @ 67.0 m.
All data are in weight percent.

	SiO_2	TiO_2	Al_2O_3	FeO*	MnO	MgO	CaO	K_2O	Na_2O	Cl	Total‡
1 (ves)§	71.81	0.123	15.97	1.159	0.06	0.042	0.792	6.27	3.15	0.109	99.50
2 (ves)	72.79	0.096	13.22	0.256	0.02	0.025	0.875	5.33	3.18	0.087	95.88
3	75.75	0.401	11.17	1.620	0.04	0.227	1.178	3.43	2.82	0.269	96.92
4	74.15	0.082	11.78	0.538	0.02	0.029	0.632	4.58	3.21	0.073	95.09
5	75.32	0.373	11.03	1.604	0.05	0.235	1.134	3.44	3.00	0.262	96.45
6a†	75.12	0.383	11.04	1.648	0.04	0.229	1.178	3.38	3.33	0.264	96.60
6b	75.12	0.381	11.05	1.633	0.04	0.234	1.186	3.34	3.39	0.266	96.65
6c	75.14	0.394	11.18	1.649	0.05	0.233	1.177	3.43	3.09	0.275	96.62
6d	75.55	0.380	11.08	1.633	0.05	0.229	1.168	3.34	3.07	0.274	96.76
7	73.07	0.075	11.63	0.969	0.04	0.040	0.859	4.69	3.12	0.083	94.57
8	75.02	0.384	11.19	1.596	0.04	0.229	1.106	3.51	3.00	0.288	96.37
9	72.92	0.089	11.70	1.060	0.04	0.053	0.850	4.52	3.14	0.079	94.45
10	75.68	0.375	11.13	1.598	0.05	0.229	1.145	3.32	2.98	0.272	96.78

* total iron as FeO

† Sample numbers with letters represent analyses of different inclusions in the same phenocryst

§ (ves) inclusion contains a bubble

‡ Difference of totals from 100 % is due to the presence of volatiles

Analyst: Dannenmann, S., Hanson, B.

Appendix A.6.1 Results of electron microprobe analyses of rhyolitic melt inclusions in quartz phenocrysts from Canajoharie @ 84.7 m.
All data are in weight percent.

	SiO_2	TiO_2	Al_2O_3	FeO*	MnO	MgO	CaO	K_2O	Na_2O	Cl	Total‡
1a†	73.72	0.205	11.54	1.810	0.067	0.237	1.841	2.23	3.04	0.257	94.95
1b	73.95	0.210	11.31	1.760	0.071	0.234	1.792	2.21	3.09	0.250	94.88
2	73.11	0.213	11.63	1.804	0.069	0.246	1.820	2.23	3.22	0.254	94.60
3	72.73	0.217	11.59	1.788	0.061	0.241	1.779	2.22	3.13	0.252	94.01
4	73.25	0.213	11.57	1.849	0.058	0.247	1.903	2.21	3.51	0.256	95.07
5	74.18	0.205	11.38	1.816	0.058	0.238	1.819	2.26	3.25	0.257	95.46
6a	73.72	0.216	11.51	1.840	0.074	0.243	1.822	2.23	3.15	0.263	95.07
6b	74.15	0.209	11.46	1.838	0.077	0.241	1.798	2.16	3.16	0.251	95.34
6c	73.70	0.219	11.52	1.816	0.064	0.243	1.831	2.25	3.15	0.257	95.05
7	73.69	0.159	11.22	1.495	0.055	0.136	1.324	2.43	3.67	0.282	94.45
8	73.31	0.210	11.58	1.828	0.068	0.241	1.787	2.24	3.24	0.261	94.77
9a	73.42	0.192	11.34	1.797	0.060	0.241	1.790	2.25	3.50	0.249	94.84
9b	73.54	0.218	11.32	1.809	0.071	0.242	1.783	2.26	3.05	0.250	94.54
11	73.12	0.214	11.66	1.805	0.062	0.247	1.786	2.31	3.34	0.269	94.81
12	73.39	0.200	11.43	1.765	0.065	0.235	1.840	2.21	3.26	0.254	94.66
13	n.a.	0.211	11.10	1.759	0.063	0.229	1.816	2.18	3.20	0.268	-
14	n.a.	0.207	11.15	1.690	0.068	0.229	1.809	2.21	3.23	0.272	-
15	n.a.	0.205	10.93	1.746	0.065	0.229	1.817	2.20	3.48	0.265	-
16	n.a.	0.208	11.17	1.748	0.068	0.230	1.819	2.22	3.20	0.275	-
17	n.a.	0.209	10.97	1.761	0.076	0.227	1.847	2.24	3.58	0.254	-
18a	n.a.	0.215	10.92	1.732	0.061	0.230	1.787	2.25	3.29	0.265	-
18b	n.a.	0.207	10.89	1.737	0.067	0.223	1.798	2.20	3.45	0.292	-

* total iron as FeO

† Sample numbers with letters represent analyses of different inclusions in the same phenocryst

n.a. = not analyzed

‡ Difference of totals from 100 % is due to the presence of volatiles

Analyst: 1-12 Dannenmann, S., Hanson, B.
13-18 Delano, J.W.

Appendix A.6.2 Results of electron microprobe analyses of rhyolitic melt inclusions in apatite phenocrysts from Canajoharie @ 84.7 m.
All data are in weight percent.

	SiO_2	TiO_2	Al_2O_3	FeO*	MnO	MgO	CaO	K_2O	Na_2O	Cl	Total‡
1	72.82	0.222	11.30	1.800	0.072	0.236	1.981	2.35	3.48	0.281	94.54
2	67.17	0.279	13.96	2.580	0.129	0.375	3.179	1.60	4.22	0.432	93.92
3	74.22	0.233	11.14	1.783	0.068	0.224	1.883	2.17	3.57	0.258	95.55
4	72.52	0.226	11.67	1.847	0.073	0.238	2.087	2.28	3.99	0.279	95.21
5	72.45	0.209	11.50	1.735	0.070	0.238	2.006	2.19	3.62	0.269	94.28
6	n.a.	0.223	n.a.	1.811	0.044	0.233	1.983	n.a.	n.a.	0.303	-
7	72.34	0.204	11.29	1.662	0.056	0.196	1.620	2.50	3.98	0.292	94.13
8	n.a.	0.226	n.a.	1.854	0.043	0.235	1.964	n.a.	n.a.	0.303	-
9	72.12	0.219	11.26	1.758	0.086	0.221	1.904	3.51	3.68	0.300	95.05
10	69.75	0.222	12.14	1.990	0.072	0.270	2.177	3.31	3.78	0.362	94.08
11	72.07	0.211	11.41	1.784	0.053	0.235	1.800	3.42	3.71	0.315	95.01
12	68.26	0.270	13.07	2.224	0.076	0.307	2.727	3.17	4.27	0.376	94.76
13	71.69	0.227	11.45	1.723	0.081	0.227	1.788	2.82	3.56	0.301	93.86
15	71.98	0.213	11.41	1.745	0.058	0.227	1.899	3.10	3.84	0.293	94.76

* total iron as FeO
n.a. = not analyzed
‡ Difference of totals from 100 % is due to the presence of volatiles
Analyst: Dannenmann, S., Hanson, B.

Appendix B

Flat Creek

Appendix B.1 Results of electron microprobe analyses of rhyolitic melt inclusions in quartz phenocrysts from Flat Creek @ 31.2 m.
All data are in weight percent.

	SiO_2	TiO_2	Al_2O_3	FeO*	MnO	MgO	CaO	K_2O	Na_2O	Cl	Total‡
1	72.88	0.168	12.43	1.710	0.029	0.075	0.504	6.44	2.50	0.029	96.77
2	70.78	0.082	12.61	1.149	0.059	0.230	0.890	5.21	3.16	0.002	94.17
3a†	71.71	0.156	11.84	0.933	0.035	0.260	1.164	8.50	3.28	0.030	97.90
3b (small)**	n.a.	0.165	n.a.	1.102	0.037	0.281	1.240	n.a.	n.a.	0.010	-
4	71.52	0.079	13.06	1.136	0.021	0.196	0.531	9.57	2.53	0.020	98.65
5	70.49	0.147	11.82	1.230	0.045	0.276	1.246	8.43	3.03	0.052	96.76
6 (small)	n.a.	0.147	n.a.	1.102	0.044	0.217	1.038	n.a.	n.a.	0.021	-
7 (small)	n.a.	0.116	n.a.	0.501	0.063	0.135	0.940	n.a.	n.a.	0.017	-
8	70.36	0.247	11.64	3.142	0.081	0.387	2.381	6.10	2.99	0.093	97.42

* total iron as FeO

† Sample numbers with letters represent analyses of different inclusions in the same phenocryst

** (small) means that the inclusion is around 8 μm

n.a. = not analyzed

‡ Difference of totals from 100 % is due to the presence of volatiles

Analyst: Dannenmann, S., Hanson, B.

Appendix B.2.1 Results of electron microprobe analyses of rhyolitic melt inclusions in quartz phenocrysts from Flat Creek @ 47.4 m.
All data are in weight percent.

	SiO_2	TiO_2	Al_2O_3	FeO*	MnO	MgO	CaO	K_2O	Na_2O	Cl
1	n.a.	0.123	11.26	0.883	0.044	0.127	1.035	4.19	2.77	0.107
2	n.a.	0.016	11.61	0.394	0.039	0.010	0.624	4.58	3.28	0.032
3a†	n.a.	0.066	11.16	0.693	0.032	0.064	0.750	4.40	2.77	0.102
3b	n.a.	0.057	11.16	0.646	0.039	0.048	0.774	4.46	2.84	0.105
3c	n.a.	0.064	11.13	0.663	0.035	0.052	0.788	4.43	2.83	0.109
4	n.a.	0.088	11.06	0.762	0.050	0.078	0.899	4.00	3.02	0.095
5	n.a.	0.024	11.61	0.813	0.089	0.047	0.746	4.35	3.42	0.037
6	n.a.	0.052	11.32	0.707	0.038	0.053	0.767	4.52	3.06	0.113
7	n.a.	0.013	11.72	0.032	0.126	0.013	0.780	4.43	3.46	0.019
8	n.a.	0.150	10.99	0.072	0.046	0.149	1.501	4.09	2.35	0.212

* total iron as FeO

† Sample numbers with letters represent analyses of different inclusions in the same phenocryst

n.a. = not analyzed

Analyst: Delano, J.W.

Appendix B.2.2 Results of electron microprobe analyses of rhyolitic melt inclusions in quartz phenocrysts from Flat Creek @ 47.4 m # 'C'.
All data are in weight percent.

	SiO_2	TiO_2	Al_2O_3	FeO*	MnO	MgO	CaO	K_2O	Na_2O	Cl	Total‡
1	72.30	0.062	11.65	1.115	0.050	0.029	0.863	4.36	3.34	0.101	93.87
2	72.49	0.050	11.79	0.893	0.072	0.045	0.951	4.48	3.09	0.103	93.96
3	74.88	0.154	11.43	0.939	0.111	0.122	0.759	2.06	4.36	0.191	95.01
4 (small)**	71.94	0.041	12.18	0.894	0.090	0.039	0.696	4.64	3.19	0.096	93.81
5 (ves?)§	71.79	0.034	14.89	1.004	0.096	0.031	0.878	5.98	3.22	0.118	98.04

* FeO as total iron

§ (ves) inclusion contains a bubble

** (small) means that the inclusion is around 8 μm

‡ Difference of totals from 100 % is due to the presence of volatiles

Analyst: Dannenmann, S., Hanson, B.

Appendix B.2.3 Results of electron microprobe analyses of rhyolitic melt inclusions in quartz phenocrysts from Flat Creek @ 47.4 m # 'E'.
All data are in weight percent.

	SiO_2	TiO_2	Al_2O_3	FeO*	MnO	MgO	CaO	K_2O	Na_2O	Cl	Total‡
1 (ves?)§	70.44	0.058	16.71	1.064	0.080	0.050	0.996	6.56	2.95	0.137	99.042
2 (ves?)§	70.07	0.059	16.55	0.781	0.073	0.028	1.068	6.53	3.23	0.154	98.549
3a†	71.80	0.024	12.18	0.823	0.076	0.031	0.673	4.37	3.46	0.027	93.464
3b	n.a.	0.026	n.a.	0.887	0.085	0.034	0.642	n.a.	n.a.	0.039	-
4	72.20	0.077	11.82	0.839	0.039	0.073	0.916	4.40	2.98	0.115	93.463
5	71.58	0.026	12.18	0.928	0.066	0.041	0.818	4.62	3.25	0.109	93.621
6	71.50	0.105	12.13	1.266	0.047	0.140	1.485	3.36	2.99	0.083	93.098

* total iron as FeO

† Sample numbers with letters represent analyses of different inclusions in the same phenocryst

§ (ves) inclusion contains a bubble

n.a. = not analyzed

‡ Difference of totals from 100 % is due to the presence of volatiles

Analyst: Dannenmann, S., Hanson, B.

Appendix B.2.4 Results of electron microprobe analyses of experimentally remelted rhyolitic melt inclusions in quartz phenocrysts from Flat Creek @ 47.4 m
All data are in weight percent and normalized to 11.8 wt.% Al_2O_3.

	SiO_2	TiO_2	Al_2O_3	FeO*	MnO	MgO	CaO	K_2O	Na_2O	Cl
1a†	n.a.	0.021	11.80	0.810	0.081	0.054	0.728	n.a.	n.a.	0.064
1b	77.45	0.034	11.80	0.854	0.092	0.047	0.724	7.42	4.35	0.101
2a	78.52	0.029	11.80	0.741	0.071	0.060	0.787	5.65	3.32	0.086
2b	80.64	0.020	11.80	0.797	0.061	0.077	0.724	6.45	3.14	0.082
2c	80.57	0.023	11.80	0.818	0.084	0.116	0.735	6.40	3.02	0.081
3a	75.85	n.a.	11.80	1.144	0.054	0.207	1.239	6.30	3.95	n.a.
3b	n.a.	n.a.	11.80	1.112	0.050	0.216	1.142	n.a.	n.a.	n.a.
4	80.13	0.027	11.80	0.820	0.078	0.071	0.695	5.84	3.12	0.078
5	80.36	0.017	11.80	0.468	0.096	0.134	0.752	6.11	2.72	0.067
6	80.30	0.015	11.80	0.820	0.083	0.185	0.708	5.23	3.46	0.087
7	79.18	0.034	11.80	0.791	0.089	0.067	0.740	5.45	3.10	0.070
8	80.07	0.028	11.80	0.809	0.080	0.056	0.708	5.48	3.66	0.076
9	78.52	0.032	11.80	0.797	n.a.	0.078	n.a.	5.90	3.19	0.086
10	77.58	0.042	11.80	0.778	0.078	0.038	0.761	4.84	3.24	0.061
11	n.a.	0.013	11.80	0.835	0.090	0.062	0.728	n.a.	n.a.	0.101
12	80.09	0.038	11.80	0.805	0.085	0.057	0.718	5.82	3.52	0.065

* total iron as FeO

† Sample numbers with letters represent analyses of different inclusions in the same phenocryst

n.a. = not analyzed

Analyst: Dannenmann, S., Hanson, B.

Appendix B.3.1 Results of electron microprobe analyses of rhyolitic melt inclusions in quartz phenocrysts from Flat Creek @ 49.5 m.
All data are in weight percent.

	SiO_2	TiO_2	Al_2O_3	FeO*	MnO	MgO	CaO	K_2O	Na_2O	Cl	Total‡
1a†	n.a.	0.209	n.a.	1.108	0.085	0.216	1.150	n.a.	n.a.	0.165	-
1b	73.51	0.231	11.34	1.104	0.085	0.213	1.150	2.74	3.29	0.160	93.83
2	72.25	0.213	11.23	1.059	0.085	0.208	1.129	2.57	3.53	0.163	92.43
3 (ves)§	n.a.	0.118	n.a.	0.844	0.090	0.127	1.249	n.a.	n.a.	0.105	-
4	n.a.	0.034	n.a.	0.671	0.037	0.046	0.791	n.a.	n.a.	0.092	-
5a	72.06	0.275	11.84	0.858	0.057	0.124	0.589	2.97	3.41	0.146	92.34
5b	71.80	0.269	11.88	1.063	0.088	0.220	1.169	3.01	3.43	0.144	93.07
5c	n.a.	0.205	n.a.	1.102	0.099	0.208	1.354	n.a.	n.a.	0.151	-
6	73.84	0.234	11.17	0.971	0.076	0.184	0.838	2.72	3.25	0.160	93.44
7	73.88	0.200	11.59	0.945	0.087	0.181	1.212	3.15	3.26	0.149	94.65
8	74.15	0.297	11.31	1.140	0.083	0.201	0.985	3.05	2.90	0.326	94.43
9	73.91	0.223	11.46	0.785	0.067	0.219	1.250	2.80	3.18	0.152	94.05
11	n.a.	0.244	n.a.	1.057	0.084	0.196	1.238	n.a.	n.a.	0.167	-
12	n.a.	0.115	n.a.	1.056	0.089	0.131	1.081	n.a.	n.a.	0.046	-
13	74.74	0.177	11.51	0.905	0.085	0.177	1.139	2.76	2.78	0.144	94.42
14	75.38	0.209	10.86	0.901	0.071	0.206	1.177	2.64	2.95	0.126	94.52
15	73.61	0.227	11.67	0.935	0.092	0.232	1.339	2.70	3.23	0.144	94.17
16	73.15	0.188	11.50	0.954	0.086	0.195	1.174	3.08	3.12	0.131	93.58
17(ves)	74.20	0.213	11.13	0.977	0.090	0.222	1.229	2.97	2.96	0.129	94.13
18	74.47	0.029	11.19	0.742	0.063	0.036	0.704	3.66	2.93	0.081	93.90

* total iron as FeO

† Sample numbers with letters represent analyses of different inclusions in the same phenocryst

§ (ves) inclusion contains a bubble

n.a. = not analyzed

‡ Difference of totals from 100 % is due to the presence of volatiles

Analyst: 1-12 Dannenmann, S., Hanson, B.
13-18 Dannenmann, S.

Appendix B.3.2 Results of electron microprobe analyses of experimentally remelted rhyolitic melt inclusions in quartz phenocrysts from Flat Creek @ 49.5 m
All data are in weight percent and normalized to 11.8 wt.% Al_2O_3.

	SiO_2	TiO_2	Al_2O_3	FeO*	MnO	MgO	CaO	K_2O	Na_2O	Cl
1	82.44	0.095	11.80	1.193	0.073	0.798	0.163	5.67	4.00	0.125
2	80.26	0.106	11.80	0.950	0.071	0.280	1.122	6.77	2.19	0.082
3a†	80.46	0.253	11.80	1.141	0.099	0.276	1.285	5.81	2.94	0.152
3b	80.15	0.255	11.80	1.168	0.092	0.423	1.240	5.67	2.88	0.167
4	80.31	0.022	11.80	0.771	0.066	0.222	0.745	2.68	4.25	0.078
5	81.27	0.050	11.80	0.874	0.060	0.054	0.798	6.36	3.28	0.091
6	80.41	0.044	11.80	0.873	0.089	0.065	0.866	6.63	2.59	0.044
7	80.46	0.214	11.80	1.035	0.087	0.194	1.120	5.45	3.76	0.155
8	77.64	0.035	11.80	0.731	0.091	0.268	0.901	7.90	1.40	0.075
9	80.02	0.240	11.80	1.051	0.130	0.314	1.207	9.13	1.42	0.173
10	75.14	0.040	11.80	0.756	0.070	0.054	0.956	7.80	1.48	0.064
11	75.61	0.035	11.80	0.835	0.088	0.081	0.979	5.76	0.90	0.078
12	82.08	0.028	11.80	0.841	0.098	0.074	0.729	5.64	2.87	0.071

* total iron as FeO

† Sample numbers with letters represent analyses of different inclusions in the same phenocryst

Analyst: Dannenmann, S., Hanson, B.

Appendix C

Chuctanunda Creek

Appendix C.1 Results of electron microprobe analyses of rhyolitic melt inclusions in quartz phenocrysts from Chuctanunda @ 42.0 m.
All data are in weight percent.

	SiO_2	TiO_2	Al_2O_3	FeO*	MnO	MgO	CaO	K_2O	Na_2O	Cl	Total‡
1	73.31	0.325	11.32	1.725	0.071	0.308	1.505	2.43	3.03	0.314	94.33
2	73.94	0.342	11.32	1.743	0.062	0.314	1.593	2.55	3.06	0.305	95.24
3	74.52	0.329	11.19	1.558	0.068	0.300	1.569	2.43	3.01	0.300	95.27
4	74.02	0.182	11.81	0.980	0.040	0.185	0.785	3.29	4.05	0.257	95.60
5	73.00	0.359	11.30	1.864	0.070	0.362	1.792	2.36	2.77	0.286	94.16

* total iron as FeO

‡ Difference of totals from 100 % is due to the presence of volatiles

Analyst: Dannenmann, S.

Appendix C.2.2 Results of electron microprobe analyses of experimentally remelted rhyolitic melt inclusions in quartz phenocrysts from Chuctanunda at 46.4 m. All data are in weight percent and normalized to 11.8 wt.% Al_2O_3.

	SiO_2	TiO_2	Al_2O_3	FeO*	MnO	MgO	CaO	K_2O	Na_2O	Cl
1a†	n.a.	0.021	11.80	0.795	0.049	0.083	0.724	n.a.	n.a.	0.067
1b	n.a.	0.013	11.80	0.803	0.089	0.076	0.712	n.a.	n.a.	0.068
2	79.31	0.021	11.80	0.763	0.046	0.083	0.838	5.06	3.43	0.080
3a	79.54	0.013	11.80	0.789	0.060	0.092	0.722	4.77	4.13	0.062
3b	79.36	0.023	11.80	0.793	0.080	0.078	0.758	5.04	3.79	0.083
4	n.a.	0.028	11.80	0.819	0.048	0.077	0.716	n.a.	n.a.	0.073
5	79.83	0.029	11.80	0.818	0.077	0.071	0.747	5.05	3.81	0.079
6a	79.82	0.041	11.80	0.802	0.091	0.077	0.690	4.83	5.78	0.071
6b	n.a.	0.023	11.80	0.785	0.056	0.069	0.639	n.a.	n.a.	0.074
7a	n.a.	0.064	11.80	0.930	0.081	0.067	0.967	n.a.	n.a.	0.072
7b	79.85	0.050	11.80	0.903	0.086	0.075	0.930	4.93	3.88	0.087
8a	77.16	0.025	11.80	0.809	0.067	0.073	0.706	4.63	3.68	0.071
8b	79.76	0.028	11.80	0.768	0.085	0.087	0.738	4.67	3.75	0.066
9	80.15	0.021	11.80	0.797	0.107	0.079	0.727	5.09	3.34	0.086
10	78.30	0.032	11.80	0.780	0.068	0.078	0.887	4.81	3.71	0.071
11a	79.63	0.022	11.80	0.432	0.058	0.084	0.705	4.95	3.84	0.068
11b	n.a.	0.035	11.80	0.821	0.084	0.082	0.715	n.a.	n.a.	0.073
12	79.75	0.028	11.80	0.825	0.067	0.087	0.712	5.41	3.52	0.063

* total iron as FeO

† Sample numbers with letters represent analyses of different inclusions in the same phenocryst

n.a. = not analyzed

Analyst: Dannenmann, S., Hanson, B.

Appendix C.2.1 Results of electron microprobe analyses of rhyolitic melt inclusions in quartz phenocrysts from Chuctanunda @ 46.4 m.
All data are in weight percent.

	SiO_2	TiO_2	Al_2O_3	FeO*	MnO	MgO	CaO	K_2O	Na_2O	Cl	Total[‡]
1 (ves)[§]	69.29	0.049	15.63	0.119	0.103	0.002	0.819	6.13	3.93	0.110	96.18
2 (ves)	70.58	0.049	15.31	1.026	0.101	0.032	0.889	5.93	3.37	0.128	97.42
3 (ves)	69.84	0.043	15.47	0.495	0.072	0.040	0.870	6.13	3.29	0.126	96.38
4a[†](ves)	70.10	0.016	15.60	0.295	0.026	0.003	1.106	5.72	3.82	0.134	96.81
4b (ves)	72.52	0.104	14.67	0.152	0.005	0.002	0.357	6.09	4.12	0.124	98.14
5 (ves)	70.49	0.090	14.67	0.256	0.002	0.000	0.351	6.32	3.68	0.092	95.94
6 (ves)	72.86	0.177	13.52	1.332	0.062	0.097	1.439	4.17	2.77	0.137	96.57
7	72.38	0.124	11.50	0.706	0.053	0.087	1.164	3.72	3.01	0.087	92.83
8	71.75	0.121	11.60	1.349	0.051	0.046	0.973	4.09	3.13	0.105	93.21
9	72.38	0.123	11.58	1.391	0.057	0.108	1.292	3.60	2.91	0.104	93.54
10 (ves)	68.92	0.050	15.75	0.784	0.089	0.031	0.971	6.12	3.71	0.134	96.56
11 (ves)	71.09	0.042	15.29	0.355	0.075	0.018	0.878	6.36	3.70	0.126	97.93
12 (ves)	72.50	0.029	15.30	0.920	0.102	0.033	0.795	6.30	2.89	0.119	98.99
13	73.52	0.133	11.34	1.213	0.032	0.083	1.065	3.38	3.46	0.071	94.30
14 (ves)	71.34	0.029	16.32	0.432	0.077	0.017	0.607	6.75	3.49	0.317	99.38
15	73.67	0.074	12.54	0.816	0.045	0.145	0.499	5.32	2.98	0.022	96.11

* total iron as FeO

[†] Sample numbers with letters represent analyses of different inclusions in the same phenocryst

[§] (ves) inclusion contains a bubble

[‡] Difference of totals from 100 % is due to the presence of volatiles

Analyst: Dannenmann, S., Hanson, B.

Appendix D

Deer River

Appendix D.1.1 Results of electron microprobe analyses of rhyolitic melt inclusions in quartz phenocrysts from Deer River @ 19.2 m.
All data in weight percent.

	SiO_2	TiO_2	Al_2O_3	FeO*	MnO	MgO	CaO	K_2O	Na_2O	Cl	Total‡
1	71.43	0.031	11.74	0.869	0.073	0.034	0.738	4.54	3.18	0.107	92.74
2	71.21	0.034	11.93	0.831	0.078	0.036	0.744	4.54	3.34	0.106	92.85
3	70.19	0.019	11.60	0.098	0.076	0.030	0.660	4.37	3.26	0.098	90.40
4	71.47	0.031	11.70	0.866	0.077	0.032	0.749	4.54	3.20	0.104	92.77
5a†	71.84	0.034	11.69	0.877	0.071	0.041	0.799	3.73	3.44	0.102	92.62
5b	72.31	0.022	11.63	0.958	0.072	0.042	0.751	3.80	3.56	0.106	93.25
6a	70.92	0.033	11.91	0.931	0.078	0.038	0.800	3.27	3.27	0.099	91.35
6b	71.41	0.043	12.05	0.889	0.072	0.040	0.804	4.48	3.31	0.104	93.20
7	71.23	0.028	11.89	0.855	0.069	0.034	0.732	4.49	3.27	0.103	92.70
8	71.46	0.053	11.79	0.919	0.071	0.058	0.897	4.40	3.06	0.105	92.81
9	71.75	0.024	11.79	0.836	0.086	0.026	0.745	4.61	3.26	0.109	93.24
10	71.24	0.029	12.01	0.905	0.080	0.040	0.847	4.57	3.07	0.111	92.90
11a	71.64	0.021	11.79	0.897	0.082	0.038	0.747	4.55	3.24	0.107	93.11
11b	71.64	0.038	11.88	0.925	0.085	0.036	0.744	4.51	3.20	0.112	93.17
12	71.47	0.026	11.88	0.846	0.080	0.031	0.722	4.57	3.20	0.104	92.93

* total iron as FeO

† Sample numbers with letters represent analyses of different inclusions in the same phenocryst

n.a. = not analyzed

‡ Difference of totals from 100 % is due to the presence of volatiles

Analyst: Delano, J.W.

Appendix D.1.2 Results of electron microprobe analyses of experimentally remelted rhyolitic melt inclusions in quartz phenocrysts from Deer River @ 19.2 m. All data are in weight percent and normalized to 11.8 wt.% Al_2O_3.

	SiO_2	TiO_2	Al_2O_3	FeO*	MnO	MgO	CaO	K_2O	Na_2O	Cl
1	80.80	0.055	11.80	0.841	0.084	0.083	0.717	5.47	4.09	0.098
2	79.82	0.028	11.80	0.809	0.072	0.296	0.889	5.31	2.33	0.098
3	81.53	0.031	11.80	0.831	0.066	0.051	0.715	4.78	4.12	0.066
4	82.68	0.115	11.80	1.042	0.051	0.910	1.113	5.66	2.68	0.080
5	81.12	0.032	11.80	0.835	0.070	0.287	0.372	5.27	2.86	0.076
6	81.59	0.073	11.80	0.835	0.043	0.328	0.861	5.67	2.42	0.082
7a†	82.08	0.044	11.80	0.825	0.073	0.270	0.760	5.12	3.35	0.059
7b	81.96	0.045	11.80	0.866	0.117	0.756	0.848	6.27	2.82	0.056
8	80.60	0.019	11.80	0.944	0.091	0.249	0.852	4.99	3.23	0.120
10	82.52	0.032	11.80	0.841	0.082	0.205	0.744	6.51	3.59	0.101
11	81.12	0.069	11.80	0.879	0.048	0.370	0.919	5.29	3.12	0.086
12	79.21	0.016	11.80	0.746	0.073	1.451	0.582	3.14	1.45	0.100

* total iron as FeO

† Sample numbers with letters represent analyses of different inclusions in the same phenocryst

Analyst: Dannenmann, S., Hanson, B.

Appendix E

Nowadaga 'B0'
Myers Road 'MC2'

Appendix E.1 Results of electron microprobe analyses of rhyolitic melt inclusions in apatite phenocrysts from Myers Road 'MC2'.
All data are in weight percent.

	SiO_2	TiO_2	Al_2O_3	FeO*	MnO	MgO	CaO	K_2O	Na_2O	Cl	Total‡
1	67.14	0.067	13.23	0.957	0.036	0.091	1.348	11.69	2.86	0.066	97.48
2	69.80	0.069	12.78	0.880	0.031	0.084	1.253	11.14	2.71	0.054	98.79
3	69.98	0.055	12.35	0.739	0.037	0.065	1.200	6.14	3.13	0.043	93.74
4	71.99	0.035	11.47	0.931	0.020	0.077	0.976	6.08	2.39	0.058	94.03
5	69.88	0.067	12.35	0.865	0.018	0.075	1.216	9.83	2.85	0.039	97.18
6	66.75	0.067	12.51	0.015	0.007	0.003	1.382	10.01	2.16	0.057	92.96
7	70.77	0.049	11.70	0.791	0.050	0.066	0.966	10.89	2.52	0.036	97.84
8	70.36	0.069	12.05	0.885	0.023	0.074	1.043	11.37	2.54	0.051	98.46
9	n.a.	0.059	n.a.	0.841	0.017	0.070	1.155	n.a.	n.a.	0.038	-

* total iron as FeO
n.a. = not analyzed
‡ Difference of totals from 100 % is due to the presence of volatiles
Analyst: Dannenmann, S., Hanson, B.

Appendix E.2 Results of electron microprobe analyses of rhyolitic melt inclusions in apatite phenocrysts from Nowadaga 'B0'.
All data are in weight percent.

	SiO_2	TiO_2	Al_2O_3	FeO*	MnO	MgO	CaO	K_2O	Na_2O	Cl	Total‡
1	71.96	0.057	11.76	0.793	0.030	0.060	0.899	6.37	2.55	0.053	94.54
2	68.27	0.073	13.50	1.221	0.053	0.115	1.453	6.13	2.80	0.065	93.68
3	70.12	0.081	12.01	0.686	0.015	0.054	1.083	5.45	3.16	0.043	92.70
4	71.74	0.088	11.79	0.735	0.039	0.058	0.813	5.64	2.65	0.048	93.60
5	70.70	0.064	12.55	0.193	0.020	0.035	1.237	5.35	3.05	0.040	93.25
6	66.32	0.373	14.89	1.200	0.032	0.101	1.862	6.14	3.25	0.065	94.24
7	70.90	0.065	12.80	0.861	0.034	0.077	1.376	5.29	2.98	0.050	94.43
8	67.43	0.341	14.86	0.190	0.028	0.039	1.579	5.51	3.45	0.054	93.48
9	70.05	0.088	13.32	0.097	0.005	0.023	1.283	6.60	2.73	0.049	94.25

* total iron as FeO

‡ Difference of totals from 100 % is due to the presence of volatiles

Analyst: Dannenmann, S., Hanson, B.